THE ROLE OF TNP-NUCLEOTIDES, LYS492 AND CA^{2+}CHELATORS IN THE SKELETAL MUSCLE SARCOPLASMIC RETICULUM CA^{2+}ATPASE CYCLE.

Thesis presented for the degree of Masters in Medical Sciences of the University of Cape Town

by

Janine Wichmann B.Sc.(Hons) (UP)

December 1997

ACKNOWLEDGEMENTS

I wish to thank my supervisors Professors David B. McIntosh and Mervyn C. Berman for their guidance, supervision and encouragement throughout this study. I also wish to extent my thanks to Mr. Abduraman Mohammad and Mr. David G. Woolley for techical assistance, and Mr. Ronnie Alexander for the routine preparation of SR vesicles.

Financial assistance for the duration of the study was provided in part by the Foundation for Research and Development (FRD). Experimental work was carried out in the Medical Research Council Biomembrane Research Unit, Department of Chemical Pathology, University of Cape Town.

ABSTRACT

In the first part of this study, the kinetics of decay of TNP-nucleotide superfluorescence was investigated with a view to understanding the role of nucleotides and Lys492 in later steps in the catalytic cycle of the skeletal muscle Ca^{2+}ATPase. It has been found previously, and verified here, that tethering TNP-8N_3-AMP to the Ca^{2+}ATPase via Lys492 retarded the Ca^{2+} initiated decay of P_i-induced superfluorescence 10-fold compared with untethered nucleotide. The rapidity of the decay upon addition of EDTA suggested that the $E_2 \leftrightarrow E_1 \rightarrow E_1Ca_2$ steps were being monitored rather than dephosphorylation per se. Tethered di- and triphospho species did not accelerate the decay. While monophasic kinetics was observed with untethered TNP-AMP and TNP-8N_3-AMP, complex kinetics were observed with the di- and triphospho TNP-nucleotides. This was shown to be due to the utilization of TNP-ADP and -ATP, and the azido derivatives, as coupled substrates of the Ca^{2+}ATPase in the forward direction of catalysis in the presence of Ca^{2+}. The hydrolysis rates of TNP-ADP, TNP-ATP, TNP-8N_3-ADP, and TNP-8N_3-ATP were 10, 5, 15 and 10 nomoles/min/mg of protein, respectively, at room temperature and pH 5.5. Ca^{2+} transport was supported by all four nucleotides. This is the first time that a diphosphonucleotide has been shown to support Ca^{2+} transport. A new nonhydrolysable triphospho TNP-nucleotide, TNP-AMP-PCP was synthesized and shown to interact with the Ca^{2+}ATPase in a similar way, in terms of superfluorescence, as the other TNP-nucleotides. It did not show the complex kinetics on inhibition of the P_i-induced superfluorescence by Ca^{2+}, but neither did it accelerate the kinetics. It was concluded that TNP-nucleotides do not

accelerate the $E_2 \leftrightarrow E_1$ transition under these conditions, possibly because of the presence of glycerol in the medium.

In the second part of the study, it was shown that addition of small amounts of chelators EGTA, EDTA, BAPTA, DTPA, HEDTA and NTA to a Ca^{2+} transport assay in which the free Ca^{2+} concentration is monitored by Fluo-3 causes the Ca^{2+}ATPase to pump to apparently lower levels as seen in the $[Ca^{2+}]_{lim}$ fluorescence. Addition of chelator retards pump function in the sense that it takes longer for 50 nmols Ca^{2+} to be accumulated. Increased thermodynamic efficiency of the pump and contaminating heavy metal ions were considered as possible mechanisms. To some extend Zn^{2+} and Cd^{2+}, but not Fe^{2+} and Cu^{2+}, appeared to reverse the partial inhibition. While interpretation of the results is difficult, it is suggested that heavy metal ions interact with luminal loops of the Ca^{2+}ATPase and enhance Ca^{2+} release under conditions of high luminal Ca^{2+} concentrations.

ABBREVIATIONS

AMP-PCP	: adenosine 5′-(β, γ-methylene)triphosphate
BAPTA	: 1,2-bis(2-aminophenoxy)ethane-N,N,N′,N′-tetraacetic acid
$[Ca^{2+}]_{free}$	: concentration of free calcium ions
$[Ca^{2+}]_{lim}$	: limiting concentration of free calcium ions
DMC	: dimethoxycoumarin
DMF	: dimethylformamide
DTNB	: 5,5′-dithio-bis(2-nitrobenzoic acid)
DTPA	: diethylenetrinitrilotetraacetic acid
EGTA	: ethylene glycol bis(β-aminoethyl ether)-N,N,N′,N′-tetraacetic acid
EDTA	: ethylenediaminetetraacetic acid
EPPS	: N-[2-Hydroxyethyl]piperazine-N′-3-propanesulfonic acid
FITC	: fluoroscein isothiocyanate
HEDTA	: N-(2-hydroxyethyl)ethylenedinitrilo-N,N′,N′-triacetic acid
MES	: 2-[N-Morpholino]ethanesulfonic acid
MOPS	: 3-[N-Morpholino]propanesulfonic acid
NBD	: 4-nirtobenzo-2-oxa-1,3-diazole
NTA	: nitrilotriacetic acid
SR	: sarcoplasmic reticulum
SRV	: sarcoplasmic reticulum vesicles
TCA	: trichloroacetic acid
TEAB	: triethylamine bicarbonate
TMAH	: tetramethylammonium hydroxide
TNBS	: 2,4,6-trinitrobenzenesulfonic acid
TNP-ADP	: 2′,3′-*O*-(2,4,6-trinitrophenyl) adenosine 5′-diphosphate
TNP-AMP	: 2′,3′-*O*-(2,4,6-trinitrophenyl) adenosine 5′-monophosphate

TNP-AMP-PCP	: 2′,3′-*O*-(2,4,6-trinitrophenyl) adenosine 5′-(β, γ-methylene)triphosphate
TNP-ATP	: 2′,3′-*O*-(2,4,6-trinitrophenyl) adenosine 5′-triphosphate
TNP-8N_3-ADP	: 2′,3′-*O*-(2,4,6-trinitrophenyl)-8-azido adenosine 5′-diphosphate
TNP-8N_3-AMP	: 2′,3′-*O*-(2,4,6-trinitrophenyl)-8-azido adenosine 5′-monophosphate
TNP-8N_3-ATP	: 2′,3′-*O*-(2,4,6-trinitrophenyl)-8-azido adenosine 5′-triphosphate
Tris	: tris(hydroxymethyl)methylamine

CONTENTS

2. EXPERIMENTAL PROCEDURES

3. RESULTS

1. INTRODUCTION

1.1 Physiological role of SR

Muscle contraction and relaxation is expedited by a system of membranes. The system consists of the plasmamembrane with its tubular infoldings (the T-system) running transversely to the fiber axis and a reticular structure (the sarcoplasmic reticulum, SR) that forms a network surrounding the myofibrils (see Fig 1)(Prescott, 1988). Depolarization of the plasmamembrane is communicated by the T-system to the interior of the muscle fiber and Ca^{2+} is released from the SR to bind troponin located on thin filaments. Muscle contraction and relaxation are induced by the release and reabsorption of Ca^{2+} by SR. The T-system and SR are further interconnected in a structure called the triad.

Biochemical studies are performed using fragmented SR isolated from muscle homogenates as vesicles. The pioneer work on the SR vesicles was performed by Hasselbach and Makinose (1961) and Ebashi and Lipmann (1962). They noticed that the isolated SR vesicles (SRV) could remove a significant amount of Ca^{2+} from the medium in the presence of ATP and Mg^{2+} . They also demonstrated that 2 mol of Ca^{2+} were transported into the SRV when 1 mol of ATP was hydrolysed. Ca^{2+}ATPase (EC 3.6.1.3.8) is a membranous enzyme found in the sarcoplasmic reticulum vesicles, which is responsible for the transport of Ca^{2+} from the reaction medium (or cytoplasm in muscle cells) into the lumen of the reticulum with ATP hydrolysis (MacLennan and Holland, 1975). In the relaxed state of the muscle, the free Ca^{2+} concentration is of the order of 0.1 μM (the limiting Ca^{2+} concentration, $[Ca^{2+}]_{lim}$), whereas the luminal free Ca^{2+} concentration is in the millimolar range (Hasselbach and Makinose, 1961, Ebashi and Lipmann,

Figure 1

The location of SR in skeletal muscle

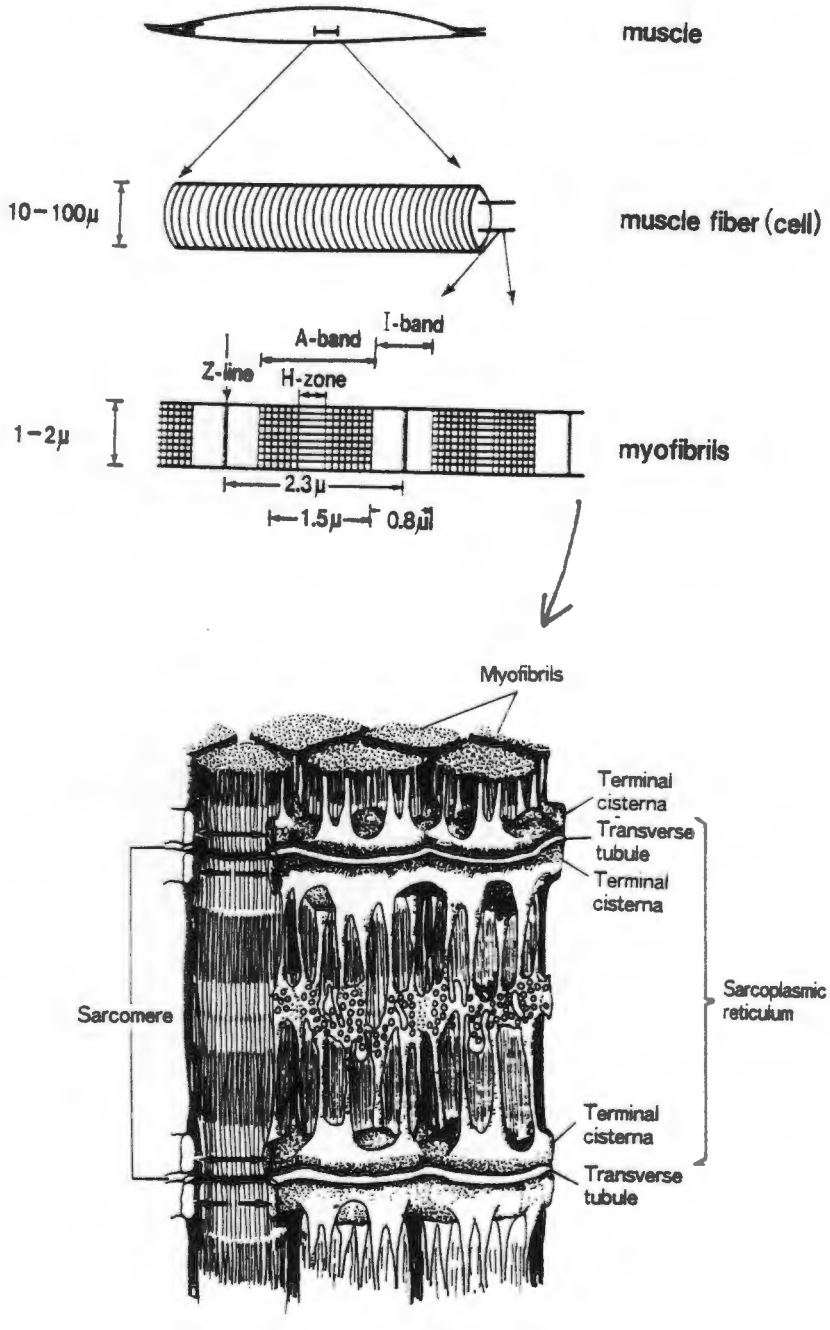

1962). The pump works against a 10^4-fold concentration gradient.

1.2 General structure of Ca^{2+}ATPase

There are three principal types of ATPases in which ATP hydrolysis is directly coupled to ion transport against an electrochemical gradient (Moller *et al.*, 1996)(see flowchart):

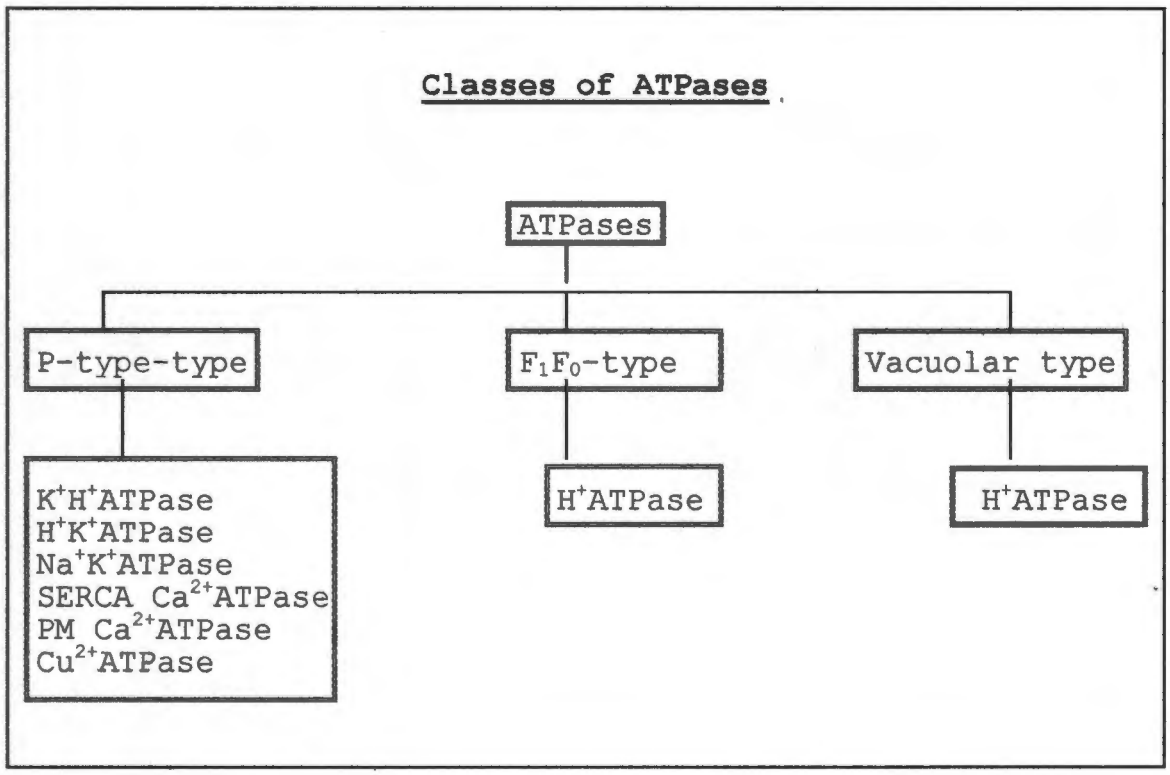

1) In the P-type of ATPases, an aspartic acid residue is phosphorylated during the transport process. From there the name, P-type. Included in this type, are the H^+K^+ATPase, Na^+K^+ATPase, K^+H^+ATPase, SERCA Ca^{2+}ATPase, plasmamembrane Ca^{2+}ATPase and Cu^{2+} transporting ATPase. In mammals the following subdivisions can also be made: Na^+K^+ATPase can be present in α1, α2 or the α3 isoform. Four different isoforms of SERCA can be distinguished: SERCA1 (found in fast-twitch skeletal muscle cells, adult and fetal isoforms have 997 and 1001 amino acid residues,

respectively), SERCA2 (present in isoform 2a (997 amino acid residues) in cardiac and slow-twitch skeletal muscle cells; and in isoform 2b (1024 amino acid residues) in many cell types), SERCA3 (found in platelets and other blood-forming cells, nonmuscle tissues eg. intestines, stomach, spleen and lungs). Plasmamembrane Ca^{2+}ATPase is present in four isoforms PMCA1, PMCA2, PMCA3 and PMCA4. The plasmamembrane Ca^{2+}ATPase is bigger than the SERCA Ca^{2+}ATPase, with 1080 to 1220 residues.

2) The F_1F_0-type is a proton transporting complex of several proteins found in eubacteria, chloroplasts and mitochondria and does not have a phospho-intermediate.

3) Vacuolar type (or V-type) is also a proton transporting complex of proteins and maintains the low pH of plant vacuoles and of lyzosomes and other vesicles in animal cells.

The fast twitch rabbit skeletal Ca^{2+}ATPase was used in our studies. It contains 997 amino acids and has a molecular weight of 110 kDa (MacLennan *et al.*, 1985; Brandl *et al.*, 1986). A structural model of the Ca^{2+}ATPase derived from the amino acid sequence is shown in Fig 2 (MacLennan *et al.*, 1985; Brandl *et al.*, 1986; Taylor and Green, 1989). The transmembrane segments and the extramembranous regions were identified from hydropathy plots (MacLennan *et al.*, 1985). The proposed structure contains ten α-helical transmembrane segments and two large extramembranous cytoplasmic loops between membrane traverses M2 and M3 (termed the β-strand domain) and M4 and M5 (the large cytoplasmic loop). Evidence that the phosphorylation site and ATP binding site are located on the latter, has mainly been provided by studies involving fluorescent and photoaffinity probes, such as Lys515 labelling with FITC (Pick and Karlish, 1980; Pick and Bassilion, 1981; Mitchinson *et al.*, 1982; Highsmith,

1986; Champeil *et al.*, 1988; Squier *et al.*, 1990) and covalent labelling of Lys492 with TNP-nucleotides (McIntosh *et al.*, 1992; McIntosh and Woolley, 1994); pyridoxal phosphate probes (Murphy, 1977; Yakamoto *et al.*, 1988) and intramolecular crosslinking studies (Murphy, 1990; Ross *et al.*, 1991; McIntosh *et al.*, 1991) as well as site-directed mutagenesis (Marayuma *et al.*, 1989; Clarke *et al.*, 1990; Vilsen *et al.* 1991).

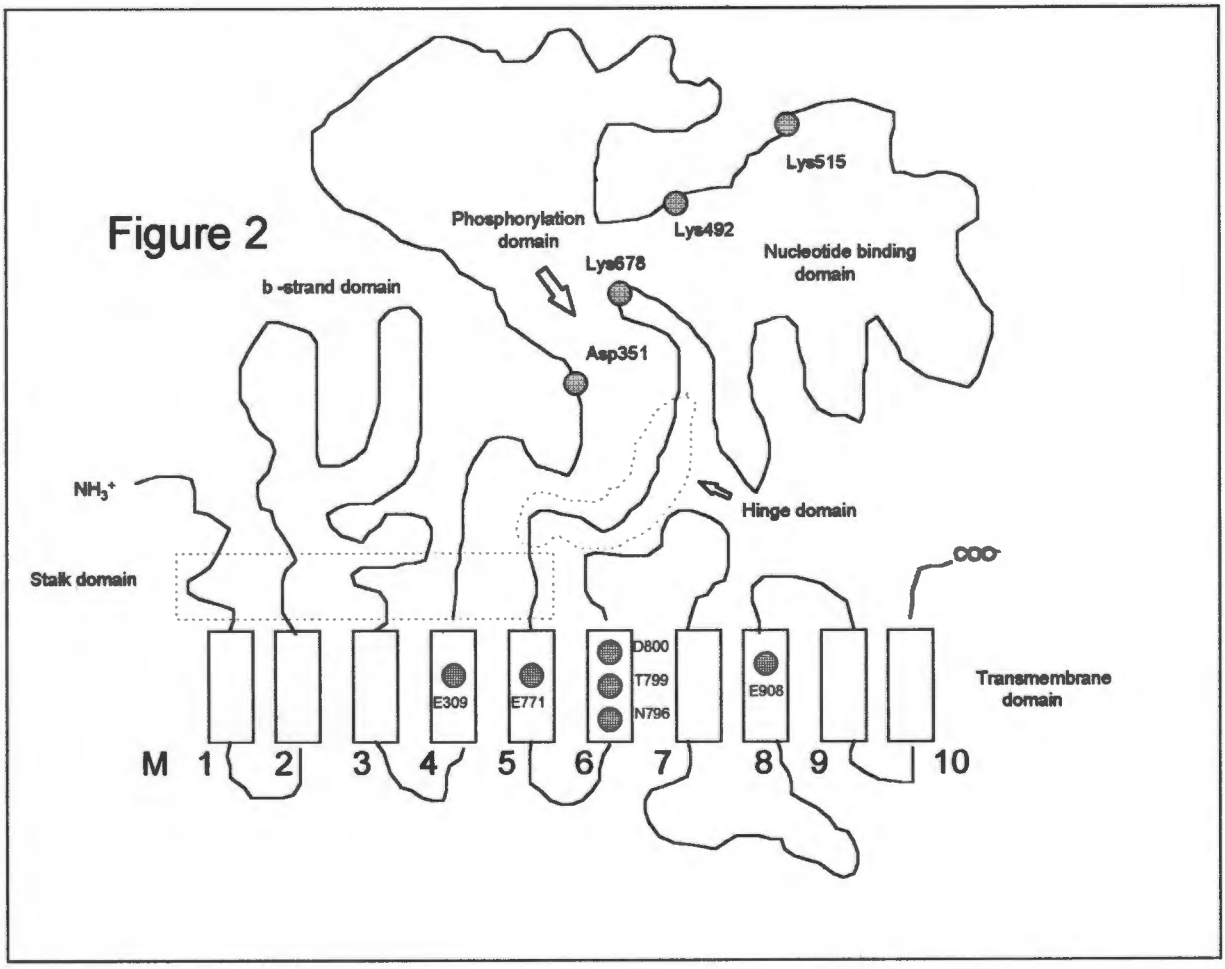

The cytoplasmic loops are connected with the transmembrane segments by a 'stalk', consisting of amphiphatic α-helices. Previously it was thought that the stalk region contained the Ca^{2+} binding sites due to the occurrence of 16 negatively charged glutamic acid

Figure 3
Proposed 3D structure of SR Ca^{2+}ATPase

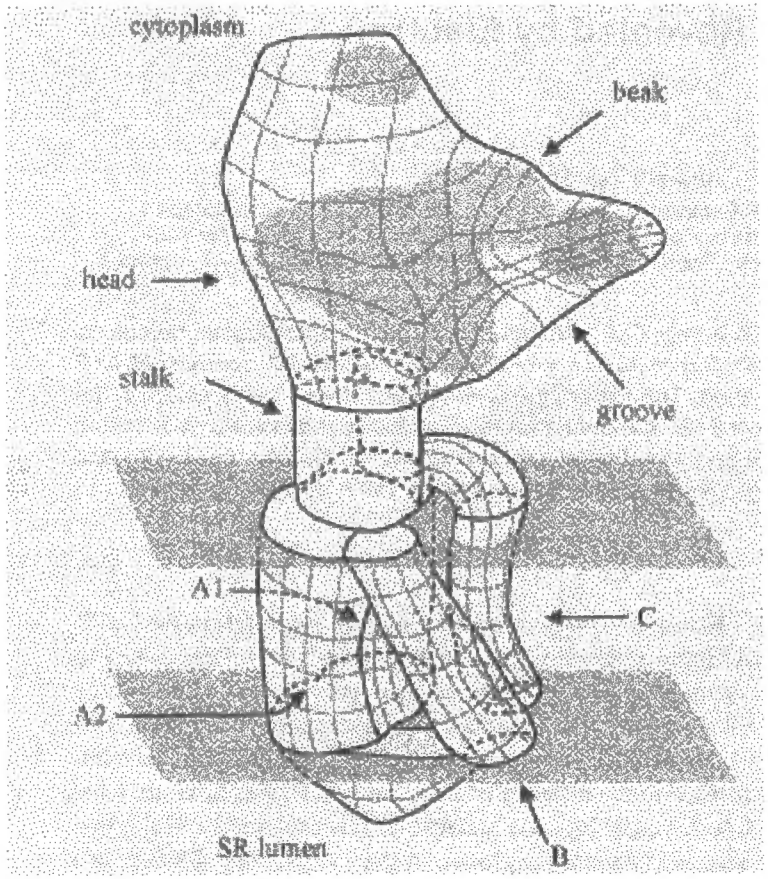

Figure 4

Proposed 3D orientation of the different domains of SR Ca^{2+}ATPase

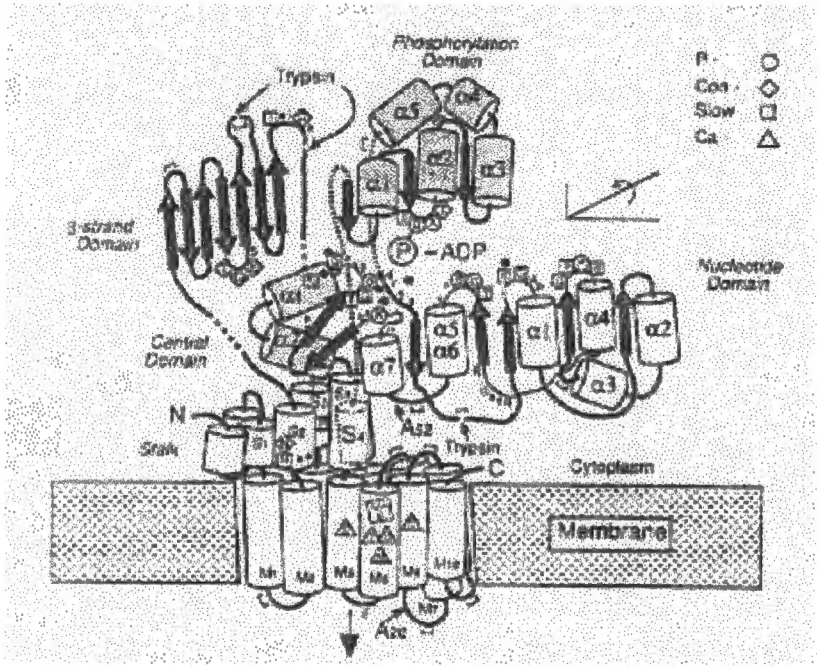

residues in the first three helices (Brandl *et al.*, 1989; Green, 1989). However, it was later shown that the Ca^{2+} binding sites are located in the transmembrane sequences M4, M5, M6, M8 (MacLennan *et al.*, 1985; Clarke *et al.*, 1990). Stalk sequences S4 and S5 appear to communicate conformational changes initiated by nucleotide binding and phosphorylation down to the Ca^{2+} binding sites in the transmembrane domain, during Ca^{2+} transport (MacLennan *et al.*, 1995, Andersen, 1995). This accounts for the coupling between ATP hydrolysis and Ca^{2+} translocation (MacLennan, 1990; MacLennan *et al.*, 1992). Previously Highsmith and Murphy (1984) had found the closest distance between the ATP and Ca^{2+} binding sites to be between 21 and 26 Å. However, more recent results, suggest that the distance is 35-40 Å (Scott, 1985; Green and Stokes, 1992; Toyoshima et al., 1993). Toyoshima *et al.*, 1993 have elucidated the tertiary structure of Ca^{2+}ATPase at 14 Å resolution, and Green and Stokes (1992) have suggested arrangements for the membrane helices (Fig 3 and 4). These models support previous predictions that two large loops are located at the cytoplasmic side and 10 α-helices are located in the membrane.

1.3 Catalytic cycle

In order to facilitate the discussion of the catalytic cycle of Ca^{2+}ATPase, a general reaction sequence, modified from McIntosh and Woolley (1994), will be used as reference.

The Ca^{2+}ATPase transports Ca^{2+} from the cytoplasm into the SR lumen and H^+ in the opposite direction. The transport of Ca^{2+} is activated by phosphorylation with ATP, and that of H^+ is associated with phosphoenzyme hydrolysis in the second part of the reaction cycle. The reaction cycle is initiated with the sequential binding of 2 Ca^{2+} to the E_1H_3

catalytic intermediate at the high affinity binding sites (K_m ~ 1 μM)(Meissner, 1973; Dupont, 1982; Orlowski and Champeil; 1991) facing the cytoplasm and the dissociation of 2-3 H^+ into the cytoplasm (de Meis and Vianna, 1979, Levy *et al.*, 1990, Forge *et al.*, 1993). Ca^{2+} binding (from the cytoplasm) at the transport sites is a crucial step in the enzyme cycle, as it induces a change in the chemical reactivity of the catalytic site, which is either phosphorylated by ATP (in the forward direction) or by P_i (in the reverse direction) in the presence and absence of Ca^{2+}, respectively.

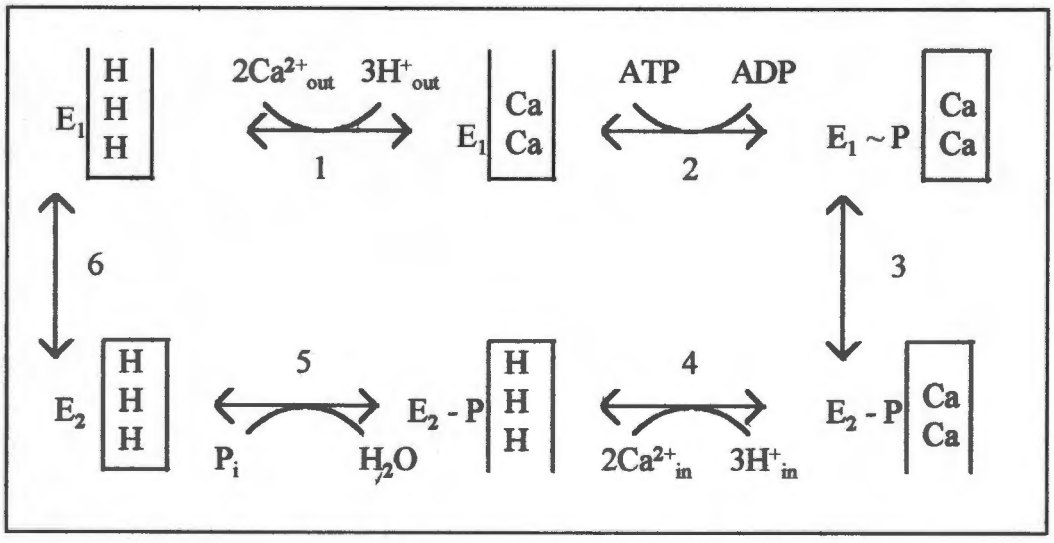

Phosphorylation by P_i and ATP, requires Mg^{2+} (Masuda and de Meis, 1973). The E_1Ca_2 form has a binding site for the catalytic Mg^{2+} ion with a K_d ~ 0.94 mM at pH 7.0, 25 °C (Punzengruber *et al.*, 1978). This is approximately 10-fold lower than that for the Ca^{2+}-free enzyme, E_1, (8.8 mM) under similar conditions (Punzengruber *et al.*, 1978). Vianna (1975) previously suggested that the substrate in the forward direction of catalysis is MgATP. However, Reinstein and Jencks (1993) have found that the dissociation rate constants of ATP and Mg^{2+} from

$E_1Ca_2ATP.Mg$, 120 s^{-1} and 60 s^{-1}, respectively. This indicates that Mg^{2+} and ATP can bind and dissociate independently; they do not have to associate or dissociate from E_1 as the MgATP complex. Incubation of free enzyme, E_1, with Mg^{2+} and ATP, causes a conformational change that activates the enzyme for phosphorylation and decreases the rate constant for the dissociation of ATP to 47 s^{-1} (Reinstein and Jencks, 1993). In the reverse direction of catalysis Mg^{2+} and Pi bind separately (Punzengruber *et al.*, 1978) or simultaneously (Champeil *et al.*, 1985). De Meis *et al* (1991) presented data that the enzyme has different binding sites for Mg^{2+} and P_i. After MgATP binding to E_1Ca_2 (K_m ~ 2 μM) (Meissner, 1973), the Ca^{2+}ATPase is phosphorylated to give E_1Ca_2P. The γ-phosphate group of bound MgATP (Allen and Green, 1976) is transferred in a rapid reaction (rate constant ≥ 1000 s^{-1}) to the Asp351 residue (Petithory and Jencks, 1986; Stahl and Jencks, 1987), forming an acid-stable acylphosphate (Degani and Boyer, 1973). Synchronous with phosphorylation, the two bound Ca^{2+} become occluded, i.e. they are retained and unable to exchange with free Ca^{2+} in either aqeous phase (Dupont, 1982; Nakamura, 1987; McIntosh et al., 1991; Vilsen and Andersen, 1992). The enzyme now undergoes a conformational change to E_2Ca_2P, in which the Ca^{2+} binding sites face the lumen of the SRV (Champeil *et al.*, 1986; Wakabayashi and Shigekawa, 1990). In this conformation, the Ca^{2+} binding affinity is greatly reduced (K_d ~ 1 mM) which permits the sequential dissociation of the 2 bound Ca^{2+} to the lumen. Yamaguchi and Kanazawa (1984, 1985) and Forge *et al.* (1993) have found that 2-3 H^+ bind from the lumen to the E_2 species. The phosphoenzyme is now dephosphorylated in a fast reaction to give E_2

($k_{forward}$ = 60 s^{-1})(Inesi *et al.*, 1983; McIntosh and Boyer, 1983). The Ca^{2+}ATPase recycles back to the E_1H_3 conformation and a new reaction cycle can be initiated.

1.4 Energy coupling mechanisms

Ca^{2+}ATPase is an ion pump, which converts chemical energy into osmotic energy. In this case the input chemical energy is the free energy (ΔG) of ATP hydrolysis and the output osmotic energy is a 10^4-fold Ca^{2+} concentration gradient. Free energy transfer from ATP to the enzyme is facilitated through the phosphorylation reaction. This interconvertion of energy is made possible by coupled vectorial processes.

It is important to notice that there are two very different meanings for the term "coupling". It often refers to

1) the relationship between changes in Gibbs energy for two processes, eg coupling of binding energies for two processes, or

2) it is also used to describe the relationship between two processes, eg the hydrolysis of ATP that is coupled with the transport of Ca^{2+} (a coupled process)(Jencks, 1982, 1992).

First, attention will be given to coupling relating to the relationship between changes in Gibbs energy for two processes. The primary function of binding energy is kinetic, as it is utilized to avoid high- or low-energy species in the Ca^{2+}ATPase catalytic cyle. High-energy species will possibly introduce a barrier to rapid enzyme turnover (Fig 5A), whilst low-energy species will possibly cause the enzyme to fall into an energy pit, which will be difficult to escape from (Fig 5B). However, the energies of the catalytic species are balanced to avoid high- or low-energy species, i.e. the Gibbs

energies of all the species are similar (Wyman, 1964; Weber, 1975; Hill, 1977; Stein and Honig, 1977; Jencks, 1980; Pickart and Jencks, 1984)(Fig 5C).

Figure 5

Gibbs energy diagram

A) Shows high-energy species and

B) low-energy species along a reaction pathway, which cause barriers in the reaction cycle.

C) Gibbs energy profile for Ca^{2+}ATPase (pH 7.0, 8 mM ATP, 5 mM Mg^{2+}, 0.1 M Ca^{2+}_{out}, and 1 mM Ca^{2+}_{in})(Pickart and Jencks, 1984).

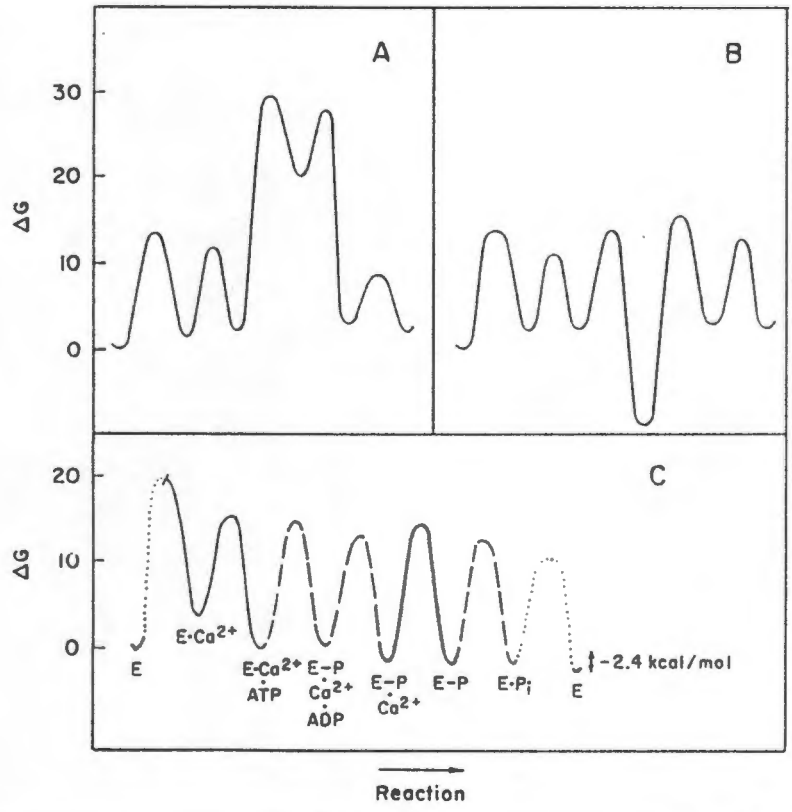

Ca^{2+}ATPase must overcome two thermodynamic barriers:

1) In the forward direction of catalysis: the conversion of "low-energy" Ca^{2+} (bound at high-affinity sites, exposed to the cytoplasm) into "high-energy" Ca^{2+} (bound at low-affinity sites, exposed to lumen), and

2) In the reverse direction of catalysis: the conversion of the "low-energy" phosphate of E_2P (which can be transferred to H_20) into "high-energy" phosphate (which can only be transferred to ADP). These barriers are overcome by mutual destabilization of the occluded Ca^{2+} and covalently bound phosphate in E_1Ca_2P (Jencks, 1983; Pickart and Jencks, 1984). The spontaneous formation of the acyl phosphate species is driven by the intrinsic binding energy of phosphate alone, whilst the strong binding of two Ca^{2+} to the high affinity sites is driven by the intrinsic binding energy of Ca^{2+} alone (Jencks, 1980; Hill and Eisenberg, 1981; Tanford, 1981). When both Ca^{2+} and the phospho group are present in E_1Ca_2P, there is mutual destabilization of the ligands by

$\Delta G_D \approx 8.0$ kcal/mol. This interaction energy increases the escaping tendency of both Ca^{2+} and the phosphate (Jencks, 1983; Pickart and Jencks, 1984).

Scheme 1

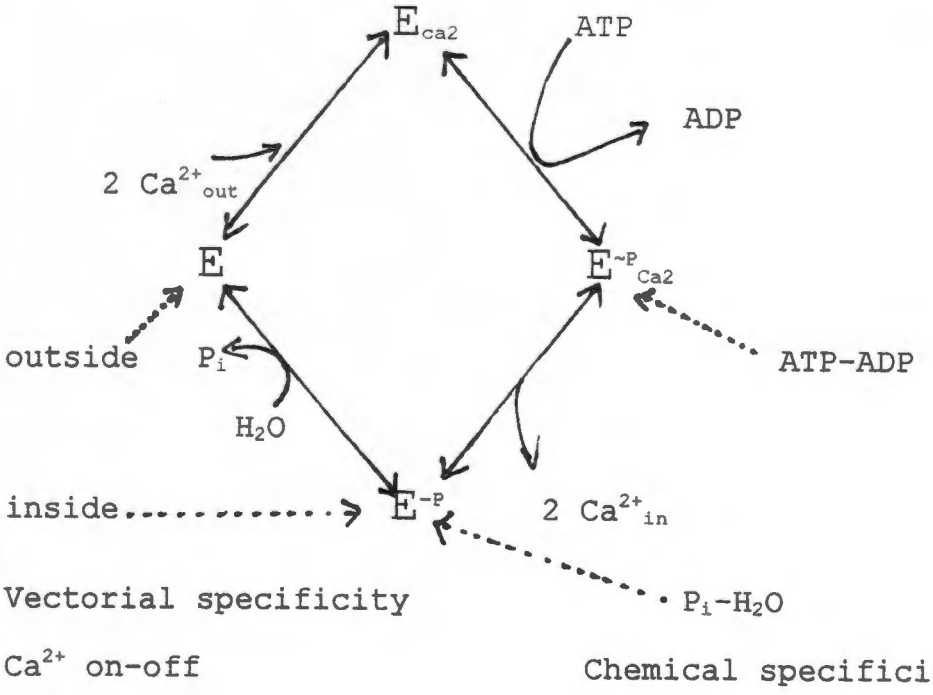

On the other hand, the coupled process of ATP hydrolysis to Ca^{2+} transport is brought about by a set of rules. These rules generally represent the chemical specificity and vectorial specificity of the enzyme (Jencks, 1980, 1992) and are based on known properties of different species of the enzyme in the catalytic cycle (de Meis and Vianna, 1979). Scheme 1 represents a simplified reaction cycle, that illustrates the set of coupling rules (Dupont, 1980; Jencks, 1982).

Chemical specificity can be explained in the following manner: In order for the enzyme in state E_1Ca_2 to transport Ca^{2+}, it is neccesary for it to be phosphorylated by ATP. In the case of ATP synthesis in the reverse direction of catalysis, the enzyme in state E_2Ca_2P must be able to transfer the phosphate to ADP. As soon as Ca^{2+} is dissociated from the enzyme, its chemical specificity changes to catalysis of the phosphorylation of the enzyme by P_i and for transfer of the phosphate from E_2P to water in the reverse direction. The vectorial specificity of the enzyme insures that in conformation E_1, it will bind and dissociate Ca^{2+} only on the cytoplasmic side of the membrane, whereas the phosphorylated enzyme, E_2P, will bind and dissociate Ca^{2+} only from to the lumen of the SRV. Thus chemical specificity is controlled by the presence or absence of bound Ca^{2+}. Vectorial specificity on the other hand, is controlled by enzyme phosphorylation: the unphosphorylated enzyme binds and dissociates Ca^{2+} only from the cytoplasm, whilst the phosphorylated enzyme, binds and dissociates Ca^{2+} only form the lumen. If this set of rules for chemical and vectorial specificity are followed, the chemical reaction of ATP hydrolysis is fully coupled to the translocation of two Ca^{2+} across the SR membrane. Violation of any of these rules, will lead to uncoupling of the system, i.e.

ATP will be hydrolysed and Ca^{2+} will not be transported or will leak out of the vesicles (Jencks, 1980, 1983). It is important to realise that there is not one specific step in the catalytic cycle that is responsible for coupling; failure of a coupling rule in any step will lead to uncoupling (Jencks, 1980; Hill and Eisenberg, 1981).

1.5 Regulation of the enzyme cycle by ATP

Micromolar ATP is required for enzyme turnover, i.e. in this concentration range it has a catalytic function. However, ATP also has a regulatory function in the millimolar concentration range. It modulates the Ca^{2+}ATPase catalytic cycle in a complex manner, so that it exhibits non-Michaelian kinetics with respect to ATP concentration (Inesi *et al.*, 1967; Yamamoto and Tonomura, 1967; Dupont, 1977; Verjovski-Almieda and Inesi, 1979). ATP accelerates the steps associated with Ca^{2+} binding ($E_2 \leftrightarrow E_1 \leftrightarrow E_1Ca_2$)(Scofano *et al.*, 1979; Guillain *et al.*, 1981; Champeil *et al.*, 1983; Stahl and Jencks, 1984; Fernadez-Belda *et al.*, 1984; Wakabayashi *et al.*, 1990; Wakabayashi and Shigekawa., 1990), Ca^{2+} dissociation to the lumen ($E_2Ca_2P \rightarrow E_2P$) (Champeil and Guillain, 1986; Wakabayashi *et al.*, 1986) and phosphoenzyme hydrolysis ($E_2P \rightarrow E_2$) (Champeil *et al.*, 1988; Mintz *et al.*, 1990). ATP accelerates therefore all the steps in the catalytic cycle, which start from a nucleotide-deprived species.

Seebregts and McIntosh (1989) have found that low concentrations of TNP-8N_3-ADP and -ATP accelerate ATPase acitivity ~1.5-fold, showing that they bind to a regulatory site. The TNP-nucleotides label Lys492 at the catalytic site. It was concluded that the regulatory and catalytic site are at the same locus. This necessitates that regulation by ATP is due to the nucleotide reentering the active site after ADP dissociates. This is

supported by other structural and kinetic evidence (Ross and McIntosh, 1987; Champeil *et al.*, 1988; McIntosh *et al.*, 1992; Lacapere and Guillain, 1993). It was suggested by Champeil and Guillain (1986) and Champeil *et al.*, (1988) that metal-free ATP is a more potent activator than MgATP for steps involving phosphoenzyme. In contrast to this model of ATP regulation, Coll and Murphy (1991) concluded that ATP accelerates phosphoenzyme hydrolysis, it must do so by binding to an allosteric site, because [γ-^{32}P]ATP formation was not inhibited when excess cold ATP was added to ADP and phosphoenzyme. Thus regulatory ATP does not appear to compete with ADP (i.e. at the phosphorylated active site).

Whether ATP executes its regulatory function at the catalytic site or at another allosteric site, is still uncertain. So far, three models for the regulatory site location with one catalytic site per 110 kDa Ca^{2+}ATPase chain, have been suggested:

1) a dimeric functional unit in which only one subunit is phosphorylated and a "silent" nonphosphorylated catalytic site in a neighboring subunit, binds the regulatory ATP (Yates and Duance, 1976; Neet and Green, 1977; Silva and Verjovski-Almeida, 1979; Moller *et al.*, 1980; McIntosh and Boyer, 1983);

2) a second physically different nucleotide site per 110 kDa chain, which binds the regulatory ATP, co-exists with the catalytic site (Coll and Murphy, 1984, 1985, 1991; Dupont *et al.*, 1985; Suzuki *et al.*, 1990, 1996), and

3) a single nucleotide site per 110 kDa chain, with the regulatory nucleotide binding site overlapping with the catalytic site. Thus for the regulatory ATP to gain access to the site the nucleotide involved in phosphorylation (ATP or ADP) must have dissociated. (Andersen *et al.*, 1982; McIntosh and Boyer, 1983;

Nakamoto and Inesi, 1984; Cable *et al.*, 1985; Bishop *et al.*, 1987; Ross and McIntosh, 1987; Champeil *et al.*, 1988; Seebregts and McIntosh, 1989)

ATP analogues, TNP-ADP and -ATP can also function in a regulatory role, but have been reported not to be hydrolysed (Watanabe and Inesi, 1982; Dupont *et al.*, 1985). TNP-ATP enhances ATP-mediated turnover (Dupont *et al.*, 1985) and both TNP-ADP and -ATP accelerate phosphoenzyme hydrolysis (Champeil *et al.*, 1988). TNP-$8N_3$-ADP and -ATP activate ATP hydrolysis (Seebregts and McIntosh, 1989; McIntosh *et al.*, 1992). This suggets that the nucleotide binding site may have different pockets, which could accomodate large substituents, so that regulation by these molecules are also possible. This will be discussed in the next section.

1.6 Structural charateristics of the ATP binding site

Besides ATP, ITP (0.8), GTP (0.7), CTP (0.55) and UTP (0.25) (numbers in parentheses represent velocities of hydrolysis relative to that of ATP) (Makinose and The, 1965; Feirrera and Verjovski-Almeida, 1988), TNP-8N3-ATP (McIntosh and Woolley, 1994), *p*-nitrophenyl phosphate (Inesi, 1971) and acetyl phosphate (de Meis, 1969; de Meis and Hasselbach, 1971; Pucell and Martonosi, 1971; Bodley and Jencks, 1987), carbamyl phosphate (Pucell and Martonosi, 1971) can also serve as substrates. Active Ca^{2+} transport is supported by all these compounds and the coupling of 2 mol of Ca^{2+} for each mol of P_i liberated, is maintained (Makinose and The, 1965; Friedman and Makinose, 1970; Inesi, 1971).

Anderson and Murphy (1983) found that both the catalytic (high affinity) and the regulatory (low affinity) site are more tolerant to changes in the 2'OH of the ribose

compared with 3'OH. The hydroxyl groups appear to be involved in stabilizing the enzyme nucleotide complex (Coan *et al.*, 1993). It appears that the catalytic and regulatory substrate specificity of Ca^{2+}ATPase appears is low, suggesting that the nucleotide binding site accommodates many different shaped molecules by utilizing different binding pockets lining the site.

Approaches such as chemical modification, photolabeling and site-directed mutagenesis of amino acids are used to delineate the ATP binding site. Some amino acids are found to be involved in complexing both catalytic ATP or regulatory ATP and others one or the other nucleotide. So far Thr532 and Thr 533 (Lacapere *et al.*, 1993); Arg678 (McIntosh, 1992); Lys684 (Yamamoto *et al.*, 1989); Lys492 (McIntosh *et al.*, 1992; McIntosh, 1992; Stefanova *et al.*, 1993; Yamagata *et al.*, 1994; Yamasaki *et al.*, 1994); and Lys515 (Mitchinson *et al.*, 1982) have been identified to ligate the catalytic ATP. The latter two amino acids were also found to aid in binding regulatory ATP on the phosphorylated enzyme. The role of Lys492 in ligating ATP is quite complex. Lys492 labelling with 7-amino-4-methylcoumarin-3-acetic acid succinidyl ester had no effect on ATPase activity (Stefanova *et al.*, 1989), but labeling with or TNP-8N3-ATP, resulted in the partial uncoupling of the enzyme (McIntosh and Woolley, 1994). Glutaraldehyde crosslinking of Lys492 to Arg678 allowed ATP-dependent Ca^{2+} occlusion and completely blocked Ca^{2+} dissociation to the lumen (McIntosh *et al.*, 1991).

Site-directed mutagenesis pointed out that the ligating role Lys515 is also complex. Mutation of Lys515 led to a lowered Ca^{2+} transport activity, because of weaker ATP binding (Maruyama *et al.*, 1988). Later it was found that mutation of Lys515 also led to complete inhibition of

ATP- and acetyl phosphate facilitated Ca^{2+} transport. McIntosh *et al.* (1996) found through mutation studies on the segment ^{487}FSRDRK^{492} and labeling with TNP-8N_3-ATP, that Lys492 does play a role in ATP binding, but is not essential for enzyme turnover. Phe487 was also indicated in playing an important role in ATP ligation, and to a lesser extent Arg489. They also found that these three residues were binding catalytic and regulatory ATP. ATP blocked the intramolecular glutaraldehyde crosslink with mutation of Lys684 (located in the hinge domain), indicating that it does not play a crucial role in nucleotide binding (Vilsen *et al.*, 1991). ATP did not inhibit the glutaraldehyde crosslink in the mutated D601 to E601 enzyme (MacLennan *et al.*, 1992). The crosslink was also not inhibited by mutating P603 to G603. This implies that the conserved ^{601}DPPR segment plays an important role in complexing ATP.

Chemical modification and photolabeling of amino acids with chromophoric probes not only provide insights into amino acid residues which ligate ATP, but also indicate the microenvironment (eg. hydrophobicity) of the site.

The ATP binding site need not be rigid, and with each step in the catalytic cycle, the amino acid residues that constitute the site, could rearrange so that the configuration, polarity of the site, and pK_a of amino acid residues as well as their reactivity are changed. The interactions between residues complexing catalytic ATP must be different from those binding regulatory ATP. Changes in nucleotide binding affinity, reactivity of residues, and polarity of the site have been detected by probes (Pick and Karlish, 1980; Ross and McIntosh, 1987; Wakabayashi *et al.*, 1990; Wakabayashi and Shigekawa, 1990; Lacapere and Guillain, 1990 and 1993; DeJesus *et al.*, 1993). The TNP-nucleotides provide a good example of

how the polarity of the nucleotide binding site changes. The transition from the ADP-sensitive phosphoenzyme (E_1PCa_2) to one which is insensitive to ADP (E_2PCa_2) is accompanied by a conformational change at the active site as can be seen from the interaction of TNP-nucleotides. The TNP-nucleotides display a large increase in fluorescence or superfluorescence either during ATP-mediated turnover in the forward direction of catalysis or in the reverse direction following phosphorylation by P_i in the absence of Ca^{2+} (Watanabe and Inesi, 1982; Nakamoto and Inesi, 1984; Davidson and Berman, 1987). Dupont and Pougeois (1983) found the polarity of the free catalytic site to be lower than that of water and a further large decrease is observed when Ca^{2+}ATPase is phosphorylated by P_i. Phosphorylation to E_2P must increase the hydrophobicity around the TNP-moiety. The fluorescent FITC probe which labels Lys515 and the crosslinking of Lys492 and Arg678 with glutaraldehyde, also provide evidence of the changes in the microenvironment of the nucleotide binding site during the catalytic cycle. The E_1Ca_2P to E_2P transition induce a large increase in FITC fluorescence, indicating a change to a more hydrophobic environment (Pick, 1981). Enzyme phosphorylation by P_i to give E_2P completely inhibits the glutaraldehyde cross-linking of Lys492 and Arg678 (Ross and McIntosh, 1987). Of the 24 Cys residues which react with SH reagents, 9 are protected by ATP binding (Mahaney *et al.*, 1995; Wawrynow and Collins, 1993). Since the cysteine residues are not conserved, the change in reactivity may be due entirely to conformational changes as a result of nucleotide binding.

1.7 Ca^{2+} binding sites

1.7.1 Structural characteristics

It was originally considered that the high affinity transport sites for Ca^{2+} may be located in the stalk

region due to the presence of 16 negatively charged glutamic acid residues in the first three helices (Brandl *et al.*, 1986; Green, 1989). However, site-specific mutagenesis has identified Glu309 in transmembrane sequence M4, Glu771 in M5, Asn796, Thr799 and Asp800 in M6 and Glu908 in M8 to be involved in Ca^{2+} binding (Brandl *et al.*, 1989; MacLennan *et al.*, 1985; Clarke *et al.*, 1989, 1990). Andersen (1995) provided evidence from site-directed mutagenesis that Glu309 and Asn796 are associated with one Ca^{2+} binding site, Glu771 and Thr799 with another site and Asp800 with both sites. According to Andersen and Vilsen (1996) Glu908 does not bind Ca^{2+} directly in the occluded state and Asn796 is possibly involved in the counter transport of H^+. Rice and MacLennan (1996) showed by mutagenesis studies that tiers 3,4 and 5 of M4, M5 and M6 contain Ca^{2+} binding and affinity mutations (Fig 6).

Figure 6

Diagram to show tiers of transmembrane helices M4, M5, M6 and M8

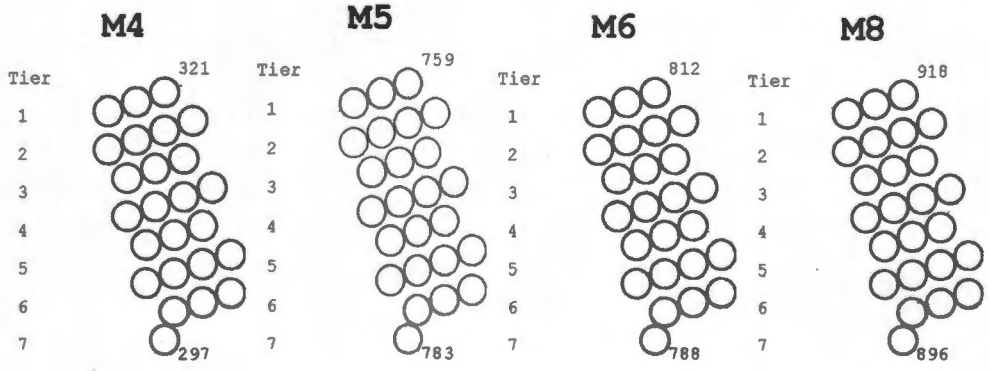

These central tiers are also implicated in the conformational changes involved in Ca^{2+} transport. M8 apparently has a peripheral role in Ca^{2+} binding and translocation in comparison to M4, M5 and M6, as mutations in M8 failed to identify residues involved in blocking conformational changes or altering Ca^{2+} affinity. Transmembrane segment M7 is considered to be obliquely angled with respect to the axis normal to the mebrane (Stokes and Green, 1994). Chen *et al.* (1996) identified short and long range roles of several amino acids within the transmembrane sequences, by site-directed mutagenesis and by modelling. Some of the short range roles include the direct involvement of Glu309, Glu771, Thr799, Asp800, Glu908 and Asn796 in M4, M5, M6 and M8, to form a Ca^{2+} binding channel; roles of several residues in the stabilization of the helical cluster for optimal channel function and Lys297 which seals the distal end of the Ca^{2+} binding channel. Long range roles include the possible involvement of several transmembrane residues in the communication between the Ca^{2+} binding sites and phosphorylation and ATP binding sites, for example, transmembrane helix M4 may rotate to allow vectorial flux of Ca^{2+} after enzyme phosphorylation by ATP.

1.7.2 Ca^{2+} binding kinetics

Ca^{2+} binding kinetics can be monitored by $^{45}Ca^{2+}$ and filtration or indirectly by Ca^{2+}ATPase intrinsic tryptophan fluorescence (Dupont and Leigh, 1978; Guillain *et al.*, 1980, 1981; Verjovski-Almeida and Silva, 1981; Champeil *et al.*, 1983; Fernandez-Belda *et al.*, 1984; Scofano *et al.*, 1985; Moutin and Dupont, 1991) or labelling an amino acid with a fluorescent sensitive probe near the Ca^{2+} binding sites, such as DMC which labels Cys344 (Stefanova *et al.*, 1992) or NBD-labelled

Ca^{2+}ATPase which monitores the $E_2 \leftrightarrow E_1$ equilibrium (Henderson *et al.*, 1994).

Ca^{2+} binding is apparently cooperative, suggesting a mechanism such as that shown in Scheme 2 (Dupont, 1976; Ikemoto *et al.*, 1978; Dupont and Leigh, 1978; Guillain *et al.*, 1980; Inesi *et al.*, 1980; Champeil *et al.*, 1983; Gould *et al.*, 1986; Froud and Lee, 1986; Inesi, 1987).

Scheme 2

$$E_2 \overset{}{\leftrightarrow} E_1 \overset{K_1}{\leftrightarrow} E_1Ca \overset{K_2}{\leftrightarrow} E_1Ca_2$$

The value of the $E_2 \leftrightarrow E_1$ equilibrium constant has been estimated as 0.5 at pH 7.2 (Froud and Lee, 1986). If Ca^{2+} binding is not cooperative the $E_2 \leftrightarrow E_1$ equilibrium constant would have been less than 0.01 if the two Ca^{2+} binding sites were of equal affinity (i.e. $K_1 = K_2$ in Scheme 2)(Inesi, 1987). Such a low value for the $E_2 \leftrightarrow E_1$ equilibrium constant seems to be inconsistent with values obtained by Pick (1982) and Froud and Lee (1986). The cooperativity of Ca^{2+} binding can be explained if the first, inner site has a higher affinity for Ca^{2+} than the outer site (i.e. $K_2 > K_1$).

Ca^{2+} binds sequentially; first to the inner, high affinity binding site exposed to the cytoplasm. A second, outer Ca^{2+} binding site is formed after Ca^{2+} binding of the first inner Ca^{2+}. The apparent binding constant for the first,

inner Ca^{2+} is lower compared with the outer Ca^{2+} (Dupont, 1982; Orlowski and Champeil, 1991), which is in agreement with the cooperative binding model. Dupont (1982) and Nakamura (1986) found that cytoplasmic dissociation of Ca^{2+} from the unphosphorylated enzyme is biphasic in the presence of excess $^{40}Ca^{2+}$. This is evidence that Ca^{2+} dissociation is sequential. Nakamura (1986) also found sequential dissociation of Ca^{2+} from the phosphorylated enzyme. Ikemoto *et al.* (1981), Inesi (1987), Moutin and Dupont (1991) and Orlowski and Champeil (1991) also support this mechanism of sequential dissociation on cytoplasmic side. Forge *et al.* (1995) found the dissociation rates in excess EGTA and Mg^{2+} (pH 8, 5 °C), to be 20 s^{-1} and 1 s^{-1} for the superficial and inner Ca^{2+}, respectively, and excess $^{40}Ca^{2+}$ blocks release of the inner $^{45}Ca^{2+}$ and leads to half of $^{45}Ca^{2+}$ being dissociated, with rate constant of 9 s^{-1} (pH 8, 5 °C).

Ca^{2+} binding kinetics is sensitive to Mg^{2+} and H^+ concentrations, and is modulated by millimolar ATP concentrations (see section 3.5). Mg^{2+} appears to compete with Ca^{2+} for binding at the Ca^{2+} sites (cytoplasmic on E_1 and luminal on E_2P)(Guillain *et al.*, 1982; Froud and Lee, 1986; Gould *et al.*, 1986; Bishop and Al-Shawi, 1988). This binding is in competition with H^+ binding (Michelangeli *et al.*, 1990; Forge *et al.*, 1993). Mg^{2+} also effects Ca^{2+} dissociation from the unphosphorylated enzyme, implying that Mg^{2+} can also bind to site(s) other than at the Ca^{2+} binding sites (Moutin and Dupont, 1991). Henderson *et al.* (1994) have found that the K_d of Mg^{2+} is pH-independent in the presence or absence of Ca^{2+} (Kd ~ 2 mM). From this the following scheme was proposed for Mg^{2+} and H^+ binding (Henderson *et al.*, 1994):

Scheme 3

Hendersen *et al.* (1994)

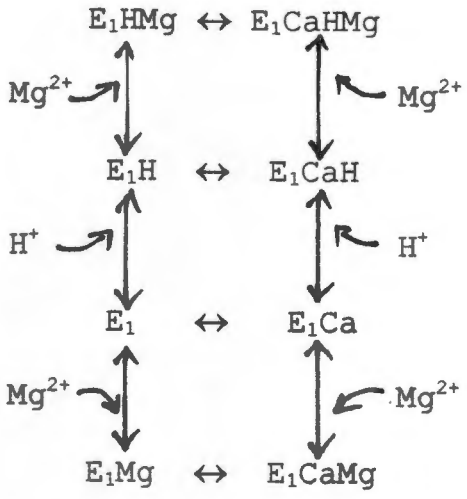

Forge *et al.* (1993) has described the inhibition effects by H^+ and Mg^{2+} on Ca^{2+} binding in the following manner. Inhibition by H^+ is described by two steps involving two H^+ and one H^+, with pK 7 and 7.9, respectively. At pH 6.0, two H^+ must dissociate to bind the first inner Ca^{2+} and a third H^+ for the second superficial Ca^{2+}. At pH 9, both Ca^{2+} bind without any H^+ exchange. Mg^{2+} on the other hand, can bind to all the species, except to the saturated Ca^{2+} species. Mg^{2+} binds tighter to the species having lost two H^+ ($\leq$ 1 mM) than to the species having three H^+ (4 mM). The deprotonated form (E_1) not only has a higher affinity for Ca^{2+}, but also binds Ca^{2+} faster than the protonated form (E_2), $k > 50\ s^{-1}$ and 1.3-2.7 s^{-1}, respectively (Forge *et al.*, 1993). Martin *et al.* (1992) has found that both Ca^{2+} and H^+ bind cooperatively at the Ca^{2+} binding sites.

Scheme 4

Forge *et al.* (1993)

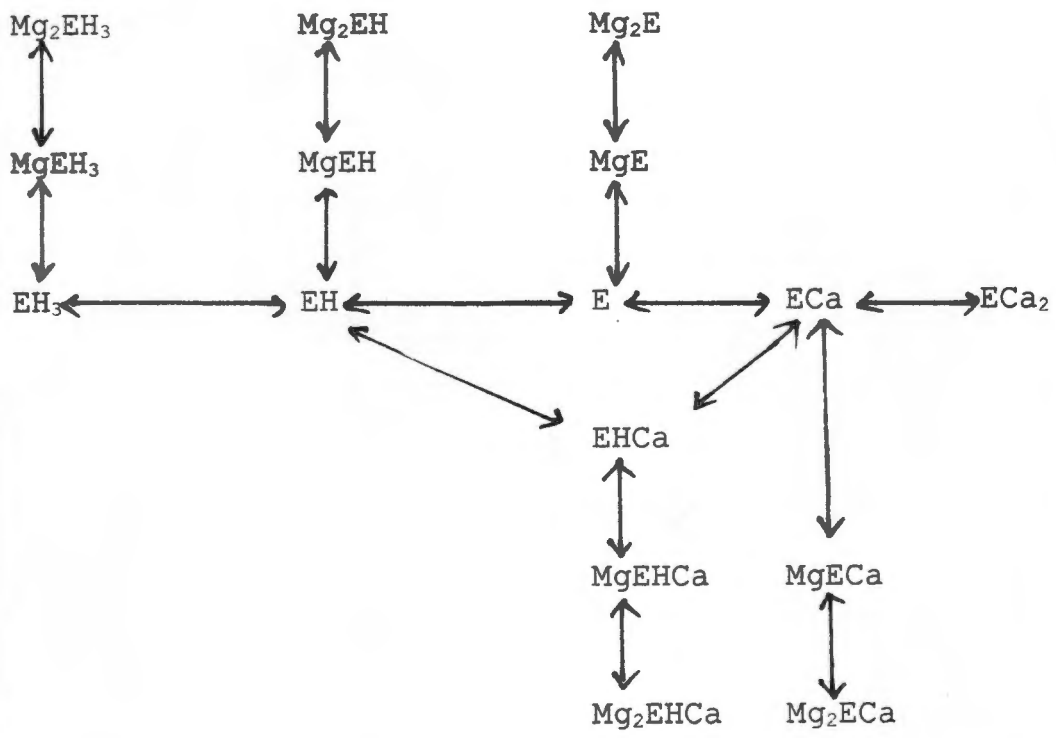

The equilibrium stability product for the two Ca^{2+} binding of log K_1K_2 = 13.2 decreases to 11.9 at pH 6.8, due to competition from protons. At pH less than 7.6, the calcium free enzyme holds two H^+ at the Ca^{2+} sites. Henderson *et al.* (1994) proposed that the pH and Mg^{2+} effect on Ca^{2+} binding is due to the their binding to a 'gating' site at the Ca^{2+} sites, which affects the affinity of the first Ca^{2+} binding site for Ca^{2+} and the rate of Ca^{2+} dissociation (see Fig 7).

Fig 7

Binding of Mg^{2+}, H^+ and Ca^{2+}

(Hendersen *et al.* (1994)

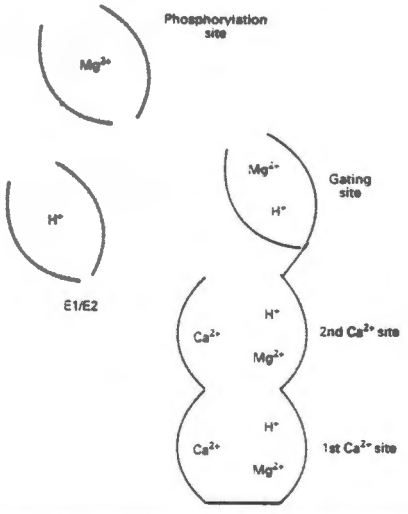

It was found by Jencks (1975, 1980) that both Ca^{2+} must bind before the enzyme cycle can be activated by ATP phosphorylation. Upon phosphorylation of the enzyme, the two Ca^{2+} become occluded, and cannot leave the sites (Dupont, 1982). Vilsen and Andersen (1992) also provided evidence consistent with the existence of two nonequivalent and interdependent Ca^{2+} occlusion sites. CrATP was used as a substrate, that stabilizes a form of the enzyme containing both Ca^{2+} ions in an occluded state, without enzyme phosphorylation, but perhaps mimicking the E_1P state. The dissociation rate constant for the first, superficial Ca^{2+} and inner Ca^{2+} was 0.99 h^{-1} and 0.25 h^{-1}, respectively. When the first site was still occupied by Ca^{2+}, the second, inner Ca^{2+} dissociated with a rate constant of 0.13 h^{-1}.

Inesi (1987) provided evidence that the first Ca^{2+} bound on the cytoplasmic side is released first to the lumen (Fig 8). It required setting up a pre-built order of $^{45}Ca^{2+}$

or $^{40}Ca^{2+}$ in the unphosphorylated ATPase and then adding ATP.

Figure 8

Sequential Ca^{2+} binding and release (Inesi, 1987)

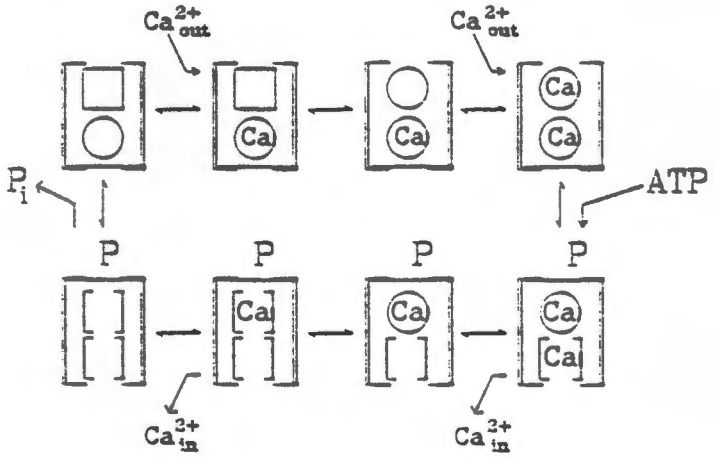

However, Hanel and Jencks (1991) and Orlowski and Champeil (1991) could not distinguised between dissociation of the two Ca^{2+} into the lumen. Later work indicated that under select conditions (5 °C, pH 8.0, 300 mM KCl) there is sequential dissociation to the lumen, since $^{40}Ca^{2+}$ slowed the release of the inner Ca^{2+} (Forge *et al.*, 1993). Canet *et al.* (1996) have further provided evidence that the Ca^{2+} are randomized during translocation, i.e. a prebuilt Ca^{2+} order is not maintained during membrane translocation of the two Ca^{2+} ions. This could indicate more than two sets of Ca^{2+} binding sites, which would be compatable with the results of Mészàros and Bak (1992, 1993), Jencks *et al.* (1993) and Myung and Jencks (1994). They proposed there are four Ca^{2+} binding sites on the Ca^{2+}ATPase in a single channel (Fig 9A). Martonosi (1995) proposed a model accounting for four possible sites with two channels. (Fig 9B).

Figure 9

Randomization of transported Ca^{2+} (Canet *et al.*, 1996)

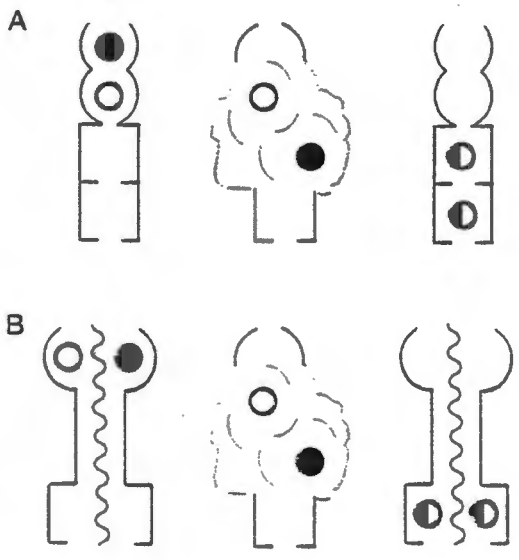

The enzyme undergoes a transition to the E_2 conformation, in which case the Ca^{2+} binding sites face the lumen and Ca^{2+} affinity is greatly reduced. Both Ca^{2+} must dissociate to the lumen before phosphoenzyme hydrolysis ($E_2P \rightarrow E_2$) can take place (Khananshvili and Jencks, 1988). De Meis (1981) postulated in the original catalytic cycle, that all E_2 states (phosphorylated or unphosphoryated) were able to bind Ca^{2+} at two low affinity sites. However, Petithory and Jencks (1988) provided evidence that the unphosphorylated E_2 state cannot bind Ca^{2+}. Forge *et al.*, (1995) have found that the Ca^{2+} transport sites of the nonphosphorylated and phosphorylated enzymes show a close similarity, although the orientation, affinities and dissociation are different, in agreement with de Meis (1981). Khan *et al.* (1997) support de Meis (1981), as they have found that Ca^{2+} (on the luminal side) can bind

to both E_2 (unphosphorylated) or E_2P (phosphorylated) intermediates with similar binding affinities.

1.7.3 Chemical properties of Ca^{2+}

Calcium and magnesium belong to the IIA(2) group of elements and are alkaline earth metal ions. They lack easily excitable unshared valence electrons, and are classified as 'hard' (Cotton and Wilkinson, 1972). They therefore tend to bind to 'hard' ligands, especially those containing oxygen atoms, and less readily to nitrogen atoms and very rarely to 'soft' sulfur atoms. Ca^{2+} binds ligands with intermediate strength and this makes it useful in control of conformational changes and cell activities (Martin, 1984). Ca^{2+} can bind to a large number of centres simulataneously. This ability is not shared by Mg^{2+} or Zn^{2+}. These factors give Ca^{2+} a selective binding chemistry. Zinc belongs to the IIB(12) group of elements. These elements form no compound in which the *d* shell is other than full, so they are regarded as non-transition elements. The metals in this group are 'softer' than the the transition metals. Zn^{2+} is less electropositive than Ca^{2+} and Mg^{2+}. Mg^{2+}, Ca^{2+} and Zn^{2+} have different sizes, with ionic radii and charge-to-radius ratios of 0.65, 0.99 and 0.69 and 3.1, 2.0 and 2.9 respectively (Cotton and Wilkinson, 1972). The coordination number is the number of liganding atoms that can pack around the cation in the first coordination sphere. The average coordination number of Mg^{2+} and Ca^{2+} ions are 6.0 and 7.3 respectively (Cotton and Wilkinson). Zn^{2+} bind to ligands with coordination numbers 4,5 and 6, with 5 especially common. The metal-oxygen distance for Mg^{2+} and Ca^{2+} are 1.95 and 2.23+ respectively (Cotton and Wilkinson).

Ca^{2+} and Mg^{2+} bind to proteins mainly by carboxylate groups, such as aspartate and glutamate. Zn^{2+}, which is a

'softer' ion compared with Mg^{2+} and Ca^{2+}, binds to cysteine and histidine via the 'softer' sulphur and nitrogen atoms respectively, and also to aspartate and glutamate via the 'harder' oxygen. Mg^{2+} and Ca^{2+} bind only in the plane of the carboxyl group. Ca^{2+} shares the two oxygen atoms of the carboxylic group equally, a characteristic that is not shared with Mg^{2+}. Mg^{2+} binding to ligands is invariably octahedral and more rigid. Ca^{2+} display more variable coordination and flexibility in the geometry of ligand binding, compared to Mg^{2+}. This geometry is is controlled by the first sphere, second coordination sphere and solvation of Ca^{2+} in solution. Ca^{2+} and Mg^{2+} kinetics differ in two aspects. Ca^{2+} exchanges water at close to the collisional diffusion limit of 10^{10} s^{-1} and its reaction on-rates are often diffusion-limited, whereas its off-rates are limited by binding strength. Mg^{2+} and Zn^{2+} exchange water with rate constants close to 10^{6} and 10^{7} s^{-1}, respectively (Cotton and Wilkinson). Proteins bind cations with strengths that depend on the size and charge of the cation. The higher the charge, the stronger it binds. The size is also important and the protein often provide a pocket of the correct size to bind the cation and it can therefore distinguish between different cations.

1.8 ATP analogues

1.8.1 Structure, stereochemistry and charateristics of ATP analogues

In order to elucidate the roles of the adenine, ribose and triphosphate moieties in the catalytic and regulatory function of ATP in the Ca^{2+}ATPase cycle and other ATP-utilizing enzymes, many ATP analogues have been synthesized (Ikehora *et al.*, 1961; Miller and Westheimer, 1966; Lecoeq, 1968). The ribose moiety has been implicated in hydrogen binding for many nucleotide binding enzymes (Banks *et al.*, 1979; Branden *et al.*,

1975; Moras *et al.*, 1975; Holbrook *et al.*, 1975). In the case of the Ca^{2+}ATPase, Anderson and Murphy (1983) have found that neither the catalytic (high affinity) nor the regulatory (low affinity) site tolerates changes in the hydroxyl substituent at the 3'OH of the ribose ring of ATP, whereas steady state rates associated with substrate binding at both sites are less affected by changes at the 2'OH position. Weaker substrate binding in the absence of a ribose hydroxyl, was also observed. They also suggested that the hydroxyls are important for substrate alignment, i.e. optimal positioning of the γ-phosphoryl group with respect to Asp351. Clore *et al.* (1982) have shown from NMR measurements, that binding of ATP to either the catalytic or regulatory site(s), produces conformational changes of the ribose moiety. The free nucleotide's predominantly 2'endo conformation of the S type is changed to a 3'endo conformation of the N type and the gauche-gauche conformation about the C4' and C5' bond is changed to gauche-trans or trans-gauche.

Photoaffinity analogues have been used to identify and characterize nucleotide binding sites (Bayley and Knowles, 1977; Chowdry and Westheimer, 1979; Guillory, 1979). The 8-azidopurine derivatives (Haley, 1974, 1975) and 3'-ribose-coupled arylazides (Jeng and Guillory, 1975; Lunardi *et al.*, 1977), have been mostly used. Substitution at the purine C-8 position represents a small structural change, but probably shifts the nucleotide's configuration about the N-glycosidic linkage from *anti* to *syn* (Tavale and Sobell, 1970; Ikehora *et al.*, 1972; Sarma *et al.*, 1974). The TNP-nucleotides are analogues of ATP, which have an environmentally sensitive chromophore or fluorophore group to provide information about the microenvironment within the ATP binding site (Murphy and Morales, 1970; Onodera and Yogi, 1971). The

visible absorption characteristics of the TNP-nucleotides are that of a typical Meissenheimer compound linking 2'OH and 3'OH groups and trinitrocyclohexyldienylidine with absorption maxima at 259 nm, 408 nm and 470 nm at neutral pH. (Foster *et al.*, 1965; Murto, 1965, Hiratsuka and Uchida, 1973). The Meissenheimer complex of the TNP-ribose linkage exhibits a pK_a of 5.1 (Hiratsuka, 1975). Ah-Kow *et al.*, 1980 had found that at acidic pH the opening of the dioxolane ring of the TNP-nucleotide occurred at the 2'-oxygen to yield a 3'-*O*-(2,4,6-trinitrophenyl) derivative as the only product.

Scheme 5

Structure of TNP-nucleotides at neutral or acidic pH values

Neutral or alkaline pH

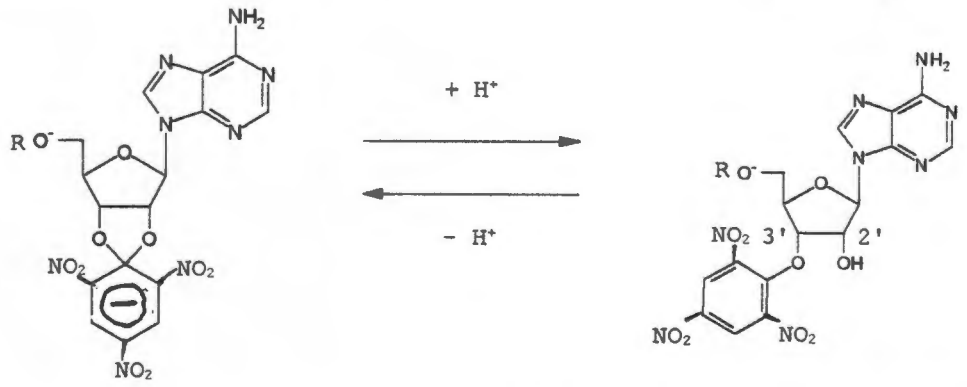

3'-O-(2,4,6-trinitrophenyl) derivative

ATP binds to Ca^{2+}ATPase with binding affinity K_d = 2 μM (Meissner, 1973). TNP-AMP, -ADP and -ATP bind tighter to the enzyme with binding affinities 7.62 nM (Suzuki *et al.*, 1990), 50-150 nM (Dupont *et al.*, 1982) and 200 nM (Dupont *et al.*, 1982), respectively. They probably exhibit an *anti* conformation about the glycosidic bond.

Their 8-azido derivatives were synthesized by Seebregts and McIntosh (1989) and probably exhibit a *syn* conformation (Tavale and Sobell, 1970; Ikehora *et al.*, 1972; Sarma *et al.*, 1974; McIntosh and Woolley, 1994) and have absorbance maxima at 281 nm (8-N_3-moiety), 408 and 468 nm (both TNP-moiety) (Seebregts and McIntosh, 1989). TNP-8N_3-AMP, -ADP and -ATP bind tighter than ATP to Ca^{2+}ATPase, but less tightly than the nonazido nucleotides, with binding affinity K_d = 0.04-0.4 μM (Seebregts and McIntosh, 1989). Irradiation at alkaline pH results in specific covalent incorporation of the 8-azido TNP-nucleotides onto Lys492. In the same concentration range, they all undergo a large increase in fluorescence (so-called superfluorescence) (Watanabe and Inesi, 1982; Nakamoto and Inesi, 1984; Bishop *et al.*, 1984, 1986; Davidson and Berman, 1987) during enzyme turnover in the presence of ATP and Ca^2, or phosphorylation from P_i in a Ca^2-depleted medium which has been ascribed to binding to the E_2P catalytic intermediate (Davidson and Berman, 1987; Wakabayashi *et al.*, 1986).

1.8.2 Synthesis of nonhydrolyzable ATP analogues

ATP plays a major important role in biological systems. Yet our understanding of its interactions with enzymes as both a substrate and as a regulator is incomplete and unsatisfactory. Analogues of ATP with modified triphosphate chains, have been synthesized to better understand these interactions. To analyze the effect of a nucleotide on the phosphoenzyme hydrolysis reaction, the use of nonhydrolysable ATP analogues is more convenient as it avoids perturbing the phosphoenzyme hydrolysis ($E_2P \rightarrow E_2$) reaction by the enzyme cycle because the phosphorylation reaction ($E_1Ca_2 \rightarrow E_1Ca_2P$) is blocked. AMP-PCP is nonhydrolysable, because of the inert stability of the P-C-P bond, that has replaced the terminal bridge

oxygen of the triphosphate chain of ATP. Thus, AMP-PCP offered the opportunity to study the interaction of an ATP-like molecule with various enzymes without the possibility of cleavage between the β,γ-phosphates. The synthesis of the TNP analogue of AMP-PCP will also provide insight into the role of the TNP and adenine moieties in the binding of the nucleotide. TNP-AMP-PCP was synthesized by the general method involving initial preparation of P^1-nucleoside-5′ P^2-diphenyl pyrophoshate from AMP and diphenyl chlorophosphate (attacking electrophile), followed by displacement of the diphenyl phosphate group (leaving group) by α,β-methylene diphosphonic acid (the attacking nucleophile) to from AMP-PCP (Michelson, 1964). The TNP-moiety was added to the ribose ring of AMP-PCP by reacting with DTNB and TNBS (see Scheme 6).

1.9 Ca^{2+} chelators

Chelating agents or chelators are often used as specific metal ion buffers in studies of metal ion-selective biological systems to maintain defined free concentrations of a specific ion in the micromolar or even nanomolar range.

Three of the chelators used in our studies will be discussed, i.e. EDTA, EGTA and BAPTA. EGTA and EDTA are regularly used as Ca^{2+} chelating agents, which have apparent calcium equilibrium constants for dissociation (K_{app}) at pH 6.8 of 9.73×10^{-7} and 9.87×10^{-8}, respectively (calculated with Fabiato programme). EGTA is the preferred buffer when the system also contains Mg^{2+}, since it exhibits a higher Ca^{2+}/Mg^{2+} selectivity than EDTA. The effectiveness of the Ca^{2+} chelators depends upon the relative rates of (a) Ca^{2+} transport and (b) Ca^{2+} uptake (or release) by the chelator. At pH 6.8, the predominant

EGTA species is H_2EGTA^{2-} . The overall complexation reaction of Ca^{2+} with a chelator can be written as:

$$Ca^{2+} + \text{Chelator} \underset{k_{off}}{\overset{k_{on}}{\leftrightarrow}} Ca^{2+}\text{Chelator} + nH^{+}$$

where k_{on} and k_{off} are rate constants.

Scheme 7

Structures of EDTA, EGTA and BAPTA

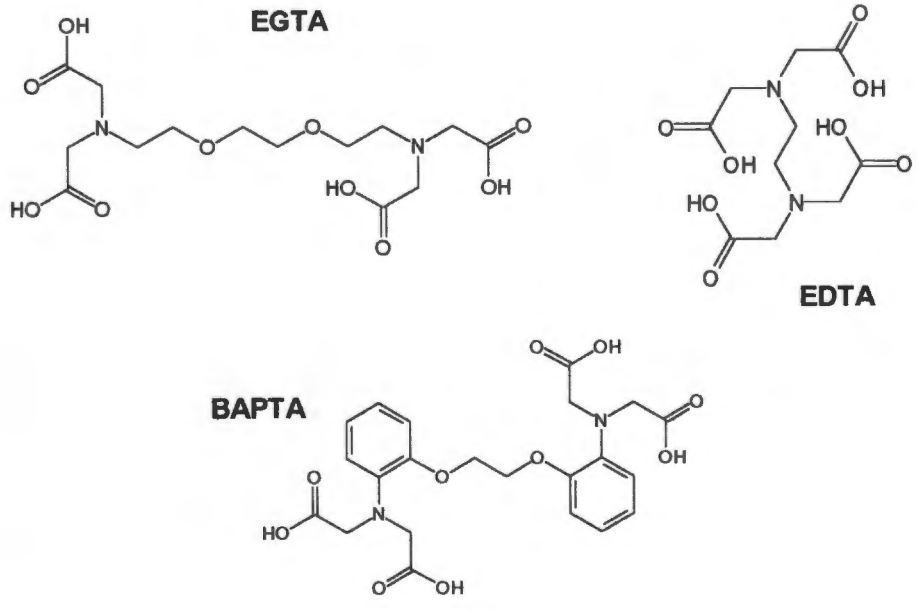

Smith *et al.*, 1977 have found that the values of the on and off rate constants for EGTA are $1.5X10^{6}$ $M^{-1}s^{-1}$ and about 0.3 s^{-1},respectively at pH 7.0 and 25°C. The Ca^{2+}/Mg^{2+} discrimination of EGTA presumably stems from a binding cavity, which has the right size for Ca^{2+} (ionic

radius, 0.95+), but which cannot constrict further to envelop the much smaller Mg^{2+} (ionic radius, 0.60) because the carboxyls at each end of the chain start butting into each other (Cotton and Wilkenson, 1972; Tsien, 1980). The nitrogens bind protons with pK_a of 8.96 and 9.58 (Martell and Smith, 1974), which makes the Ca^{2+} buffering level of EGTA strongly dependent on pH variations near 7.0. The positively charged protonated nitrogens greatly slow down the uptake and release of Ca^{2+}, as Hellam and Podolsky (1969) have found. The apparent forward and backward rate constants for the reaction of Ca^{2+} with EGTA, are $10^{6.3}$ $M^{-1}s^{-1}$ and $0.4s^{-1}$, respectively.

Scheme 8

Structures of DTPA, NTA and HEDTA

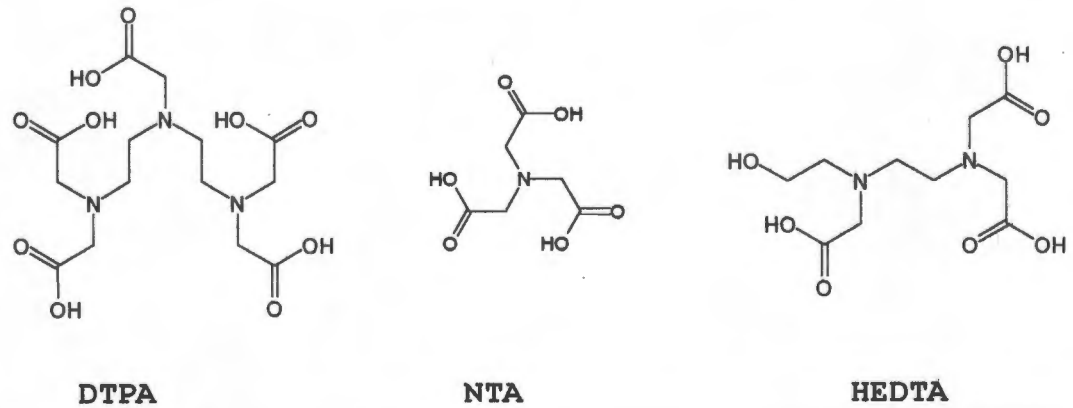

DTPA **NTA** **HEDTA**

At physiological pH, EGTA binds Ca^{2+} 2 to 3 orders magnitude more slowly than ligands without blocking protons. It therefore takes EGTA several seconds to buffer Ca^{2+} transiently. BAPTA is one of the newer chelators, which also has a large binding cavity, but it binds Ca^{2+} at a much faster rate (10^{8} $M^{-1}s^{-1}$) than EGTA (Tsien, 1980). In BAPTA, benzene rings have replaced the methylene groups found in EGTA connecting nitrogen to oxygen. The nitrogen pK_as are lowered from 8 or 9 to 5 or

6. Ca^{2+} chelation by BAPTA is thus pH insensitive in the range 7 to 10 (Tsien, 1980). It has K_{app} values for Ca^{2+} and Mg^{2+} of $1.07x10^{-7}$ and $1.70x10^{-2}$, respectively (calculated with Fabiato programme). The Ca^{2+}/Mg^{2+} ratios for EGTA, BAPTA and EDTA are $5.3x10^{4}$, $1.6x10^{5}$ and $1.0x10^{2}$, respectively (Calculated with Fabiato programme).

2. EXPERIMENTAL PROCEDURES

2.1 Materials:

The sources of materials were as follows: deionized water was used in all the experiments; amylase, Boehringer Mannheim; Fluo-3 (pentammonium salt), Molecular Probes, Inc.(Eugene, OR); standard atomic absorption Zn^{2+} solution, SMM Chemicals; trichloro acetic acid, Analar; zinc acetate and $LaCl_3$, Hopkin and Williams. $CaCl_2$ stock solution solution was prepared from Analar $CaCO_3$. $CdSO_4$, $FeSO_4$ and $CuSO_4$, from Analagar. Buffers Tris, MOPS, EPPS, MES and NH_4CO_3H, sodium oxalate, AMP, tri-*n*-octylamine, α,β-methylene diphosphonic acid, 5,5'-dithio-bis(2-nitrobenzoic acid), imidazole, $MgCl_2$, ATP, chelators NTA, EGTA, EDTA, BAPTA, HEDTA and DTPA, from Sigma; 2,4,6-trinitrobenzenesulfonic acid and triethylamine, Fluka; [^{45}Ca]$CaCl_2$, Amersham; glycerol, dimethylformamide, acetonitrile, from Merck; diphenyl chlorophosphate, Aldrich; tri-*n*-butylamine, BDH Chemicals; methanol, Burdick and Jackson; pyridine, Analgar. TNP-8N_3-ATP, -ADP and -AMP were used from stock, synthesized originally by the method of Seebregts and McIntosh (1989). HPLC purified TNP-ATP, -ADP and -AMP stock was used, synthesized originally by the method of Hiratsuka and Uchida, 1977.

2.2 Preparation of skeletal muscle sarcoplasmic reticulum vesicles:

Sarcoplasmic reticulum vesicles were prepared from the back and hind leg muscle of rabbits by the method of Champeil *et al.* (1985). In brief, the muscle was homogenized in a blender and the vesicles isolated by differential centrifugation. Amylase, 1 µg/ml, was added to the initial homogenate in order to decrease glycogen content and

phosphorylase contamination to less than 5%, as determined by polyacrylamide gel electrophoresis in sodium dodecyl sulphate. Protein concentrations were determined from the optical absorbance at 280 nm in 50 mM sodium phosphate, pH 7.0, 1%(w/v) sodium dodecyl sulphate, using a conversion factor of 1 absorbance unit = 1 mg of protein/ml. The factor was based on the Lowry method (Lowry *et al.*, 1951) using bovine serum albumin as standard. The vesicles were finally resuspended in a medium of 5 mM imidazole, pH 7.4 and 0.3 M sucrose at a concentration of about 35 to 40 mg of protein/ml and stored at -70°C.

***2.3 Photolabeling*:**

TNP-8N_3-nucleotides (5 µM) were irradiated in a medium containing 25 mM NH_4HCO_3/TMAH (pH 8.5), 1 mM $MgCl_2$, 20% (w/v) glycerol, 0.5 mM EGTA and 1.0 mg of SRV protein/ml Ca^{2+}ATPase. Irradiation was performed at room temperature in quartz cuvettes with a Xenon light source of 150 W and with a front facing reflector located behind the cuvette. The light beam was filtered in front and behind by toluene contained in standard (1 cm path length) quartz cuvettes. The irradiation time was 2 min. Under these conditions and in the absence of azido nucleotide, inactivation of ATPase activity was less than 3% (Seebregts and McIntosh, 1989). Following irradiation, 0.1 mM ATP was added to the samples and then passed through a column (0.3 X 1 cm) of Dowex AG1X4 resin (HCO_3^- form), equilibrated with 25 mM NH_4HCO_3, to remove noncovalently attached nucleotide. Loss of protein was approximately 10% and the fluorescence of the samples was compared to controls that has also been passed through the columns. The addition of ATP aided removal of noncovalently bound TNP-8N_3-nucleotides (Seebregts and McIntosh, 1989).

2.4 TNP-nucleotide superfluorescence:

ATP-induced superfluorescence was measured with SRV (0.2 mg of protein/ml) in a medium containing 100 mM EPPS/TMAH (pH 8.0), 5 mM $MgCl_2$, 20% (w/v) glycerol, 50 μM $CaCl_2$. The TNP-nucleotides were added to the cuvette as indicated in the appropriate traces. Phosphorylation of Ca^{2+}ATPase was initiated by the addition of 100 μM ATP. EGTA (0.5 mM) was added to quench the superfluorescence signal.

P_i-induced superfluorescence was measured in the following manner: SRV (final concentration, 1.0 mg of protein/ml) was added to 25 mM NH_4HCO_3/TMAH (pH 8.5), 1 mM $MgCl_2$, 20% (w/v) glycerol, 0.5 mM EGTA (the irradiation medium, see later). The suspension was diluted 5-fold into a medium containing 100 mM MES/TMAH (pH 6.4), 6 mM $MgCl_2$, 0.4 mM EGTA and 20% (w/v) glycerol, prior to fluorescence measurements. The final pH was 6.5. Phosphorylation of Ca^{2+}ATPase was initiated with 10 mM P_i (potassium salt, pH 7.0). $CaCl_2$ (total concentration 0.6 mM) was added to quench the superfluorescence signal. Fluorescence measurements were performed with a SPEX FluoroMax spectrofluorometer with the excitation and emission wavelengths set at 418 and 530 nm, respectively.

2.5 P_i-induced superfluorescence in the reverse direction of catalysis:

2.5.1 Tethered TNP-nucleotides:

The TNP-$8N_3$-nucleotides were tethered to Ca^{2+}ATPase as described previously in the irradiation buffer. Noncovalently bound TNP-$8N_3$-nucleotides were removed as before. Prior to the fluorescence measurements, the sample was diluted 5-fold into a medium containing 100 mM MES/TMAH

(pH 6.4), 6 mM $MgCl_2$, 0.4 mM EGTA and 20% (w/v) glycerol (the fluorescence medium). The final pH was 6.5. Phosphorylation of Ca^{2+}ATPase was initiated upon the addition of 10 mM P_i (potassium salt, pH 7.0). Superfluorescence was quenched by the addition of 1.0 mM total $CaCl_2$ (pH 5.5) or 0.6 mM total $CaCl_2$ (pH 6.0 and 6.5). The reaction was also monitored at pH 5.5 and 6.0. The irradiation mixture was then diluted into the following buffer solutions instead: 100 mM MES/TMAH (pH 5.35) and 100 mM MES/TMAH (pH 5.8) containing 6 mM $MgCl_2$, 0.4 mM EGTA and 20% (w/v) glycerol, respectively.

2.5.2 Free TNP-nucleotides:

The reaction was also monitored with free TNP-nucleotides. The irradiation buffer, containing SRV (1.0 mg of protein/ml), was diluted 5-fold into the appropriate buffer as before. The free TNP-nucleotide was added to the cuvette as indicated in the appropriate traces.

Phosphorylation of Ca^{2+}ATPase was also initiated in the forward direction upon the addition of 1.0 mM total $CaCl_2$ (pH 5.5), using 5 μM free TNP-$8N_3$-ATP, -ADP, TNP-ATP or -ADP as substrate. The irradiation buffer was diluted 5-fold into the appropriate buffer as before and the nucleotides were added to the cuvette as indicated in the figures.

The superfluorescence signal (in the forward direction of catalysis) was enhanced by the presence of 10 mM P_i (potassium salt, pH 7.0), but this time the enzyme was pre-incubated with 1.2 mM total $CaCl_2$ (pH 5.5).

***2.6 Hydrolyis of TNP-nucleotides*:**

SR-catalyzed hydrolysis of the TNP-ATP and -ADP and of TNP-8N_3-ATP, -ADP was performed (in the dark for the latter two) at 20 °C in 25 mM MES/TMAH pH 5.5 containing 0.1 mM $CaCl_2$ or 10 mM EGTA, 5 mM $MgCl_2$, 0.1 mg/ml Ca^{2+}ATPase and 5 µM nucleotide. In some cases thapsigargin (3-fold molar excess over Ca^{2+}ATPase, i.e. 0.3 µM) was included in the medium. At timed intervals, the reaction was stopped by the addition of neat acetonitrile (to 50%), 10 mM EDTA and 20 mM Tris. The acetonitrile was blown off under a N_2 stream and the sample chromatographed on a C_{18} column using a System Gold HPLC system (Beckman Instruments) with the dual-pump Programmable Solvent Module 126 and Scanning Detector Module 167. The nucleotides were monitored at 408 nm and eluted with a linear gradient of 10 mM KP_i / 60% (v/v) acetonitrile, 10 mM KP_i pH 6.0. Quantitation was by peak area.

***2.7 Ca^{2+} transport*:**

Transport supported by TNP-ATP and -ADP, TNP-8N_3-ATP and -ADP was performed (in the dark for the latter two) in the same media and temperature as for the hydrolysis except that $^{45}CaCl_2$ was used. Aliquots were filtered on Millipore 0.45 µm filters at timed intervals and washed with ice-cold assay medium containing 10 mM EGTA, instead of Ca^{2+}. The filters were assayed for radioactivity.

***2.8 TNP-AMP-PCP synthesis*:**

AMP was phosphorylated to the triphosphate form using the anion-exchange procedure of Michelson (1964). 10 µmoles AMP.H_2O (free acid, Sigma grade) was dissolved in 100 µl absolute methanol containing 10 µmoles tri-*n*-octylamine

(3.53 mg). The methanol was removed under a N_2 stream. The residue was dissolved in 50 µl DMF. The reaction was carried out in a 50 µl Hamilton syringe. The solubilized residue was taken up first, followed by 3 µl diphenyl chlorophosphate (15 µmoles) and 4 µl tri-*n*-butylamine (20 µmoles). The contents were expelled and retaken up quickly and the reaction was allowed to continue for 2 h at room temperature. If a precipitate formed, it was dissolved by taking up a small aliquot of tri-*n*-butylamine. The product, P^1-adenosine P^2-diphenyl pyrophosphate, was added slowly to a solution of methylenediphosphonic acid (20 µmoles, 3.52 mg), tri-*n*-butylamine (40 µmoles, 9.4 µl) and 100 µl pyridine. After reacting for 3 h at room temperature, the sample was freeze-dried. The residue was dissolved in 400 µl water and 1.2 ml dry diethyl ether was added. The two phases were separated by freezing the water layer at -20 °C. The purity of the formed product was monitored by TLC using PEI cellulose plates and 1 M LiCl. The AMP-PCP was purified on a Whatmann DE52 (HCO_3^- form, 1.5 cm x 3 cm) anion exchange column using an linear gradient up to 250 mM TEAB buffer. The TEAB buffer was freshly prepared by bubbling CO_2 through a 1 M triethylamine solution until pH 7.4 was reached, and the necessary dilution was made. Fractions (10 ml) were collected and absorbance determined at 259 nm . The fractions that contained the majority of the AMP-PCP were pooled and concentrated. Quantitation of AMP-PCP was by absorbance at 259 nm using the extinction coefficient of ATP (15.9 au/mM/cm). Addition of the TNP-group (trinitrophenyl) to the ribose ring was accomplished in the following manner: 10 µmoles AMP-PCP was dissolved in 250 µl water and added to 250 µl freshly prepared 0.8 M $Na_2CO_3/NaHCO_3$ buffer containing

10 mg (34 µmoles) 2,4,6-trinitrobenzene sulfonic acid. The reaction was continued overnight for 16 h at room temperature. The TNP-AMP-PCP was then purified on a column (4 cm X 0.5 cm) of Whatman DE52 anion exchange resin equilibrated with water. The column was developed with 0.2, 0.5 and 1 M ammonium formate. The desired product eluted with the highest concentration. Quantitation of TNP-AMP-PCP was measured by absorbance at 408 nm using the extinction coeffient of TNP-ATP (26.4 au/mM/cm). The yield was 19%. The purity of the synthesized TNP-AMP-PCP was checked by C_{18} HPLC. (Solvent A: 10 mM KP_i, pH 6.0; Solvent B: 60% (v/v) acetonitrile/10 mM KP_i, pH 6.0)

2.9 Fluorescence measurements relating to the chelator effect on $[Ca^{2+}]_{lim}$ and Ca^{2+} transport activity:

Free $[Ca^{2+}]$ was determined by measuring the fluorescence of Fluo-3, using a SPEX FluoroMax spectrofluorometer. The emission and excitation wavelengths were 535nm and 509nm respectively.

$[Ca^{2+}]_{free}$ was calculated according to Molecular Probes:

$$[Ca^{2+}]_{free} = K_d[(F-F_{min})/(F_{max} - F)]$$ where

K_d = Binding constant of Ca^{2+} to Fluo-3 (450 nM)
F = Fluorescence of the indicator at experimental Ca^{2+} levels
F_{min} = Fluorescence in the absence of Ca^{2+}
F_{max} = Fluorescence of the Ca^{2+}-saturated dye

SRV, (final concentration: 0.25 mg of protein/ml) were diluted in 20 mM Tris/MOPS, pH 6.8, containing 20 nM Fluo-3, 5 mM $MgCl_2$ and 5 mM potassium oxalate (standard buffer). The

appropriate chelator concentration was added and the fluorescence signal measured. The Ca^{2+}ATPase was activated by the addition of ATP (final concentration 2 mM). The F_{max} and F_{min} were determined by the addition of 400 µM $CaCl_2$ and 10 mM EGTA, respectively. $CaCl_2$ (20 µM) aliquots, were added to the mixture as indicated in the appropriate figures.

EGTA effect on Ca^{2+} activation of transport was measured by a Ca^{2+}-infusion method. The experiments were carried out in the standard buffer solution containing 2.5 µM EGTA. The enzyme was activated as before by 2 mM ATP and at time t_1, the infusion of 1 mM $CaCl_2$ at a convenient rate was started, using an ABU 80 Autoburette (Radiometer Copenhagen). Transport is presumed to be equivalent to the infusion rate. The slopes of the plots were extrapolated to time t_0 and the fluorescence intensity was recorded and $[Ca^{2+}]_{free}$ calculated.

2.10 Determination of $[Zn^{2+}]$ in SRV preparations:

SR vesicles were prepared for Zn^{2+} analysis by the modified method of Davies *et al.*, 1968. SRV were diluted 10-fold with metal-free water and added to 1 ml of 10% TCA. The mixture was left for 10 min, with mixing in between, and centrifuged at 30 000 rpm on Beckman Model TJ-6 centrifuge. The supernatant was used for the zinc analysis. Standard zinc solutions were prepared from an atomic absorption commercial zinc solution (10 000 ppm in 0.1 N percloric acid): 4, 8, 16, 20 and 24 µM. The measurements were performed with a Varian Atomic Absorption Spectrometer AA-10, using a Zn^{2+} hollow cathode lamp. A 10% (w/v) TCA solution was used as blank.

2.11 Influence of [Zn^{2+}] on the Fluo-3 fluorescence signal:

SRV (0.25 mg of protein/ml), were incubated in 20 mM Tris/MOPS, pH 6.8, containing 20 nM Fluo-3, 5 mM $MgCl_2$ and 5 mM potassium oxalate. The Ca^{2+}ATPase was activated by the addition of 2 mM ATP. Aliquots of a zinc acetate solution were added in steps of increasing concentration. The increase in fluorescence after each Zn^{2+} aliquot was recorded and plotted against total Zn^{2+} added. The effect of 1 µM HEDTA on ZnFluo-3 fluorescence was performed under the same reaction conditions.

2.12 Effect of Zn^{2+}, Cd^{2+}, Fe^{2+} and Cu^{2+} on Ca^{2+} transport rate measured with Fluo-3:

SRV (0.25 mg of protein/ml), were incubated in 20 mM Tris/MOPS, pH 6.8, containing 20 nM Fluo-3, 5 mM $MgCl_2$ and 5 mM potassium oxalate. The Ca^{2+}ATPase was activated as before by 2 mM ATP. An aliquot of 20 µM Ca^{2+} was added before and after the addition of 1.0 µM HEDTA. 1.0 µM Zn^{2+}, 0.1 µM Cd^{2+}, 0.8 µM Fe^{2+} or 0.8 µM Cu^{2+} was then added as indicated in the appropriate traces. After the addition of the heavy metals, an aliquot of 20 µM Ca was added again.

3. RESULTS

3.1 TNP-nucleotides

ATP accelerates most steps of the Ca^{3+}ATPase transport cycle, including $E_1P \rightarrow E_2P$ and Ca^{2+} release to the lumen (Champeil and Guillain, 1986; Wakabayashi and Shigekawa, 1986), E_2P hydrolysis, P_i binding (Champeil *et al.*, 1988; Mintz *et al.*, 1990), and the Ca^{2+}-induced conformational change, $E_2 \rightarrow E_1Ca_2$ (Sumida *et al.*, 1978; Takisawa and Tonomura, 1978; Scofano *et al.*, 1979; Inesi *et al.*, 1980; Guillain *et al.*, 1981; Pickart and Jencks, 1984). To analyze the effect of a nucleotide on the enzyme catalytic cycle, the use of nonhydrolysable ATP analogues is more convenient than ATP, as it avoids perturbing the experimental results by the phosphorylation reaction. Previously it has been found that TNP-ATP and TNP-ADP are not substrates or hydrolyzed by Ca^{2+}ATPase (Watanabe and Inesi, 1982; Dupont *et al.*, 1985) and that low concentrations of TNP-ATP and TNP-ADP accelerate ATP hydrolysis (Seebregts and McIntosh, 1989; Dupont *et al.*, 1985) and E_2P hydrolysis (Champeil *et al.*, 1988). Lys-492 has been implicated in binding both catalytic and regulatory ATP by affinity labeling and site-directed mutagenesis (Murphy, 1977; Seebregts and McIntosh, 1989; McIntosh *et al.*, 1992; Yamagata et al., 1993; Stefanova *et al.*, 1993; McIntosh and Woolley, 1994; Yamasaki *et al.*, 1994; McIntosh *et al.*, 1996). Covalent tethering TNP-$8N_3$-ATP to Lys-492 by light activation partially uncouples the pump (McIntosh and Woolley, 1994), but still permits the large fluorescence enhancement of the nucleotide on formation of E_2P (Seebregts and McIntosh, 1989; and see below). There was an indication from prior results (Seebregts and McIntosh, 1989) that the quenching of

tethered TNP-8N_3-AMP superfluorescence by Ca^{2+} is retarded compared with the situation of the untethered TNP-nucleotide.

The following series of experiments were designed to explore the role of free and tethered TNP-nucleotide regulation of steps $E_2P \rightarrow E_2 \rightarrow E_1Ca_2$ and the involvement of Lys-492, through studying the rate of superfluoresence quenching by Ca^{2+}. First, the experimental system and superfluorescence are explained.

3.1.1. The phenomenon of TNP-nucleotide superfluorescence:

3.1.1.1 ATP-induced superfluorescence:

The Ca^{2+}ATPase is phosphorylated by ATP in the presence of Ca^{2+} in the forward direction of catalysis. ATP-induced superfluorescence was initiated at pH 8.6 in the presence of TNP-8N_3-AMP, SRV, Mg^{2+} and Ca^{2+} as indicated in Fig 10. Note that ATP-induced superfluorescence is greater at alkaline pH. Adding TNP-8N_3-AMP to SRV produced in increase of fluorescence intensity, due to its binding to Ca^{2+}ATPase. ATP addition led to a pronounce increase in fluorescence, the so-called superfluorescence. The reason for this is the binding of TNP-8N_3-AMP to the phosphoenzyme (E_2P) formed during enzyme turnover (Watanabe and Inesi, 1982; Nakamoto and Inesi, 1982; Bishop *et al*, 1984, 1987; Davidson and Berman, 1987). The superfluorescence was quenched by EGTA addition, which chelated Ca^{2+} and inhibited subsequent enzyme turnover and E_2P formation. The rate constant for the decay in superfluorescence is possibly a combination of the rate constants of phosphoenzyme hydrolysis ($E_2P \rightarrow E_2$) and the conformational change ($E_2 \rightarrow E_1$).

Figure 10

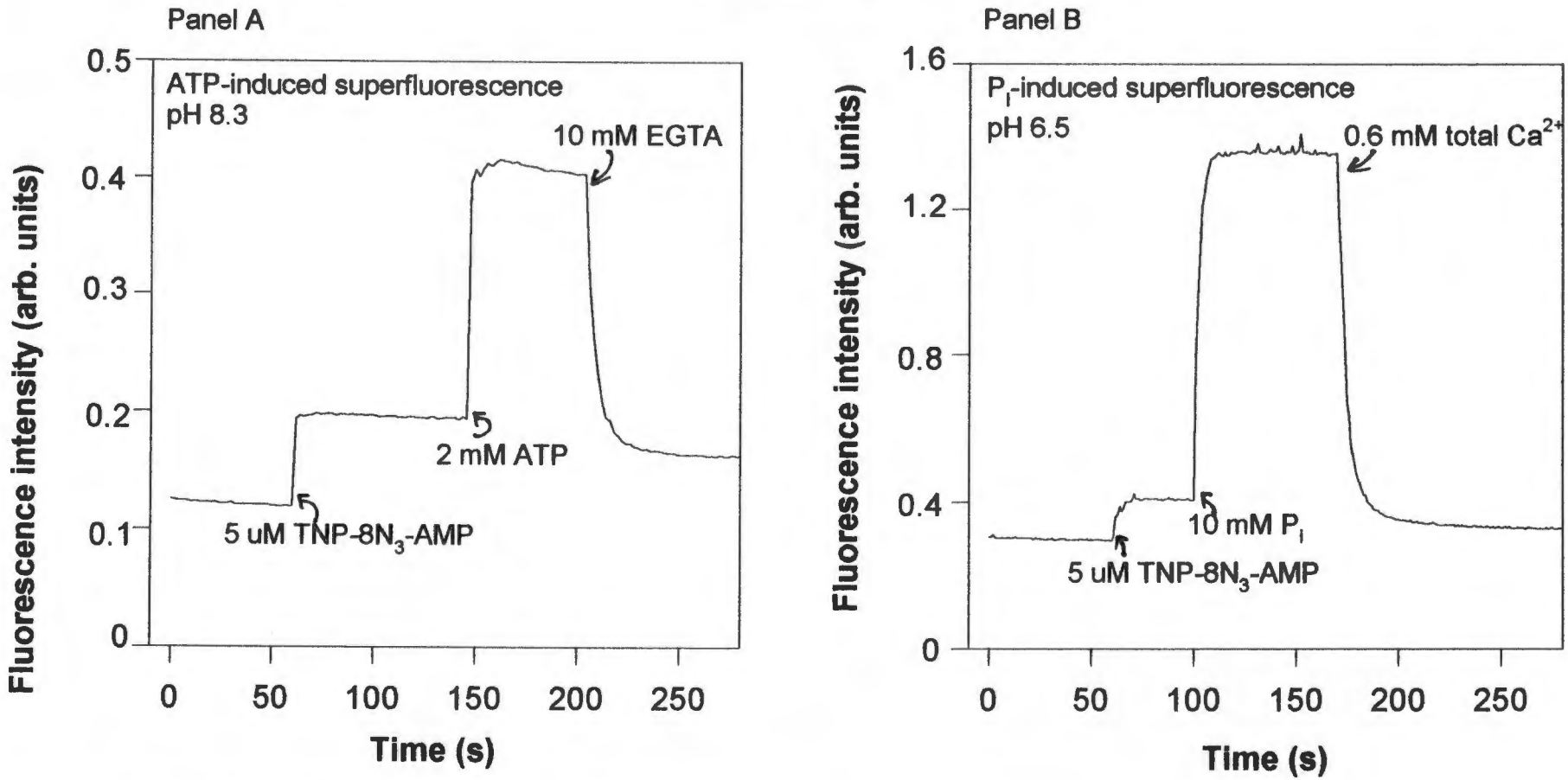

Comparison between ATP- and P_i-induced superfluorescence

Panel A, SRV (0.2 mg of protein/ml) were incubated at 25 °C in 100 mM EPPS/TMAH, pH 8.3, 5 mM $MgCl_2$, 20 % (w/v) glycerol and 50 µM $CaCl_2$.

Panel B, SRV (1.0 mg of protein/ml) were incubated at 25 °C in 25 mM NH_4HCO_3/TMAH, pH 8.5, 1 mM $MgCl_2$, 20 % (w/v) glycerol and 0.5 mM EGTA (the irradiation buffer). The suspension was diluted 5-fold into 100 mM MES/TMAH, pH 6.4, 6 mM $MgCl_2$, 20 % (w/v) glycerol and 0.4 mM EGTA, prior to fluorescence measurements. Final SRV, $MgCl_2$, EGTA concentrations were 0.2 mg of protein/ml, 6.2 mM and 0.5 mM respectively. The final pH was 6.5. TNP-$8N_3$-AMP (5 µM), 2 mM ATP, 10 mM EGTA, 10 mM P_i (potassium salt, pH 7.0) and 0.6 mM total $CaCl_2$ were added to the reaction mixtures as indicated in the panels.

3.1.1.2 P_i-induced superfluorescence:

Phosphorylation of Ca^{2+}ATPase with P_i requires that the enzyme is in a Ca^{2+}-free form (de Meis and Vianna, 1979). This is accomplished by chelation of Ca^{2+} with excess EGTA. Binding of TNP-$8N_3$-AMP to Ca^{2+}ATPase increased the fluorescence (Fig 10). P_i-induced superfluorescence in contrast to ATP-induced superfluorescence is maximal low pH. The latter ensures that the enzyme is predominantly in the E_2 species, which is reactive to P_i. Addition of P_i yields a superfluorescence signal, because of the binding of TNP-$8N_3$-AMP to the same E_2P species as generated in the forward direction of catalysis, as seen above. The superfluorescence was quenched by Ca^{2+}, due to phosphoenzyme hydrolysis ($E_2P \rightarrow E_2$) and the formation of a low fluorescence E_1Ca_2.TNP-$8N_3$-AMP complex. The decay rate of superfluorescence is dependent on the rate constants of three steps $E_2P \leftrightarrow E_2$ and $E_2 \leftrightarrow E_1 \rightarrow E_1Ca_2$.

3.1.2. Rate of Ca^{2+} inhibition of P_i-induced superfluorescence:

3.1.2.1 Free vs. tethered TNP-$8N_3$-AMP:

As mentioned before, results from Seebregts and McIntosh (1989) indicated that quenching of tethered TNP-$8N_3$-AMP superfluorescence by Ca^{2+}, is retarded compared to the situation of free TNP-$8N_3$-AMP. This was verified in Fig 11. The P_i-induced superfluorescence and quench by Ca^{2+} shown above for TNP-$8N_3$-AMP is compared with results obtained with the tethered nucleotide (Panels A and B). In the case of free TNP-$8N_3$-AMP, 90% of the decay of fluorescence was described by a single rate constant $k = 0.25\ s^{-1}$. Addition of P_i to tethered TNP-$8N_3$-AMP SRV produced an increase in fluorescence, although smaller than in the case of free TNP-$8N_3$-AMP, compatible with partial derivatization of

Figure 11

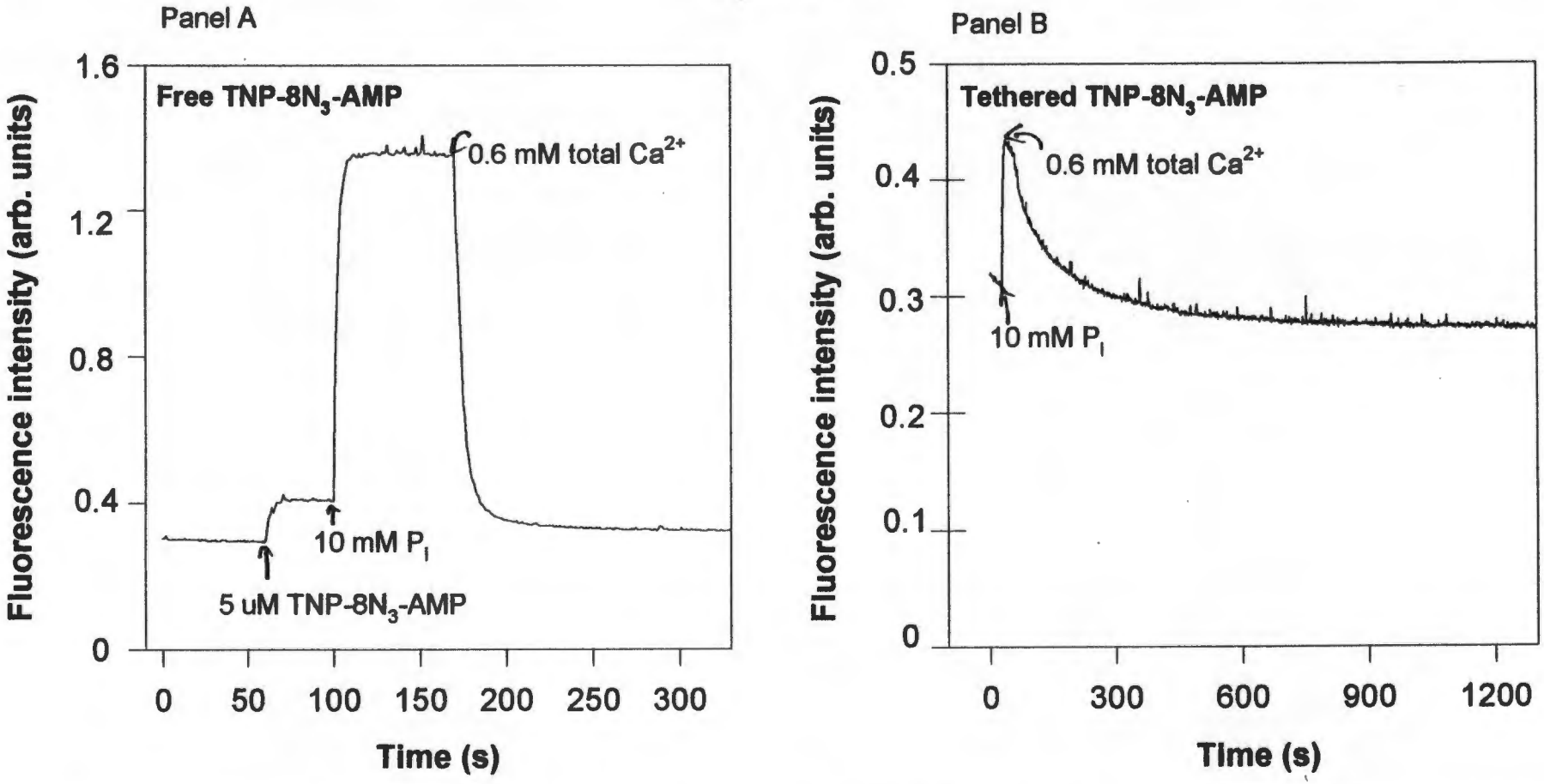

Rate of P_i-induced superfluorescence quench by Ca^{2+}: Free vs tethered TNP-$8N_3$-AMP

Panel A, See legend of Fig 10 (Panel B)

Panel B, SRV were photolabeled with TNP-$8N_3$-AMP (5 μM) the irradiation buffer. Noncovalently attached TNP-$8N_3$-AMP was removed by passing the medium through a column (0.3 x 1 cm) of Dowex AG1X4 resin (HCO_3^- form), equilibrated with 25 mM NH_4HCO_3. The eluate was diluted 5-fold into 100 mM MES/TMAH, pH 6.4, 6 mM $MgCl_2$, 20 % (w/v) glycerol and 0.4 mM EGTA, prior to fluorescence measurements. Final SRV, $MgCl_2$, EGTA concentrations were 0.2 mg of protein/ml, 6.2 mM and 0.5 mM respectively. The final pH was 6.5. P_i, (10 mM, potassium salt, pH 7.0) and 0.6 mM total $CaCl_2$ were added to the reaction mixtures as indicated in the panel.

Lys-492. Addition of Ca^{2+} again led to superfluorescence decay, but the quench kinetics was more complex. The decay in fluorescence was biphasic (k_{fast} = 0.02 s^{-1} and k_{slow} = 0.0035 s^{-1}). Unfortunately there was a high background drift in fluorescence with tethered nucleotides and this is possibly the cause of the slow phase. If the fast phase is taken as representing the true decrease in superfluorescence, it can be concluded that the rate constant for this decrease is at least 10-fold slower compared with the situation with the free nucleotide.

3.1.2.2 Comparison between tethered TNP-8N_3-ATP, -ADP and -AMP:

Ca^{2+} quenching of superfluorescence involves at least three steps, two of which are probably associated with significant reverse reactions, $E_2P \leftrightarrow E_2 \leftrightarrow E_1 \rightarrow E_1Ca_2$. It is known from the literature that ATP accelerates: phosphoenzyme hydrolysis ($E_2P \rightarrow E_2$)(Champeil *et al.*, 1988; Mintz *et al.*, 1990), and the Ca^{2+}-induced conformational change, $E_2 \rightarrow E_1Ca_2$ (Sumida *et al.*, 1978; Takisawa and Tonomura, 1978; Scofano *et al.*, 1979; Inesi *et al.*, 1980; Guillain *et al.*, 1981; Champeil *et al.*, 1983; Pickart and Jencks, 1984; Fernandez-Belda *et al.*, 1984; Wakabayashi *et al.*, 1990). We therefore investigated whether the Ca^{2+} quenching of tethered TNP-8N_3-ATP and/or -ADP may be faster than that with TNP-8N_3-AMP. A comparison of Ca^{2+} quenches with TNP-8N_3-AMP, -ADP and -ATP is shown in Fig 12 and the rate constants listed in Table 1. The software package SigmaPlot 2.01 was used to determine the rate constants by regression analysis.

Figure 12

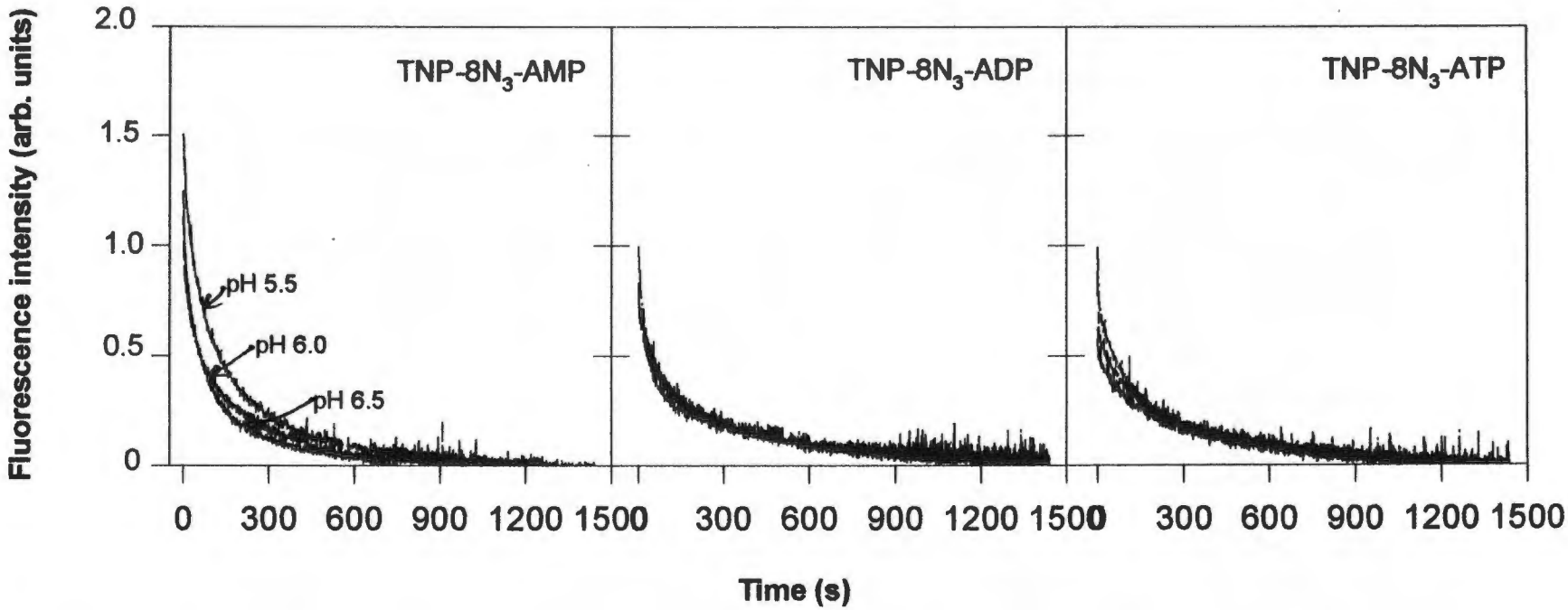

pH dependence of P_i-induced superfluorescence quench rate by Ca^{2+} with tethered TNP-$8N_3$-AMP, -ADP and -ATP
The SRV were photolabeled with TNP-nucleotides as described in the legend of Fig 2. The suspensions were diluted 5-fold into 100 mM MES/TMAH, pH 6.4, 6 mM $MgCl_2$, 20 % (w/v) glycerol and 0.4 mM EGTA, prior to fluorescence measurements at 25 °C. Final pH was 6.5. For final pH 5.5 and 6.0, the suspension was diluted into 100 mM MES/TMAH, pH 5.35 and 5.8, respectively, containing 6 mM $MgCl_2$,
20 % (w/v) glycerol and 0.4 mM EGTA. Superfluorescence was quenched by the addition of 1.0 mM total $CaCl_2$ (pH 5.5) or
0.6 mM total $CaCl_2$ (pH 6.0 and 6.5). The panels display only the time frame covered for the fluorescence to decrease to the baseline value. The solid, dashed and dotted lines refer to pH 5.5, 6.0 and 6.5 respectively.

Table 1

Rate constants of tethered TNP-nucleotides superfluorescence quench rates[a]

Nucleotide	pH	Rate constant (s^{-1})
TNP-8N_3-AMP	5.5	0.018
	6.0	0.020
	6.5	0.020
TNP-8N_3-ADP	6.5	0.025
TNP-8N_3-ATP	6.5	0.023

a: 60 to 80% of of the superfluorescence quench was described by a single rate constant.

As mentioned earlier, there was a high background drift in fluorescence with tethered nucleotides and this is possibly the cause of the slow phase (k_{slow} = 0.0025 to 0.0035 s^{-1}). This slow phase always represented less than half of the signal. The quench was performed at pH 5.5, 6.0 and 6.5 for all three nucleotides. No acceleration of the superfluorescence quench rate constant of the faster phase was oberved for the tethered TNP-8N_3-ATP and -ADP compared to TNP-8N_3-AMP, as can be seen from Table 1. The decay profiles for TNP-8N_3-ATP and -ADP were superimposable (Fig 12) and the rate constants are only given for pH 5.5. Increasing the pH also had no effect on the quench rate constant.

3.1.2.3 Complicated kinetics with free TNP-nucleotides:

3.1.2.3.1 TNP-8N_3-ATP, -ADP and -AMP:

The pH dependence (5.5, 6.0, 6.5) of the Ca^{2+}-induced quench kinetics with TNP-8N_3-ATP, -ADP and -AMP is shown in Fig 4. In these experiments, P_i-induced superfluorescence was initiated in 0.5 mM EGTA and inhibited by the addition of 1.0 mM (pH 5.5) or 0.6 mM total $CaCl_2$ (pH 6.0 and 6.5) (Fig 13). The overall level of superfluorescence was greater at lower pH. The quench kinetics with TNP-8N_3-AMP was monophasic 80-90% of the time course at each pH and increased with increasing pH (k = 0.023, 0.090 and 0.25 s^{-1} at pH 5.5, 6.0 and 6.5 respectively). The kinetics was more complicated with the other two nucleotides. In the case of TNP-8N_3-ADP at pH 5.5, there was an initial rapid quench of superfluorescence and then it increased transiently and finally ceased after 500 s. With TNP-8N_3-ATP the initial drop was barely visible and the final cessation delayed to 600 s. At higher pH the extended plateau of superfluorescence was shorter, and hardly detectable at pH 6.5. One explanation for the complex kinetics observed could be enzyme turnover. It is possible that Ca^{2+} plus a substrate could promote phosphorylation in the forward direction of turnover, yielding E_2P and hence superfluorescence. This could perhaps be expected for TNP-8N_3-ATP, because it has been shown previously that the nucleotide is a substrate and supports Ca^{2+} transport (McIntosh and Woolley, 1994). It was however unexpected for TNP-8N_3-ADP to display such a phenomenon, because neither ADP nor any ADP analogue has yet been identified as a substrate of Ca^{2+}ATPase in the forward direction of catalysis. Other possibilities that we considered were time-dependent reversible aggregation at low pH, ATP contamination of the preparation and TNP-nucleotides,

Figure 13

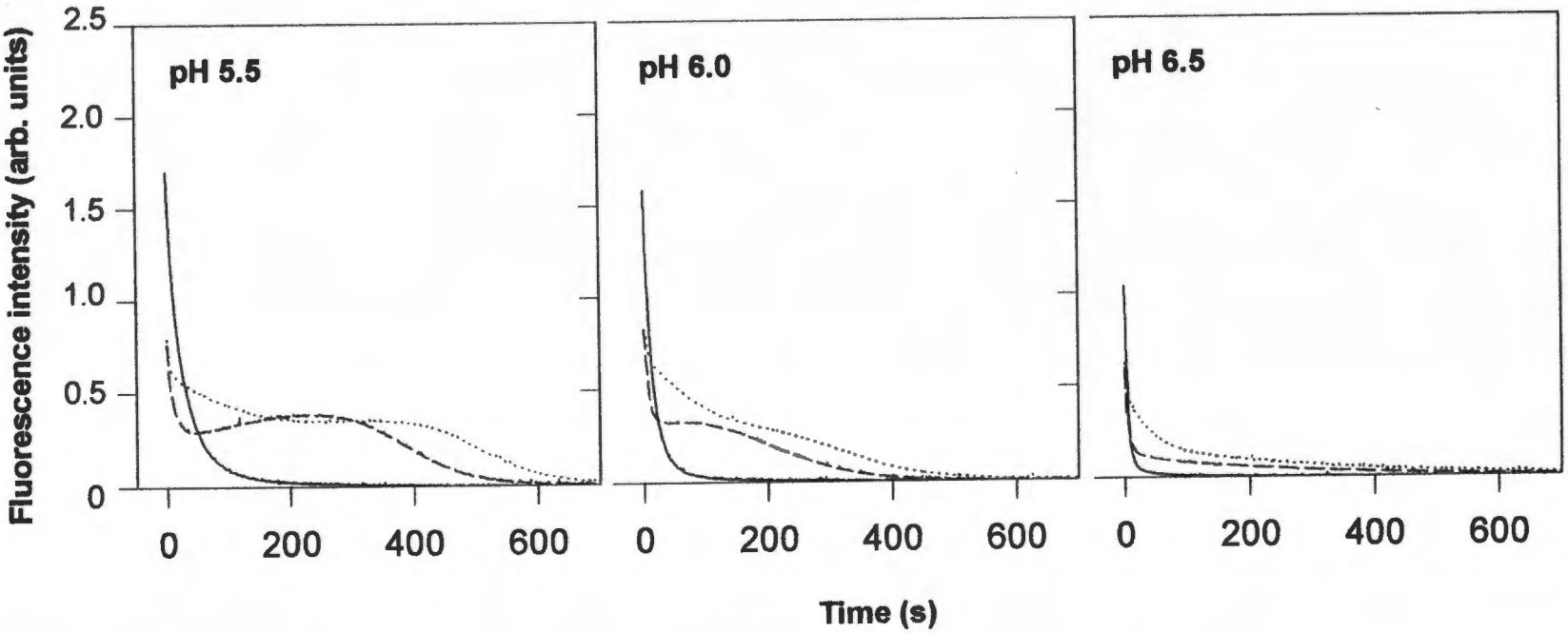

pH dependence of P_i-induced superfluorescence quench rate by Ca^{2+} with free TNP-8N_3-AMP, -ADP and -ATP
The irradiation buffer (25 mM NH_4HCO_3/TMAH, pH 8.5, 1 mM $MgCl_2$, 20 % (w/v) glycerol and 0.5 mM EGTA) was diluted into 100 mM MES/TMAH (pH 6.4) or 100 mM MES/TMAH (pH 5.8) or 100 mM MES/TMAH (pH 5.8) containing 6 mM $MgCl_2$, 20 % (w/v) glycerol and 0.4 mM EGTA to give final pH 6.5, 6.0 and 5.5, respectively. SRV (0.2 mg of protein/ml) were incubated at 25 °C in the diluted buffer. TNP-nucleotide (5 µM) and 10 mM P_i were added to give the superfluorescence and 1.0 mM total $CaCl_2$ (pH 5.5) or 0.6 mM total $CaCl_2$ (pH 6.0 and 6.5) was added to quench the superfluorescence. The panels display only the time frame covered for the fluorescence to decrease to the baseline value. The solid, dashed and dotted lines refer to TNP-8N_3-AMP, -ADP and -ATP, respectively.

contaminating enzymes converting the TNP-nucleotides into ATP or TNP-$8N_3$-ADP into TNP-$8N_3$-ATP. An aggregation phenomenon was ruled out by the absence of similar changes in the baseline fluorescence. The other possibilities will be addressed at a later stage.

3.1.2.3.2 TNP-ATP, -ADP and -AMP:

Whilst TNP-$8N_3$-ATP has been shown to be a substrate of the pump, the nonazido parent TNP-nucleotides are apparently not (Watanabe and Inesi, 1982; Dupont *et al.*, 1985). Therefore the same experiments were performed with the nonazido TNP-nucleotides and the results are shown in Fig 14. Again the overall superfluorescence diminished with increasing pH, and the kinetics for TNP-AMP was monphasic. The quench kinetics for TNP-ADP and TNP-ATP were again complex and very similar to the azido compounds except that the secondary plateau of superfluorescence was shorter.

3.1.2.4 Extremely fast inhibition of P_i-induced superfluorescence by EDTA:

As mentioned previously, Ca^{2+} quenching of superfluorescence involves at least three steps, two of which are probably associated with significant reverse reactions,

$E_2P \leftrightarrow E_2 \leftrightarrow E_1 \rightarrow E_1Ca_2$. In order to acertain whether the kinetics we were observing was related to phosphoenzyme hydrolysis or a subsequent step, EDTA was used to quench the reaction. The results obtained with the TNP-$8N_3$-nucleotides, the nonazido TNP-nucleotides, and with the tethered azido nucleotides are shown in Fig 15. In all cases EDTA quenched the superfluoresence faster than could be monitored manually.

Figure 14

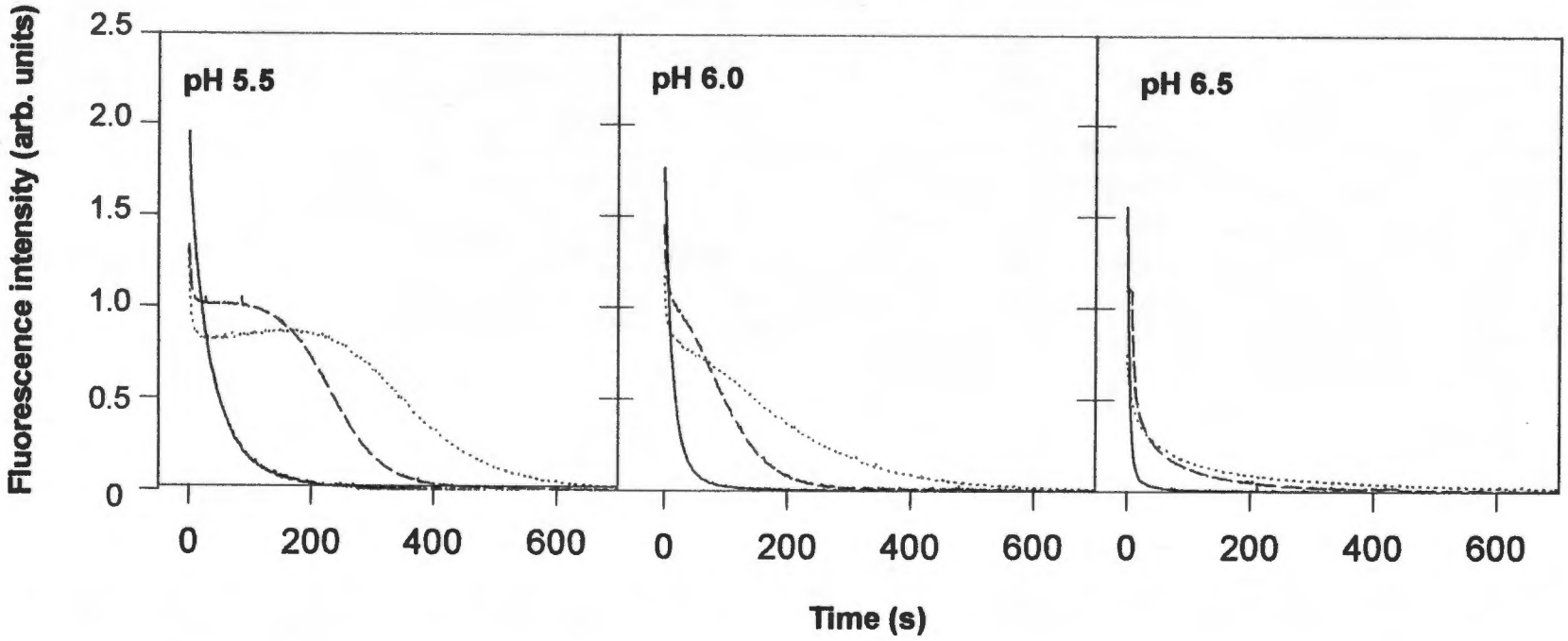

pH dependence of P_i-induced superfluorescence quench rate by Ca^{2+} with TNP-AMP, -ADP and -ATP
See legend of Fig 13 for details. The solid, dashed and dotted lines refer to TNP-AMP, -ADP and -ATP, respectively.

Figure 15

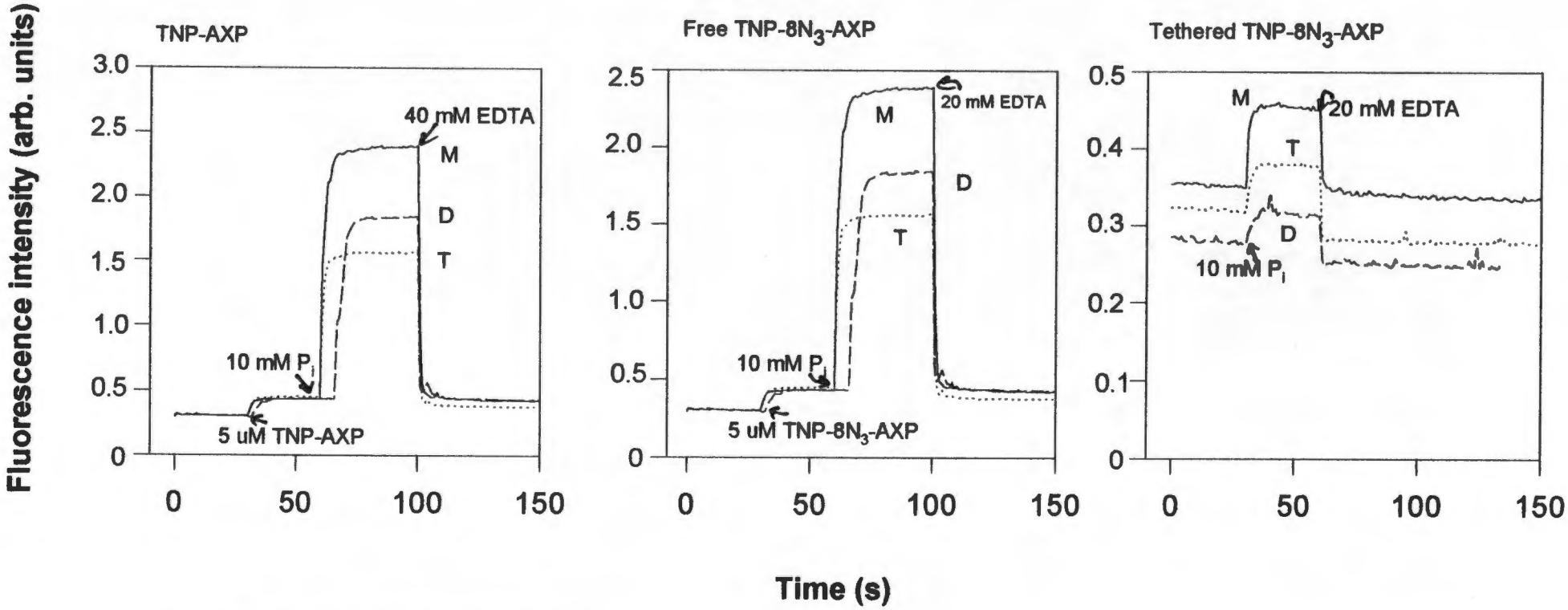

Inhibition of P_i-induced superfluorescence by EDTA
See legend of Fig 13 for details. In this situation, the superfluorescence was quenched with 20 mM EDTA (for free and tethered azido nucleotides) and 40 mM EDTA (for nonazido nucleotides).

It is concluded that the kinetics observed with the Ca^{2+} quench, monitors a reaction subsequent to dephosphorylation. Most likely this is the $E_2 \rightarrow E_1$ conformational change.

3.1.3. Hydrolysis of TNP-nucleotides by SRV:

3.1.3.1 TNP-8N$_3$-ATP and -ADP:

The possible hydrolysis of TNP-nucleotides by Ca^{2+} ATPase was tested directly by measuring the individual TNP-species by HPLC. Representitive HPLC profiles of the time dependence of hydrolysis of TNP-ATP, pH 5.5, are shown in Fig 16. At 0 min ~95% of the nucleotide is present as the triphosphate species. With increasing time this species was converted into the di- and monophosphate nucleotide. Quantitation of the reaction by peak area provided the results shown in Fig 17. In the case of TNP-8N_3-ATP (top frames) and in the presence of Ca^{2+} (first frame) there is a time dependent hydrolysis of the triphosphate, with the concommitant formation of first TNP-8N_3-ADP, reaching a steady state level after 2 min, and then TNP-8N_3-AMP gradually increases in concentration. In the absence of Ca^{2+} (second frame) hydrolysis is only evident after 6 min. There is no formation of TNP-8N_3-AMP during the entire time course. In the presence of thapsigargin (a specific inhibitor of Ca^{2+} ATPase), hydrolysis of TNP-8N_3-ATP is very slow and again there is no hydrolysis of the diphosphate to monophosphate nucleotide. The Ca^{2+}-dependent component of hydrolysis is obtained by subtracting the activity in the presence of EGTA from the total activity and the result is shown in the last frame. There is a burst of TNP-8N_3-ADP formation, followed by a slower increase in TNP-8N_3-AMP.

Figure 16

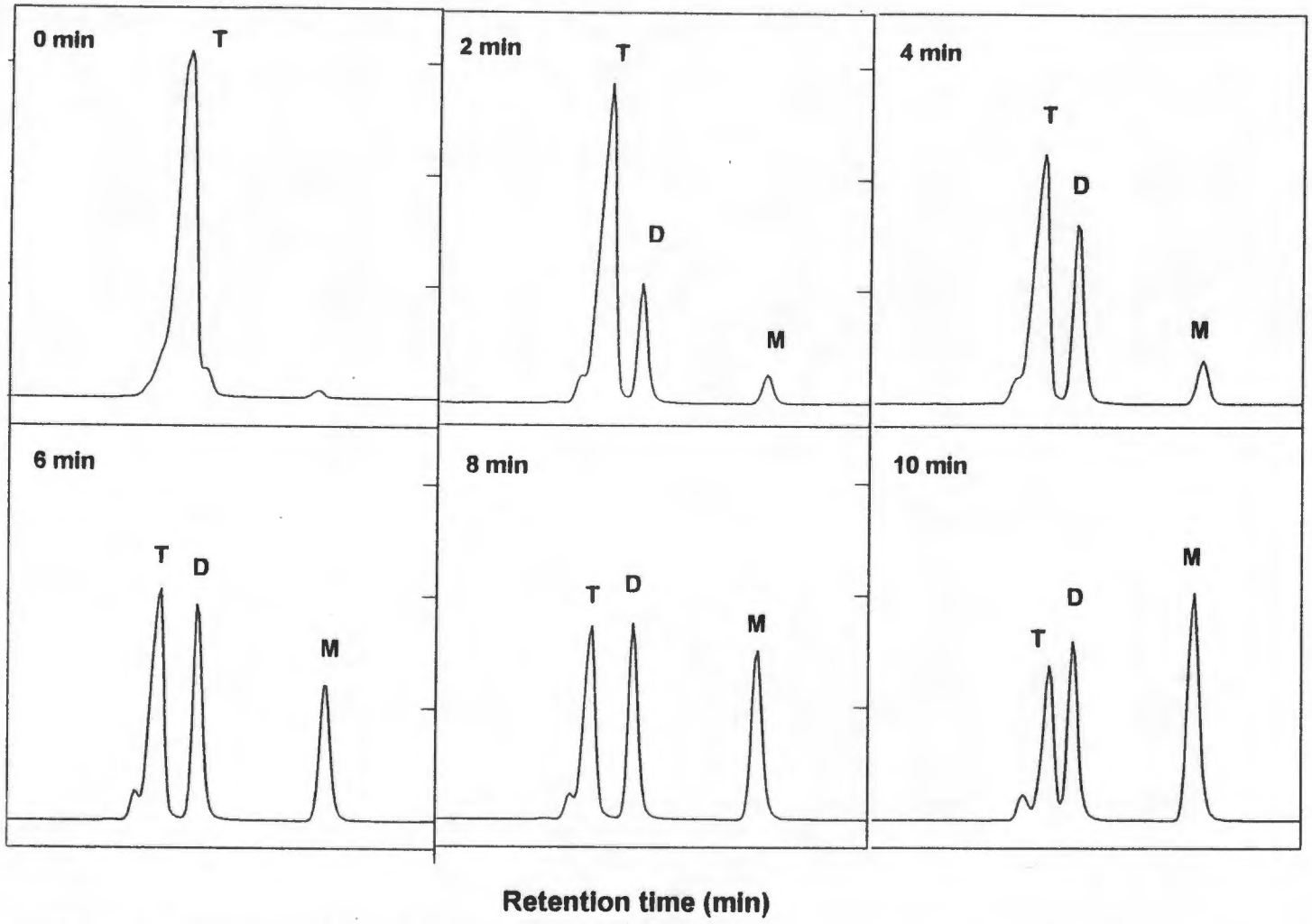

Representitive HPLC profile of TNP-ATP hydrolysis by SRV

SR-catalyzed hydrolysis of 5 μM TNP-ATP was performed at 20 °C in 25 mM MES/TMAH, pH 5.5 containing 0.1 mM $CaCl_2$, 5 mM $MgCl_2$, 0.1 mg of protein/ml. At timed intervals, the reaction was stopped by the addition of acetonitrile (end concentration 50 %), 10 mM EDTA and 20 mM TRIS. The acetonitrile was blown off under a N_2 stream and the sample chromatographed on a C_{18} column. TNP-ATP was monitored at 408 nm and eluted with a linear gradient of 10 mM KP_i/60 % (v/v) acetonitrile, 10 mM KP_i, pH 6.0

Figure 17

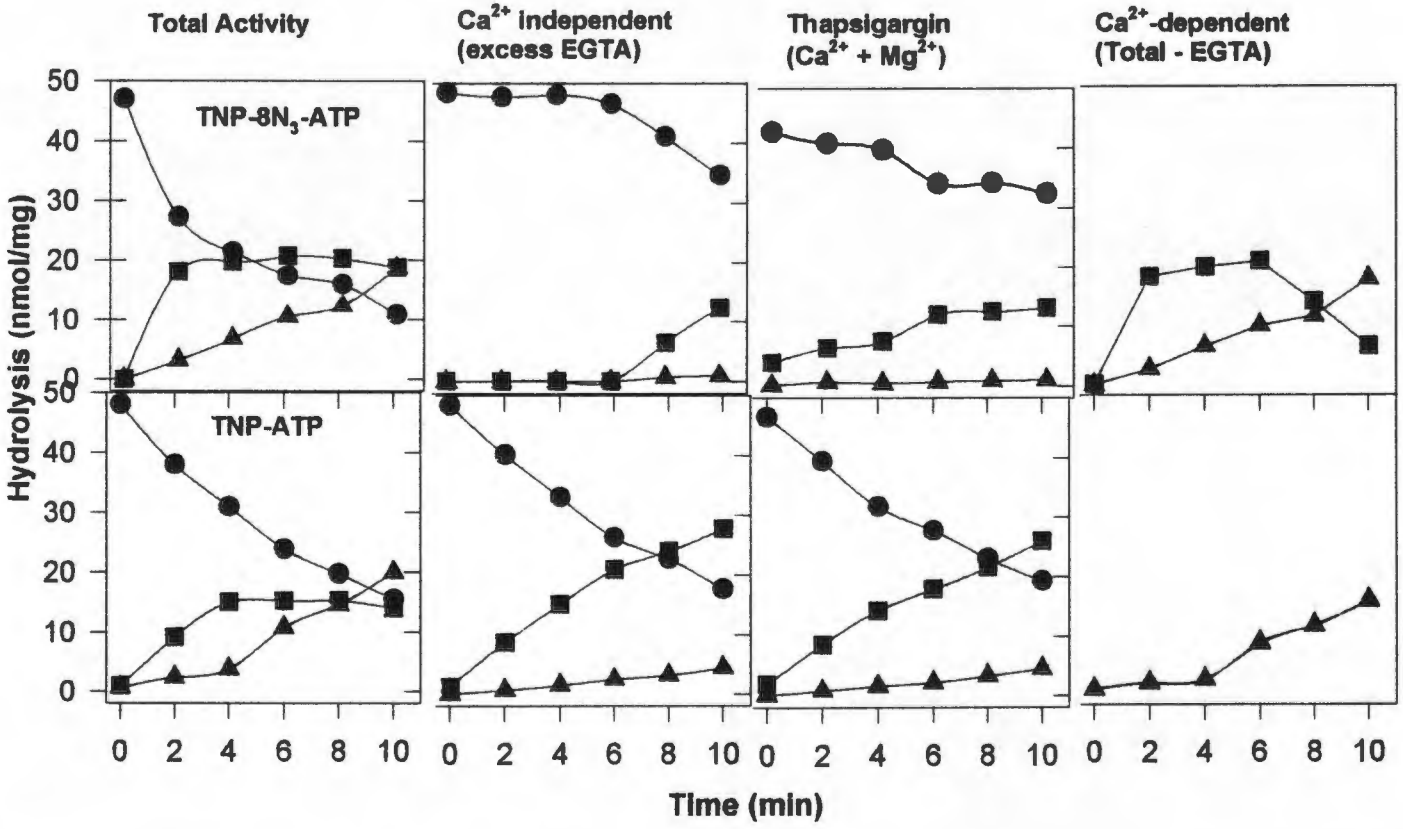

Hydrolysis of TNP-$8N_3$-ATP and TNP-ATP by SRV
The plots were obtained from HPLC profiles of each TNP-nucleotide as described in the legend of Fig 16. Quantitation was by peak area. TNP-nucleotide hydrolysis (5 µM) was performed (in the dark for the azido nucleotide) at 20 °C in 25 mM MES/TMAH, pH 5.5 containing 0.1 mM $CaCl_2$ (under total activity conditions) or 10 mM EGTA (under Ca^{2+}- independent conditions), 5 mM $MgCl_2$, 0.1 mg of protein/ml. Thapsigargin (3-fold molar excess over Ca^{2+}-ATPase, 0.3 µM) was included in the medium to monitor the hydrolysis of TNP-nucleotides by contaminating enzymes in the SRV. The Ca^{2+} dependent hydrolysis was determined by subtracting the Ca^{2+} independent hydrolysis from the total activity.

Figure 18

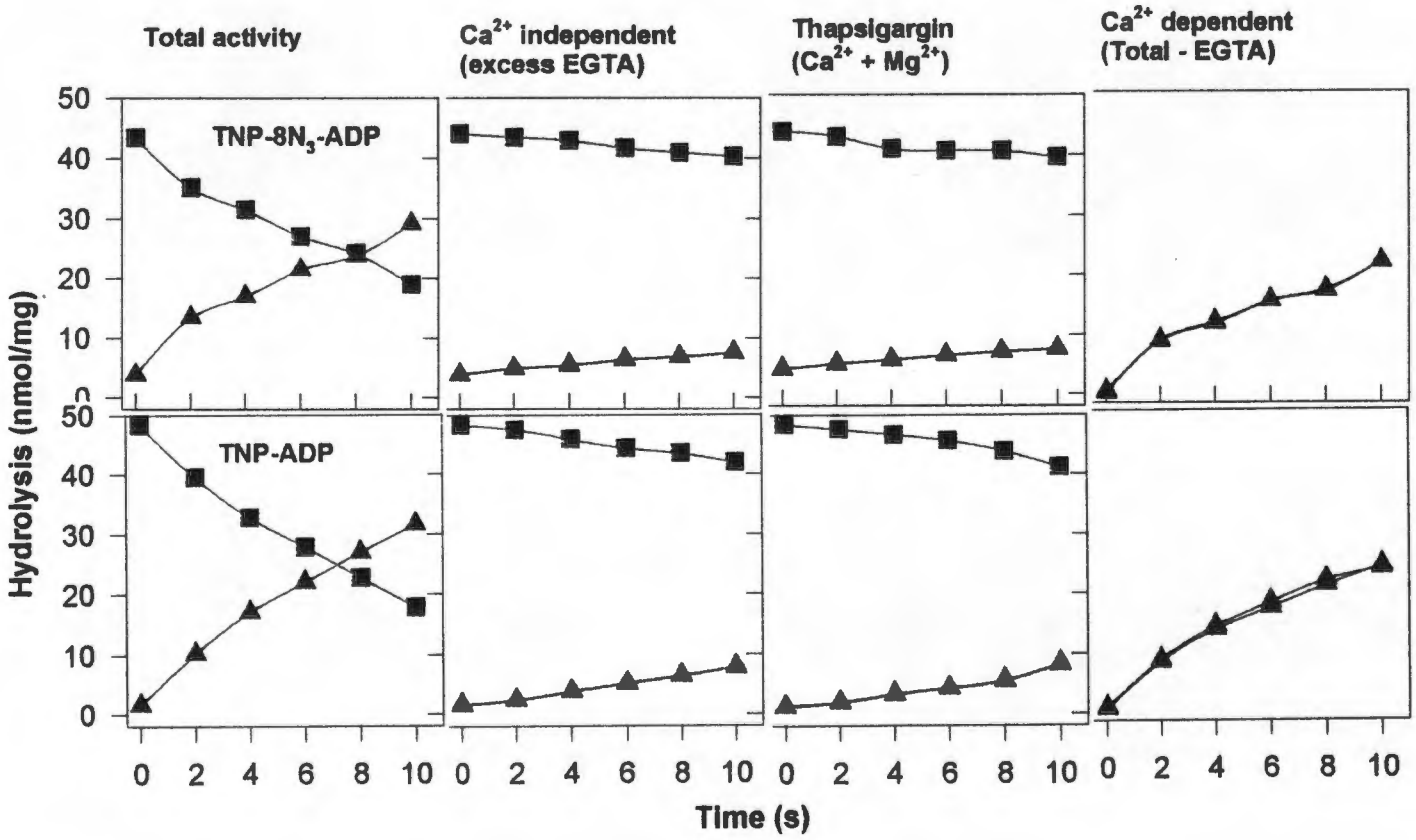

Hydrolysis of TNP-8N$_3$-ADP and TNP-ADP by SRV
See legend of Fig 17 for details.

3.1.3.2 TNP-ATP and -ADP:

In the case of TNP-ATP, hydrolysis in the presence of Ca^{2+} is slower and the slower promotion of TNP-ADP and subsequently TNP-AMP is evident. The situation is not very different in the absence of Ca^{2+} (second frame) except that there is virtually no hydrolysis of TNP-ADP. Similar results were obtained in the presence of thapsigargin. The high hydrolysis rates of TNP-ATP in the absence of Ca^{2+} preclude measurements of a Ca^{2+}-dependent component. However, there was a clear Ca^{2+}-dependent and thapsigargin-inhibitable conversion of TNP-ADP into TNP-AMP.

The results suggest that TNP-$8N_3$-ATP and -ADP as well as TNP-ADP are substrates of Ca^{2+}ATPase. TNP-ATP may be as well but such activity is masked by a high non Ca^{2+}ATPase activity. It should be borne in mind that the conditions used in the above experiments were somewhat different from those performed in Fig 13 and 14 (i.e. glycerol was absent) and the protein concentration was less).

Similar experiments using TNP-$8N_3$-ADP and TNP-ADP are shown in Fig 18. In these cases hydrolysis from the diphospho to monophospho species were the same and almost entirely Ca^{2+}-dependent. The rates of hydrolysis for each nucleotide is listed in Table 2.

3.1.4. $^{45}Ca^{2+}$ transport studies:

The ability of the TNP-nucleotides to support Ca^{2+} transport under the same conditions as used for the hydrolysis experiments is shown in Fig 19. TNP-ATP and -ADP supported low rates of Ca^{2+} transport. The low rate coupled with apparent tight binding did not permit distinction between

Figure 19

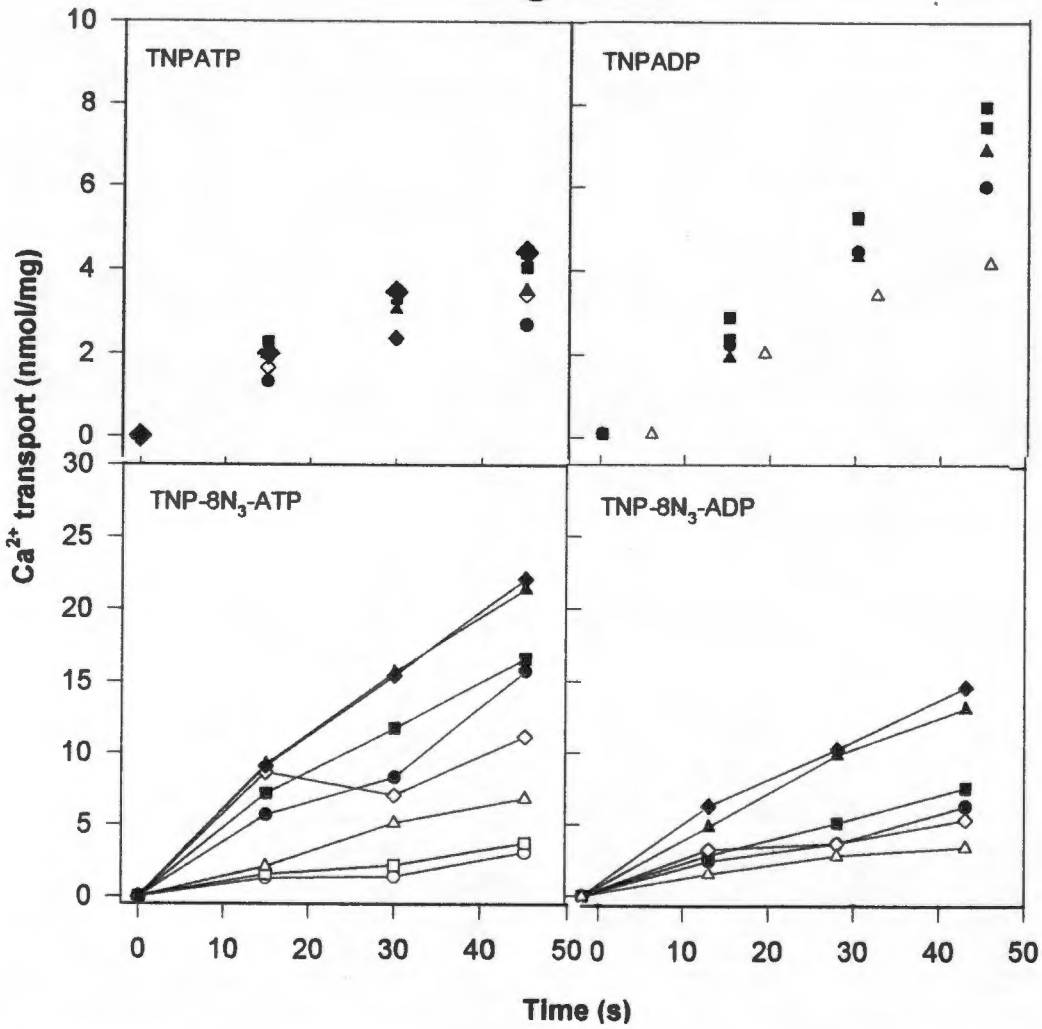

TNP-nucleotide supported Ca^{2+} transport
Transport supported by TNP-ATP and -ADP, and TNP-$8N_3$-ATP and -ADP was performed (in the dark for the latter two) in the same media and temperature as for the hydrolysis, except that $^{45}CaCl_2$ was used. Aliquots were filtered on Millipore 0.45 μM filters at timed intervals and washed with ice-cold assay medium containing 10 mM EGTA. The filters were assayed for radioactivity.Open circle, square, triangle, diamond represent 0.05; 0.1; 0.5 and 1.0 μM TNP-nucleotide, respectively and closed circle, square, triangle, diamond represent 2.0; 5.0; 10.0 and 20.0 μM TNP-nucleotide, respectively.

rates at different nucleotide concentration. The initial rate of transport by the two nucleotieds is similar (i.e. 2-2.3 nmoles/15 s/mg of protein or 8-10 nmoles/min/mg of protein). The lack of any lag in activation of transport suggests that TNP-ATP is in fact a substrate of Ca^{2+}ATPase. Transport was more rapid with the azido nucleotides (up to 32 and 25 nmoles/min/mg of protein for TNP-$8N_3$-ATP and -ADP respectively) and an approximate K_m of 0.5 μM for both nucleotides.

Table 2

Rates of TNP-nucleotide hydrolysis and Ca^{2+} transport (nmoles/min/mg of protein)

TNP-nucleotide	Ca^{2+} transport	Hydrolysis	Coupling ratio
TNP-$8N_3$-ATP	32	15	2.1
TNP-$8N_3$-ADP	25	10 - 12	2.5 - 2.1
TNP-ATP	8 - 10	Unmeasurable	Unmeasurable
TNP-ADP	8 - 10	5	1.6 - 2.0

3.1.5. TNP-superfluorescence in the forward direction of catalysis:

The demonstration that at least three of the free TNP-nucleotides are coupled substrates of Ca^{2+}ATPase and the complicated kinetics following quenching of superfluorescence by Ca^{2+} suggested that TNP-superfluorescence could be followed in the forward direction of catalysis. An attempt to demonstrate this is shown in

Figure 20

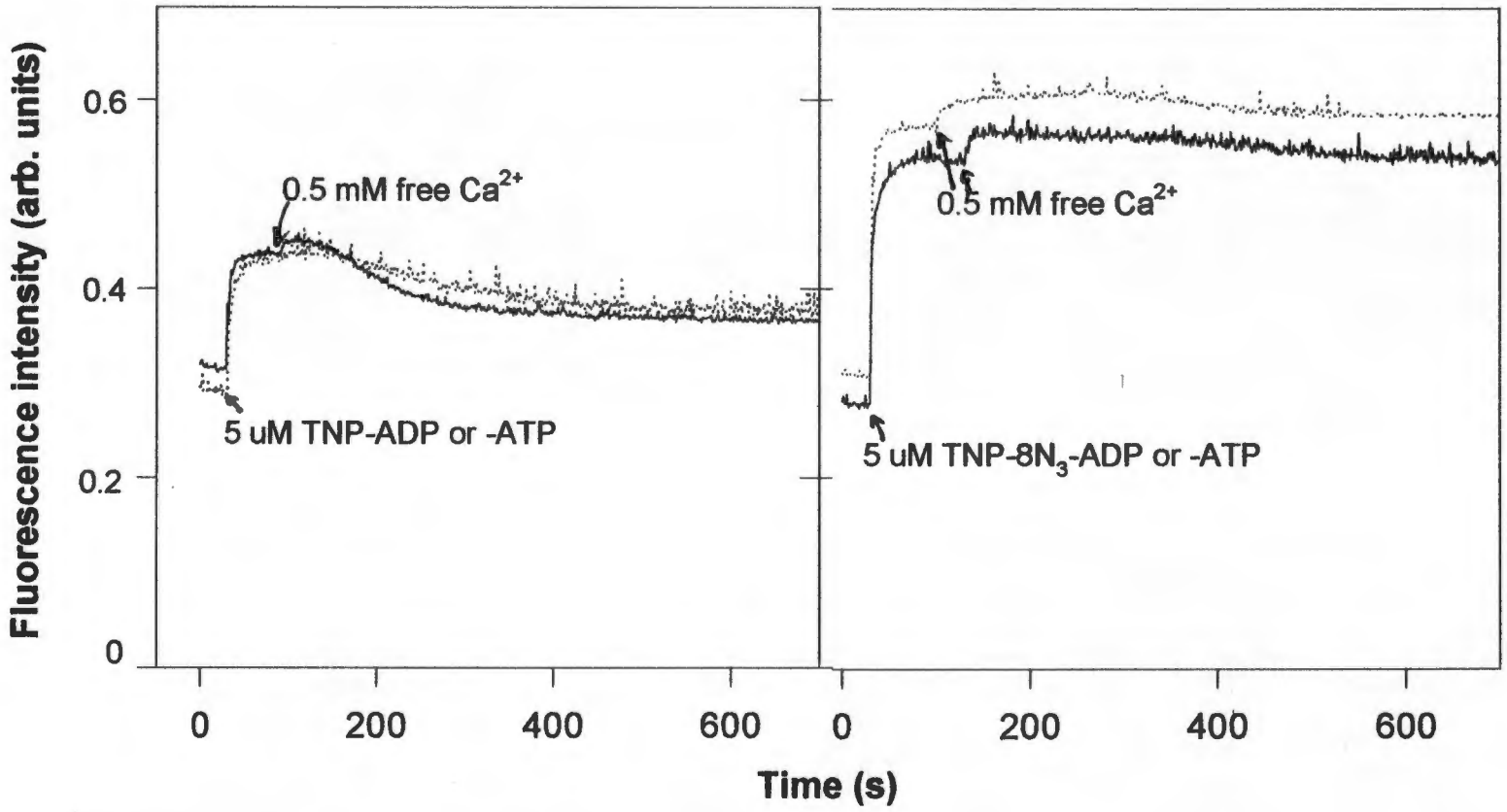

TNP-superfluorescence in the forward direction of catalysis
Phosphorylation of Ca^{2+}ATPase (0.2 mg of protein/ml SRV) was initiated in the forward direction of catalysis at 25 °C and pH 5.5, upon the addition of 1.0 mM total $CaCl_2$, using 5 µM free TNP-$8N_3$-ATP, -ADP, TNP-ADP or -ADP as substrates. The irradiation buffer was diluted 5-fold into the fluorescence buffer, as was described previously in the legend of Fig 4. The solid and dotted lines refer to TNP-$8N_3$-ATP (TNP-ATP) and TNP-$8N_3$-ADP (TNP-ADP), respectively.

Fig 20. Addition of Ca^{2+}, produced a very small immediate change in fluorescence which was followed by a slow decline over approximately 300 s. This time span is compatible with hydrolysis of the nucleotide. A larger initial rise was found with TNP-ADP, and the subsequent slower phase of quenching was more evident and faster compared with the triphospate nucleotide.

In the case of the azido nucleotides the initial rise in superfluorescence on the addition of Ca^{2+} was more significant, but the slower quench less obvious.
If the slower phases are associated with hydrolysis of the nucleotides, it seems that the nonazido species are hydrolysed faster that the azido ones. This is contrary to what was found in Fig 13 and Fig 14. The difference could be due to the presence of glycerol in the fluorescence medium.
There still appears to be a discrepancy between the low levels of fluorescence obtained in the above experiments in the forward direction of catalysis compared with the high levels found in P_i-induced fluorescence following quenching with Ca^{2+} (Fig 15 and 16).

3.1.6. P_i enhances TNP-nucleotide fluorescence in the forward direction of catalysis:

Accordingly, the above experiments were repeated in the presence of 10 mM P_i (Fig 21). It can be seen that there is a very much larger transient increase in superfluoresence, particularly in the case of the nonazido species. This transient increase appears to be dependent on enzyme turnover since the monophosphate species did not exhibit the same phenomenon. Notice the difference in scale on the time axis between the nonazido and azido nucleotides. It is clear that the nonazido species are better substrates than the

Figure 21

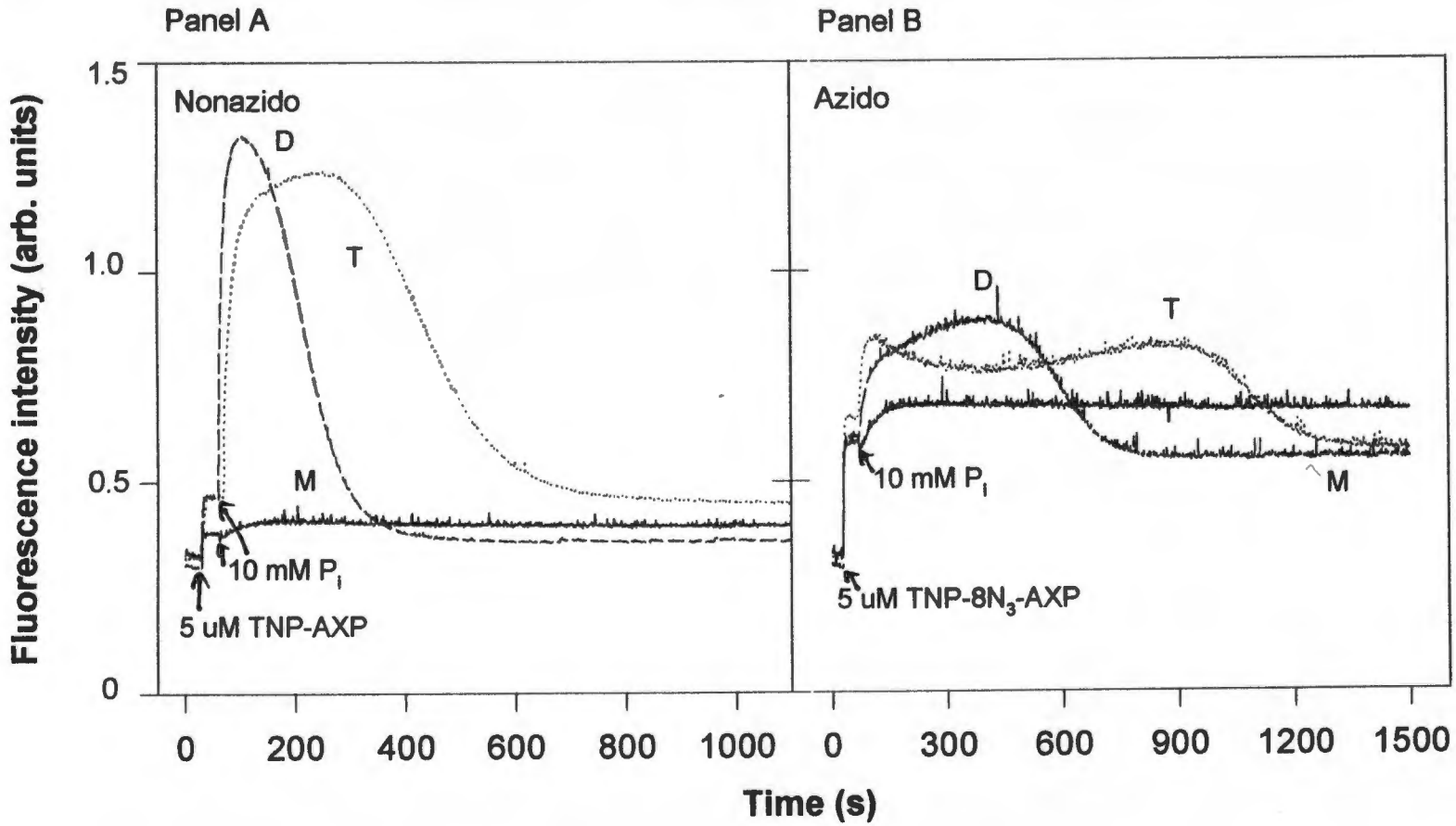

P_i enhancment of TNP-fluorescence in the forward direction of catalysis
The conditions were the same as in Fig 20, except that the enzyme was pre-incubated with 1.2 mM total $CaCl_2$ at 25 °C, pH 5.5. TNP-nucleotide (5 μM) and 10 mM Pi were added as indicated on the traces.

azido ones. It is also apparent that the length of time taken to hydrolyse the triphospho nucleotide is approximately double that of the diphospho species suggesting, as found above, that the two species are hydrolysed at similar rates and that the triphospho form is hydrolysed twice to yield the monophosphate. Note also that there is no time lag in the rise in the superfluorescence associated with TNP-ATP hydrolysis suggesting that the latter is directly a substrate for the Ca^{2+}ATPase and does not need to be converted into the diphospho form by contaminating enzymes.

3.1.7. Similar rates with free TNP-8N$_3$-AMP, TNP-AMP and TNP-AMP-PCP:

Coming back to the original problem as whether TNP-nucleotides can accelerate the quench of P_i-induced superfluorescence by Ca^{2+}, it is clear from the above results that TNP-ATP and -ADP and the azido derivatives cannot be used.

We therefore synthesized the nonhydrolysable analogue TNP-AMP-PCP (see flow diagram, Fig 22). AMP-PCP was purified on a DE 52 HCO_3^- anion exchange column with a 0-250 mM TEAB gradient. The product was present in fractions 10 to 16. The reaction solvent and excess diphenyl chlorophosphate eluted in fractions 0 to 2 and unreacted AMP in fractions 4 to 8 (Fig 23). TNP-AMP-PCP was formed by the reaction of purified AMP-PCP with DTNB and TNBS. The product was purified on a DE52 anion exchange column and developed with 0.2, 0.5 and 1 M ammonium formate. Fractions 8 to 13 contained the product (Fig 23). A 19% yield from AMP was obtained. The purity of TNP-AMP-PCP was monitored by TLC (Fig 24) and HPLC (Fig 25). From this can be seen that TNP-AMP-PCP has a

Scheme 6
Synthesis of TNP-AMP-PCP

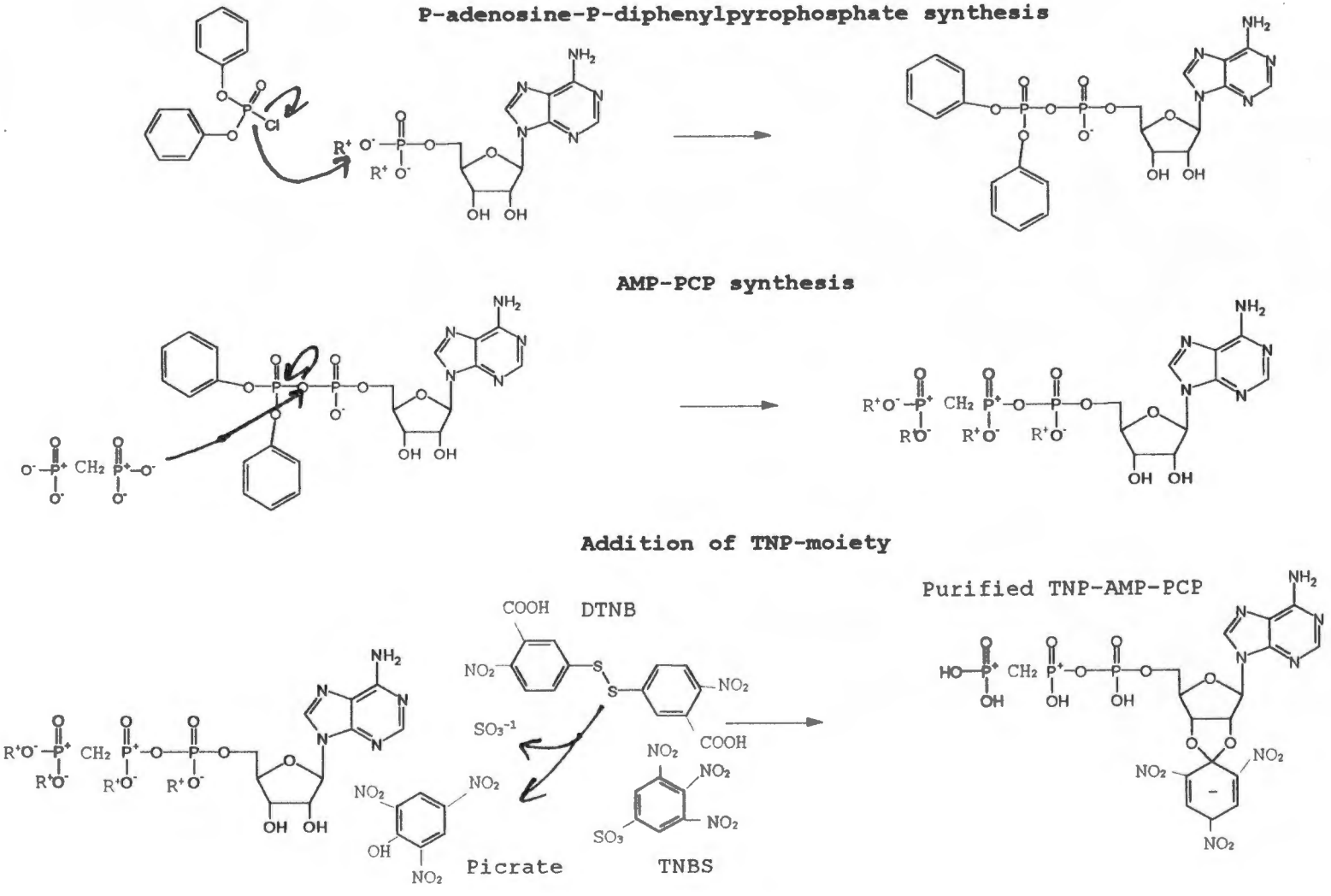

Figure 22

Flow diagram for the synthesis of TNP-AMP-PCP

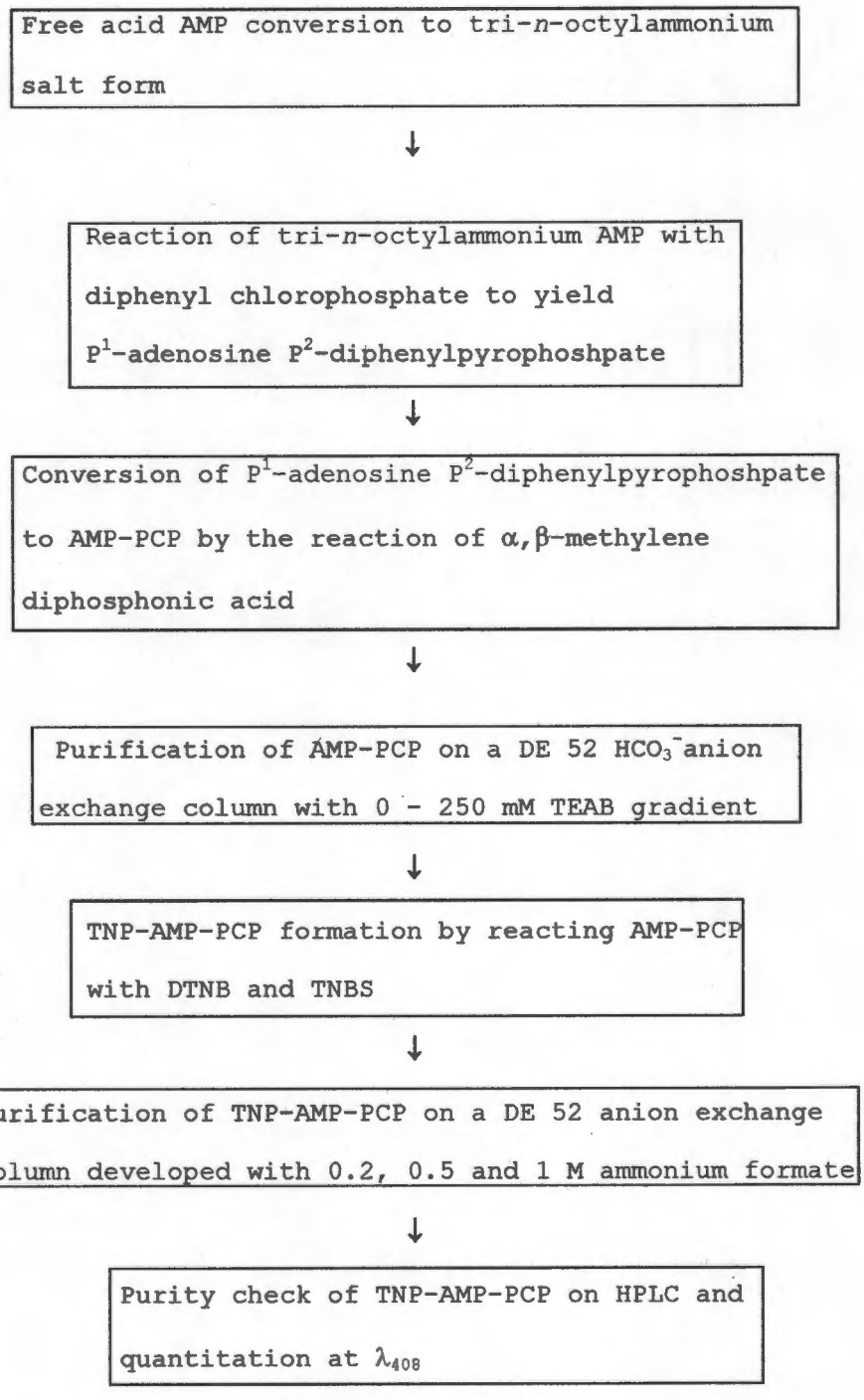

Figure 23

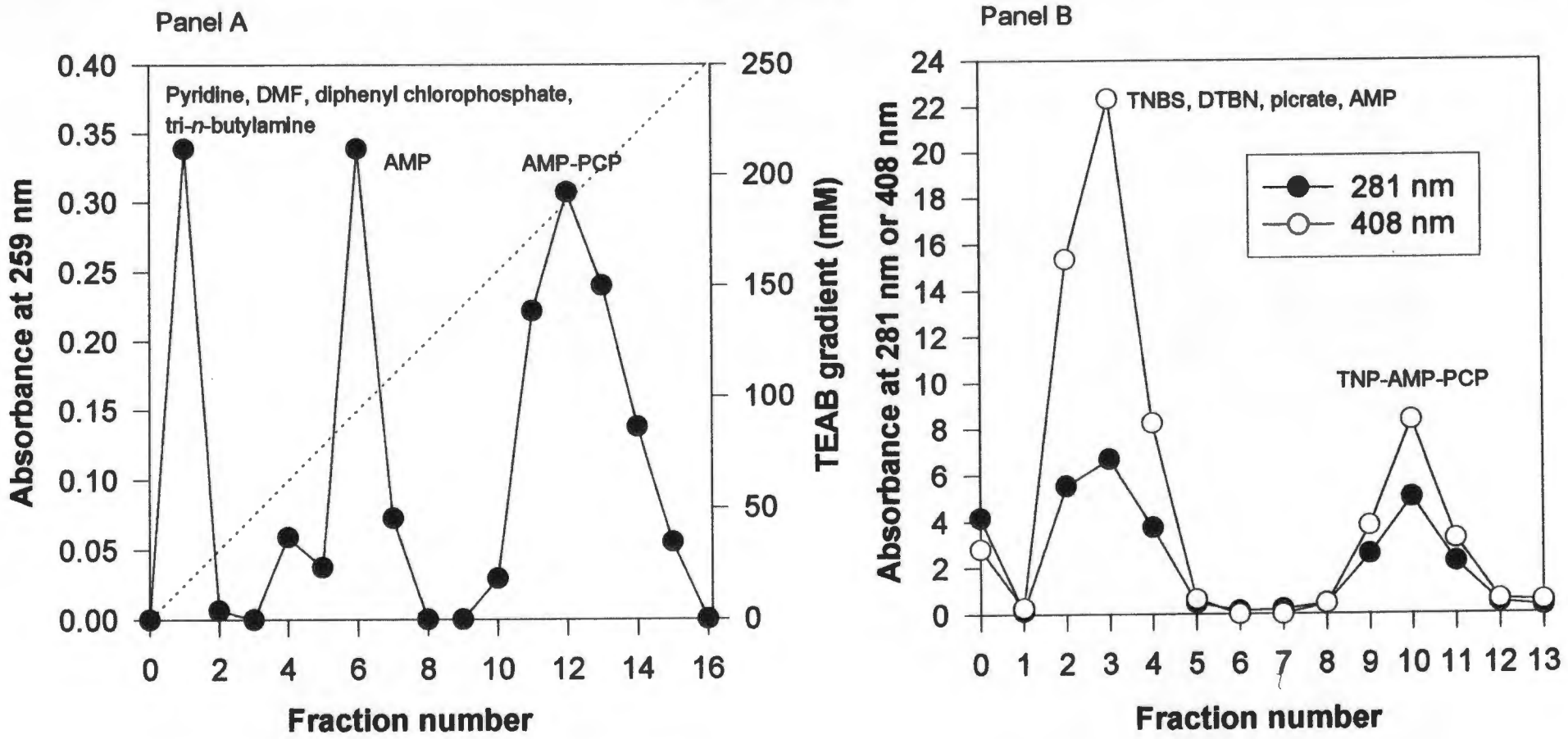

Purification of AMP-PCP and TNP-AMP-PCP

Panel A, AMP-PCP was purified on a DE 52 (HCO_3^- form, 1.5 x 3 cm) anion exchange column using a linear gradient up to 250 mM TEAB buffer. Fractions (10 ml) were collected and absorbance determined at 259 nm. The fractions that contained the majority of the AMP-PCP were pooled and concentrated.

Panel B, TNP-AMP-PCP was purified on a column (4 x 0.5 cm) of DE 52 anion exchange resin, equilibrated with water. The column was developed with 5 ml aliquots of 0.2, 0.5 and
1 M ammonium formate. Fractions (5 ml) were collected and absorbance determined at 408 nm and 281 nm. The fractions that contained the majority of the TNP-AMP-PCP were pooled and concentrated.

similar R_f value and retention time as TNP-ATP TNP-AMP-PCP showed the same absorbance profile as the TNP-nucleotides, with absorbance maxima at λ_{259} , λ_{408} and λ_{470} (Fig 26). TNP-AMP-PCP displayed a similar P_i-induced superfluorescence signal as TNP-AMP (Fig 27).

Figure 24

Purity check of TNP-AMP-PCP by TLC

TNP-AMP-PCP, TNP-ATP, -ADP and -AMP were spotted on a PEI cellulose plate and developed in 1 M LiCl

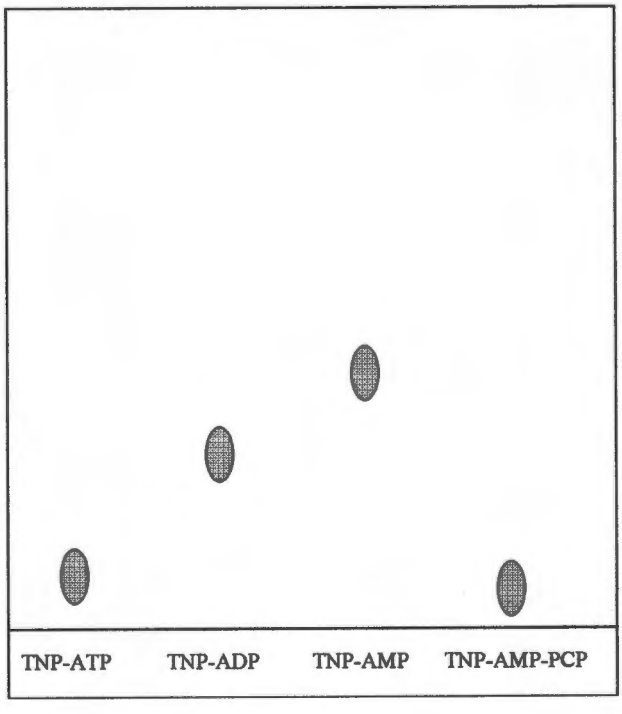

The earlier experiments involving Ca^{2+} quenching of TNP-AMP and TNP-$8N_3$-AMP were repeated and compared with results obtained with TNP-AMP-PCP (Figure 28 and Table 3). As can be seen TNP-AMP-PCP did not accelerated the quench of superfluoresence by Ca^{2+}, in the pH range 5.5 - 6.5, compared with TNP-AMP and TNP-$8N_3$-AMP. In general, 80-91% of

Figure 25

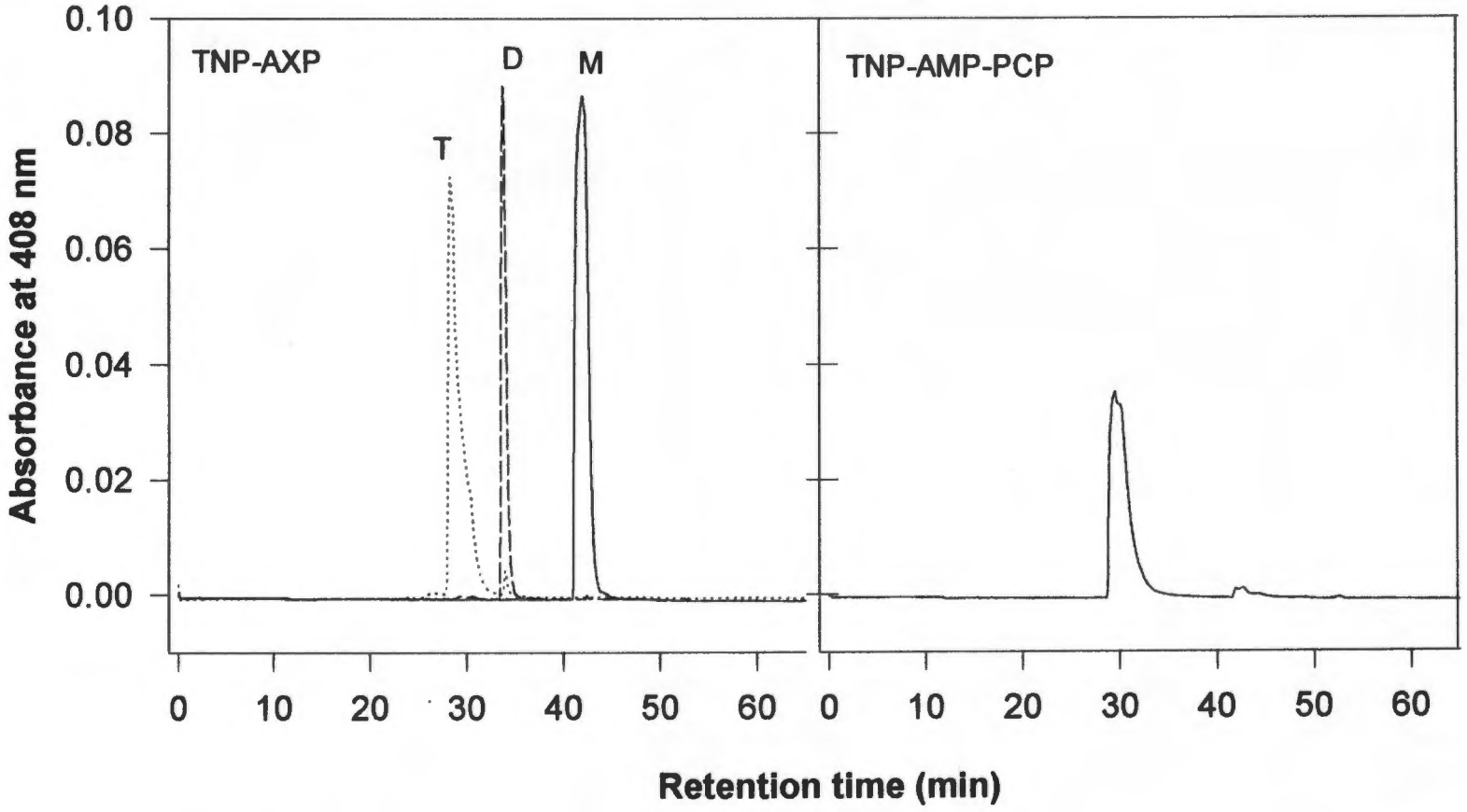

Purity check of TNP-AMP-PCP by C_{18} HPLC
TNP-AMP-PCP was monitored at 408 nm and eluted with a linear gradient of 10 mM KP_i, pH 6.0, 10 mM KP_i/60 % (v/v) acetonitrile.

Figure 26

Panel A

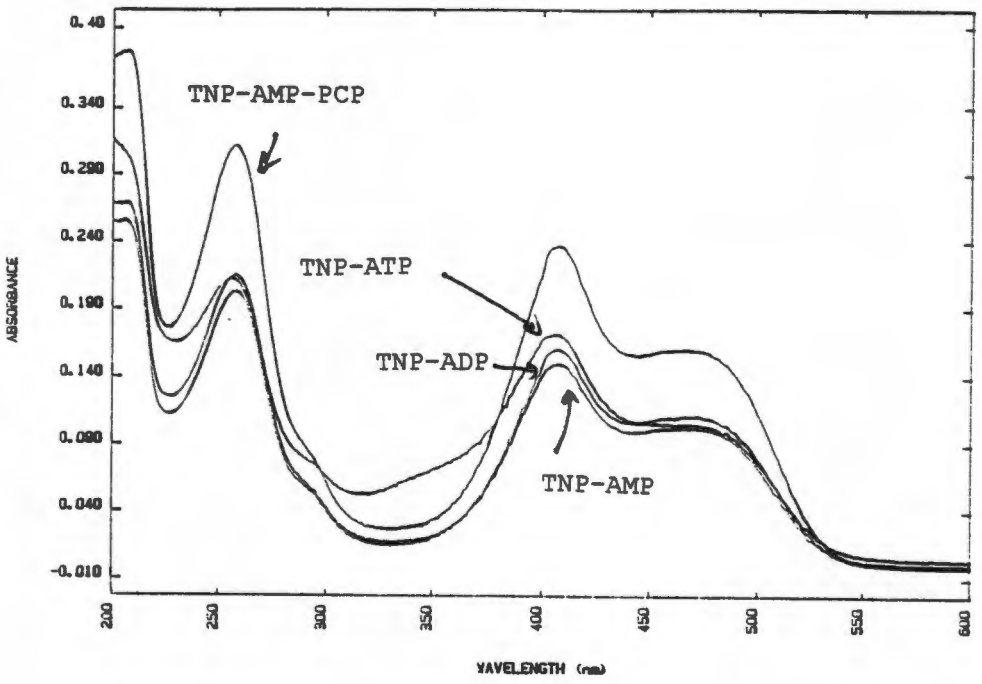

Panel B

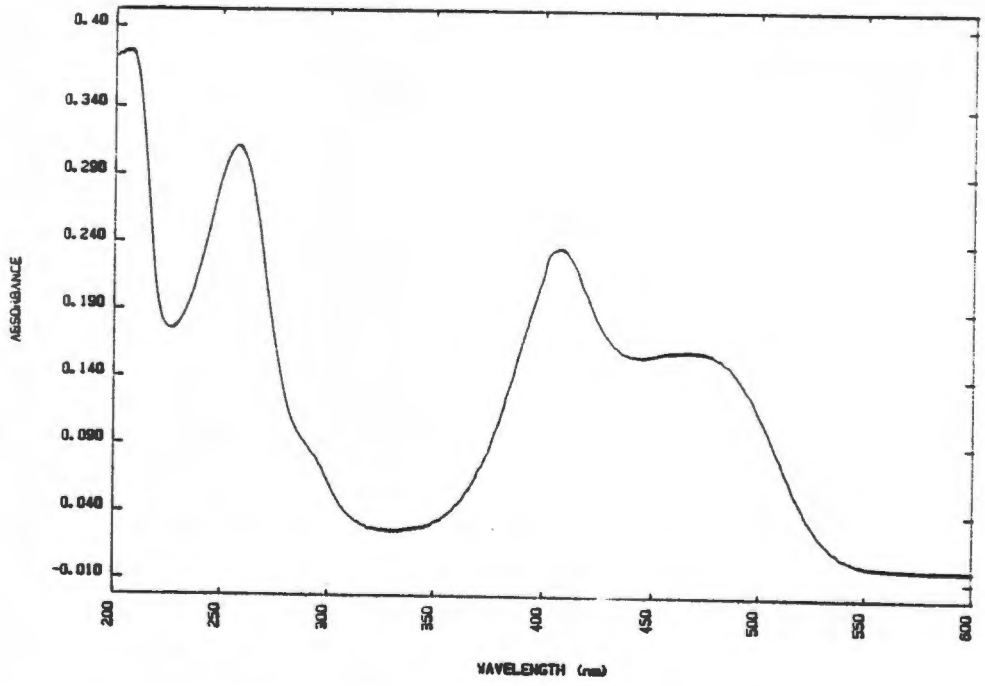

Absorbance scan of purified TNP-AMP-PCP
Panel A, Comparison between TNP-AMP-PCP, TNP-ATP, -ADP and -AMP. The nucleotides were diluted in 10 mM KP_i (pH 7.0) with 10 mM KP_i (pH 7.0) used as blank.
Panel B, Purified TNP-AMP-PCP was diluted as above.

Figure 27

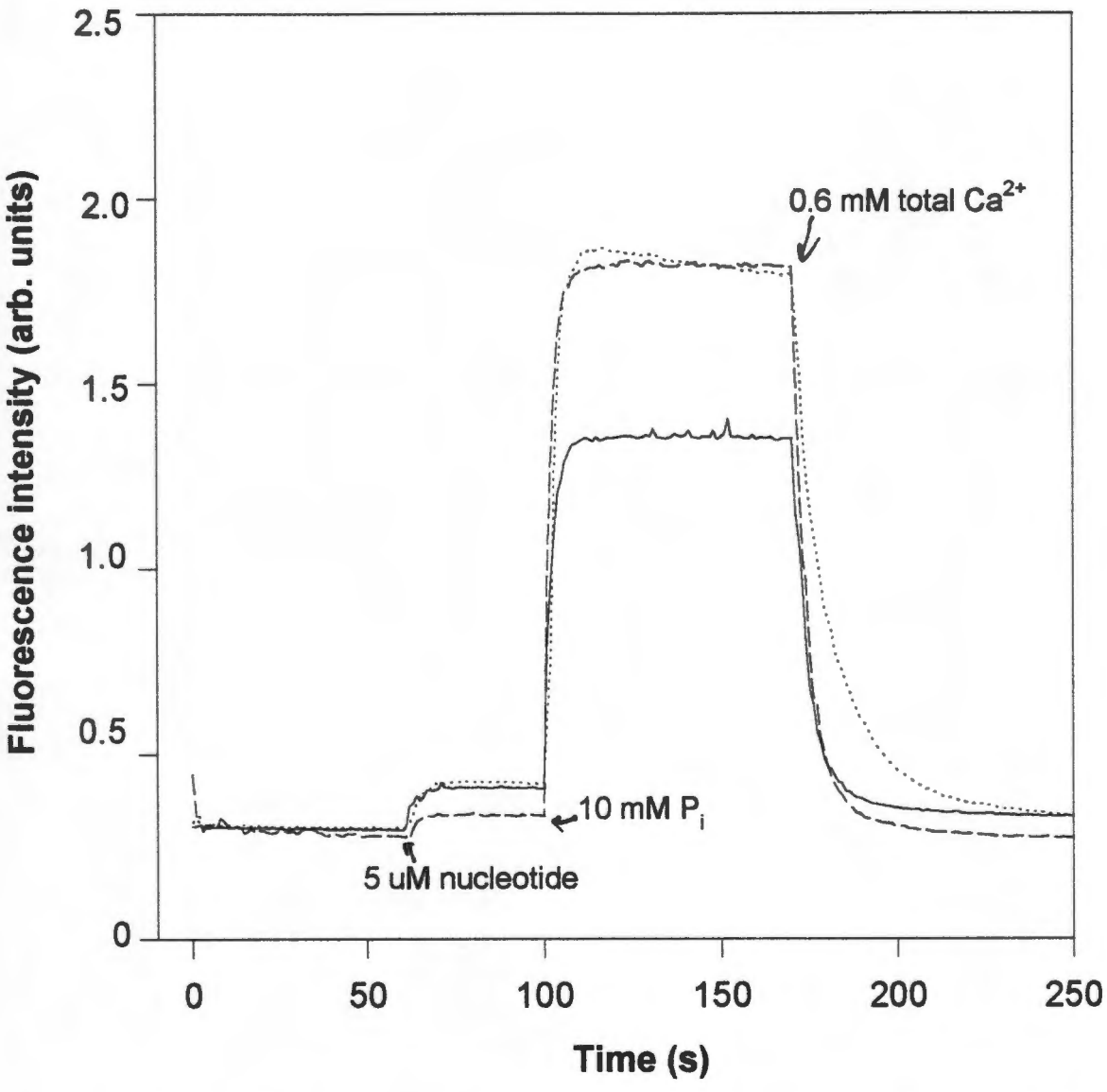

TNP-AMP-PCP fluorescence characteristics compared to TNP-AMP and TNP-$8N_3$-AMP

See legend of Fig 13 for details. The solid, dashed and dotted lines refer to TNP-$8N_3$-AMP, TNP-AMP and TNP-AMP-PCP, respectively.

Figure 28

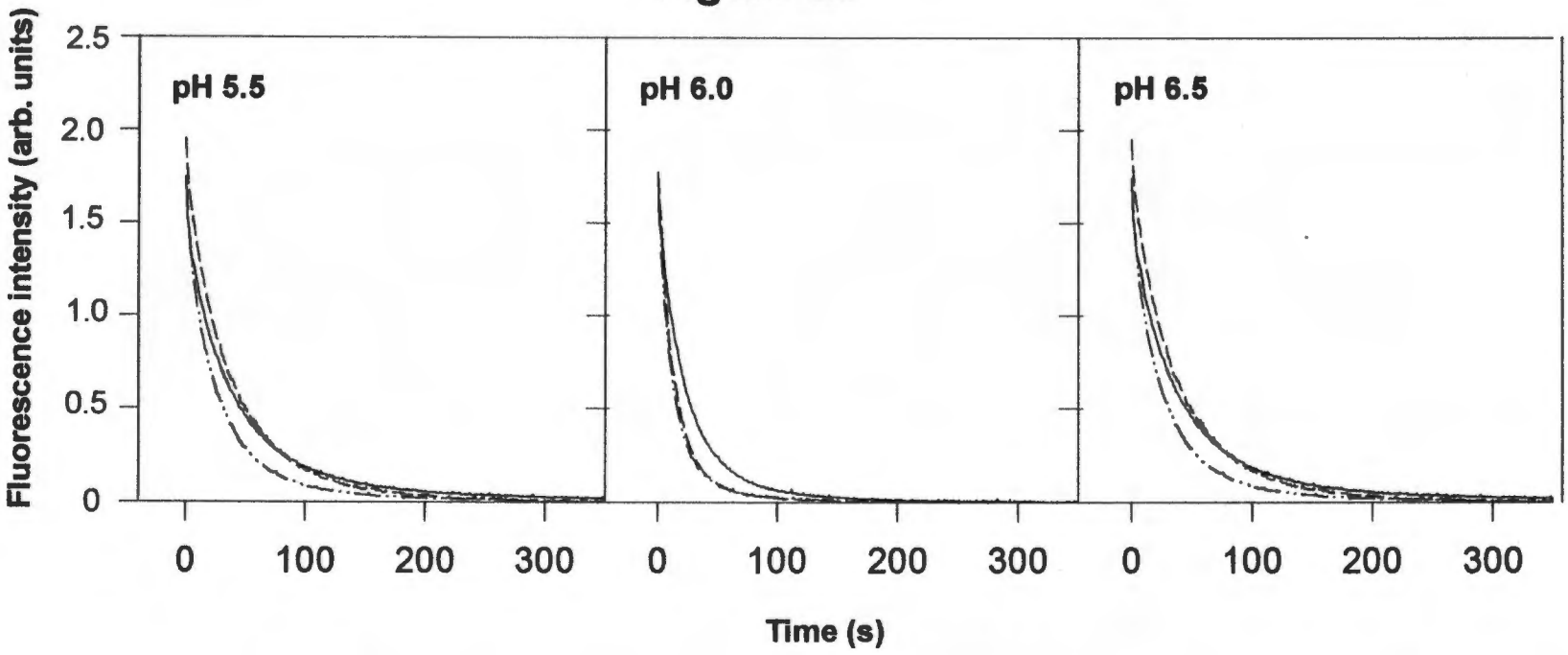

pH dependence of P_i-induced superfluorescence quench rate by Ca^{2+} with TNP-AMP, TNP-$8N_3$-AMP and TNP-AMP-PCP
The earlier experiments were repeated (see legend of Fig 13) at pH 5.5, 6.0 and 6.5. The solid, dashed and dotted lines refer to TNP-AMP-PCP, TNP-AMP and TNP-$8N_3$-AMP, respectively.

the superfluorescence quench can be described by a single rate constant (listed in Table 3).

Table 3

Comparison between free TNP-8N_3-AMP, TNP-AMP and TNP-AMP-PCP superfluorescence quench rates

Nucleotide	pH	Rate constant (s^{-1})
TNP-8N_3-AMP	5.5	0.023[a]
	6.0	0.09
	6.5	0.25
TNP-AMP	5.5	0.023
	6.0	0.09
	6.5	0.28
TNP-AMP-PCP	5.5	0.03
	6.0	0.05
	6.5	0.12

a: A fast and slow component of 47% (k_{fast} = 0.09 s^{-1}) and 53% (k_{slow} = 0.023 s^{-1}), respectively, were found for free TNP-8N_3-AMP at pH 5.5.

The presence of a small slow phase (0.008 to 0.025 s^{-1}) was attributed to background drift. Over the pH range 5.5, 6.0 and 6.5 there was a general increase in the superfluorescence quench rate (0.023-0.03, 0.05-0.09 to 0.12-0.25 s^{-1}, respectively) for all three nucleotides. It can be concluded that, under these conditions, the

Figure 29

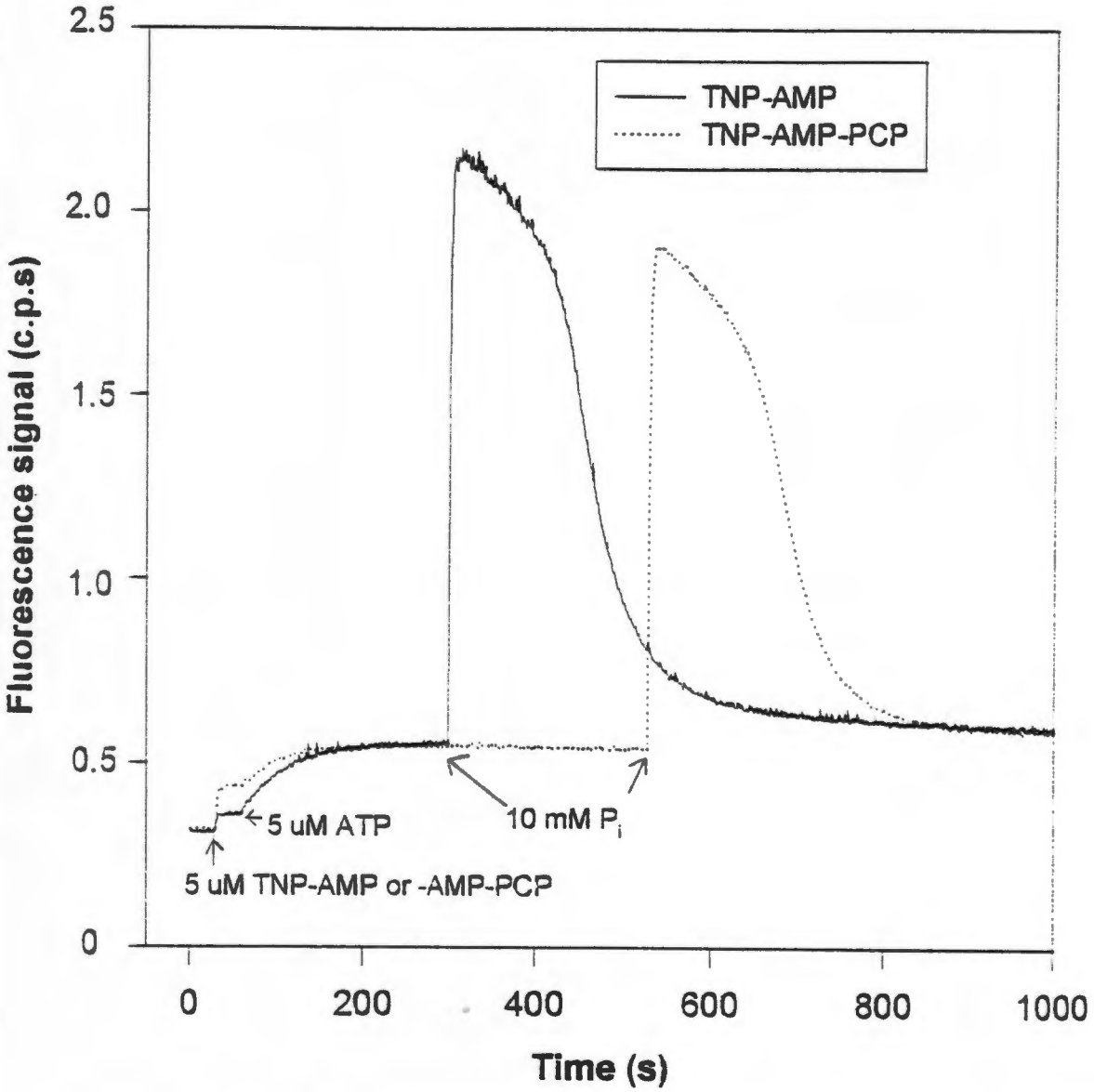

Hydrolysis of ATP compared to the hydrolysis of TNP-nucleotides
The irradiation buffer was diluted as previously described into the fluorescence buffer (see legend of Fig 13). SRV (0.2 mg of protein/ml) were incubated in the medium at 20 °C for a minute and then 5 μM TNP-AMP or TNP-AMP-PCP, 5 μM ATP and 10 mM P_i were added as indicated. The solid and dashed lines refer to TNP-AMP and TNP-AMP-PCP, respectively.

triphospho nucleotide does not accelerate the step associated with the Ca^{2+} quench.

3.1.8. Hydrolysis of ATP is comparable to the hydrolysis of TNP-nucleotides under these reaction conditions:

The preceding experiments are somewhat unusual in that glycerol is present in the medium. It was therefore of interest to compare the results obtained with the TNP-nucleotides to that obtained with ATP under the same conditions.

Such an experiment, using TNP-AMP or TNP-AMP-PCP as fluorescent probes, is shown in Fig 29. It can be seen that it takes approximately 200 s to hydrolyse 5 μM ATP, i.e. about the same time as it takes to hydrolyse 5 μM TNP-ADP (Fig 21). It can be concluded that, under the conditions used, Ca^{2+}-ATPase utilizes ATP and TNP-nucleotides with approximately equal facility.

3.2 Ca^{2+}chelators

Skeletal muscle sarcoplasmic reticulum Ca^{2+}ATPase binds cytoplasmic Ca^{2+} with high affinity ($K_d \cong 1$ μM) and positive cooperativity ($n_H \cong 2$). In the relaxed state of the muscle, the free Ca^{2+} concentration in the cytoplasm is in the order of 0.1 μM (the limiting Ca^{2+} concentration, $[Ca^{2+}]_{lim}$), whereas the luminal free Ca^{2+} concentration is in the millimolar range (Hasselbach and Makinose, 1961; Ebashi and Lipmann, 1962).

The Ca^{2+} chelator EGTA is routinely used to lower and maintain low, free Ca^{2+} concentrations in solutions to study

various reactions in the Ca^{2+}ATPase enzyme cycle. An example is the phosphorylation of the enzyme in the reverse direction of catalysis by P_i, where no Ca^{2+} must be bound to the enzyme to ensure that the majority of the enzyme will be present as the reactive E_2 species. Ususally it is assumed that the chelator and/or Ca^{2+}chelator complexes do not alter the kinetic or binding characteristics of Ca^{2+}ATPase. However, so-called EGTA effect has been reported in various systems.

Ca^{2+} transport by islet cell plasmamembrane $Ca^{2+}Mg^{2+}$ATPase is activated by millimolar EGTA, but not stimulated further by calmodulin addition (Kotagel *et al.*, 1983). On the other hand, calmodulin stimulation is inhibited by the presence of millimolar EGTA suggesting that the ability of CaEGTA to activate the $Ca^{2+}Mg^{2+}$ATPase and increase Ca^{2+} transport is possibly mimicking the effect of a physiological activator. Schatzmann (1973), Al-Jobore and Roufogalis (1983) and Weiner and Lee (1972) reported that EGTA increases the apparent affinity of the red blood cell Ca^{2+}ATPase for Ca^{2+}, without enhancing its maximum velocity. Al-Jobore and Roufogalis (1981) found that a low Ca^{2+} affinity site is converted to a high affinity site in the presence of EGTA, and that CaEGTA appears to be associated with this interconversion. Orlov *et al.* (1983) provided further evidence that EGTA increases the Ca^{2+} affinity of Ca^{2+}ATPase. They proposed two models for the EGTA effect:
1) $Ca^{2+}Mg^{2+}$ATPase might contain two types of Ca^{2+} binding sites, with low and high affinity for Ca^{2+}. The latter is manifest in the presence of EGTA. 2) EGTA or CaEGTA enhance the Ca^{2+} affinity for the enzyme either through direct interaction with the enzyme or by modifying its microenvironment in the membrane. Rossi and Rega (1989)

investigated the effect of EGTA on the red blood cell Ca^{2+}ATPase affinity for ATP. They found that EGTA does not increase the apparent affinity for ATP, which means that EGTA has its effect at or near the transport sites, unrelated to the activation by ATP. It was reported by Frey *et al.* (1981) that EDTA, CDTA and EGTA stimulate GTP pyrophosphatelyase, by increasing its affinity for MgGTP (the substrate). Segel *et al.* (1981) investigated the effect of EGTA on the lymphocyte plasma membrane Na^+K^+ATPase. Ca^{2+} is an inhibitor of the enzyme in the 50-100 μM concentration range, therefore EGTA must be present in the assay medium to chelate contaminating Ca^{2+}. However, they concluded that the enhancement of the enzyme activity is explained by Zn^{2+} chelation, and not of Ca^{2+}. Kronman and Bratcher (1982) provided evidence that CaEGTA binds directly to bovine α-lactalbumin. This binding causes a conformational change in the protein, resulting in a larger apparent association constant for Ca^{2+}. EGTA, EDTA and CDTA all increase initial rates of Ca^{2+} transport by cardiac sarcolemma Na^+Ca^{2+}ATPase (Trosper and Philipson, 1984). They suggested that the Ca^{2+}chelator complex causes the stimulation. CaEGTA also appears to activate the SR muscle Ca^{2+}ATPase (Berman, 1982). The effect is specific for EGTA as EDTA did not provide a similar stimulation.

3.2.1. Ca^{2+} transport characteristics measured by Fluo-3 fluorescence:

Extravesicular free [Ca^{2+}] was measured at 25 °C, pH 6.8 with the Ca^{2+} indicator Fluo-3. The Ca^{2+}ATPase was activated by adding 2 mM ATP, which resulted in a decrease of fluorescence to a baseline value (Fig 30). The decrease in fluorescence was due to Ca^{2+} (in the medium) being transported from the medium into the SRV. Upon addition of

Figure 30

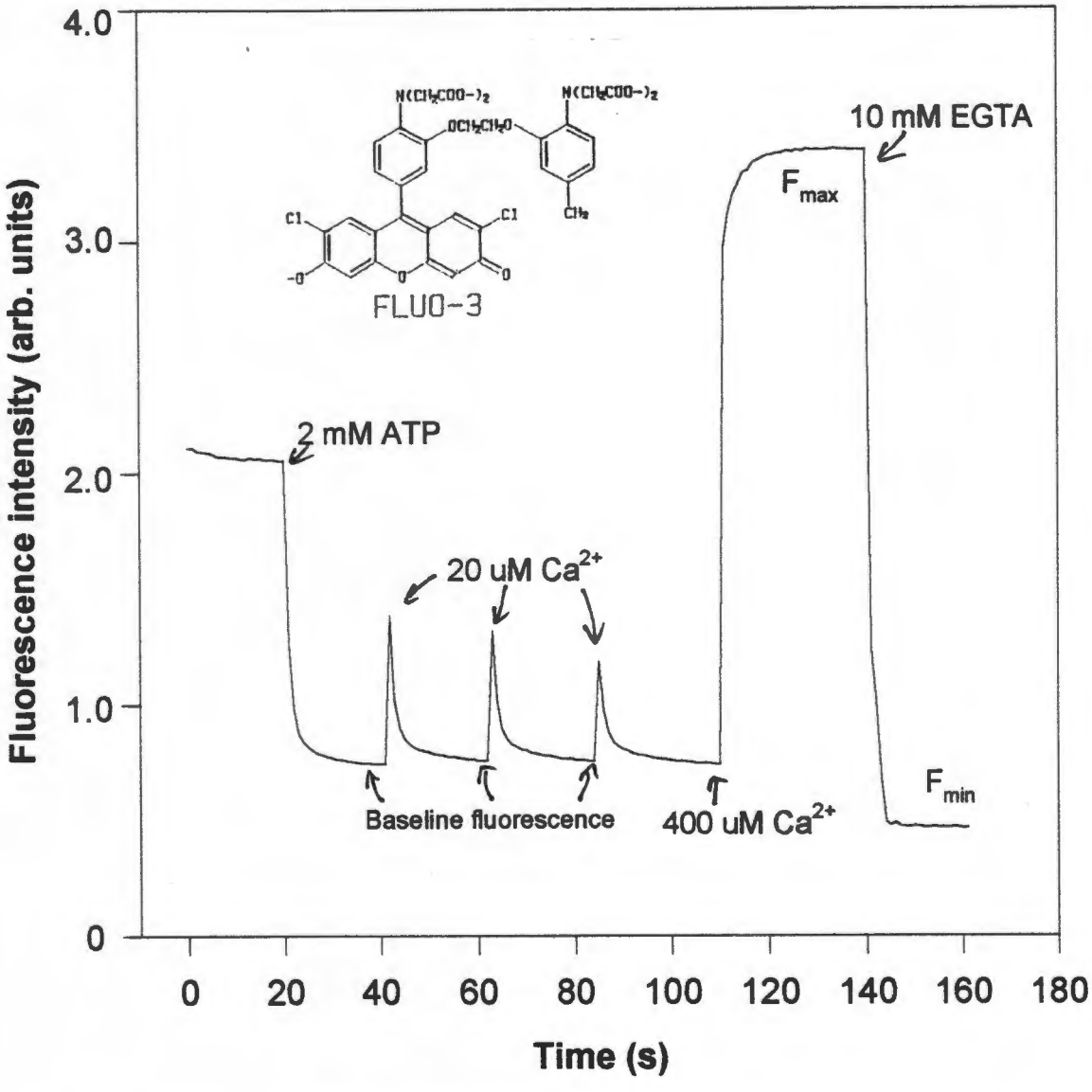

SRV Ca^{2+} transport characteristics measured by Fluo-3 fluorescence
Free Ca^{2+} was determined by measuring the fluorescence of Fluo-3, using a SPEX FluoroMax spectrofluorometer. The emission and excitation wavelenghts were 535 nm and 509 nm, respectively. SRV (0.25 mg of protein/ml) were incubated at 25 °C in 20 mM MOPS/TRIS, pH 6.8, 20 nM Fluo-3, 5 mM $MgCl_2$ and 5 mM potassium oxalate. The Ca^{2+}ATPase was activated by the addition of 2 mM ATP. $CaCl_2$ (20 µM) aliquots were added to the mixture as indicated in the plot. F_{max} and F_{min} were obtained by the addition of 400 µM $CaCl_2$ and 10 mM EGTA, respectively.

Figure 31

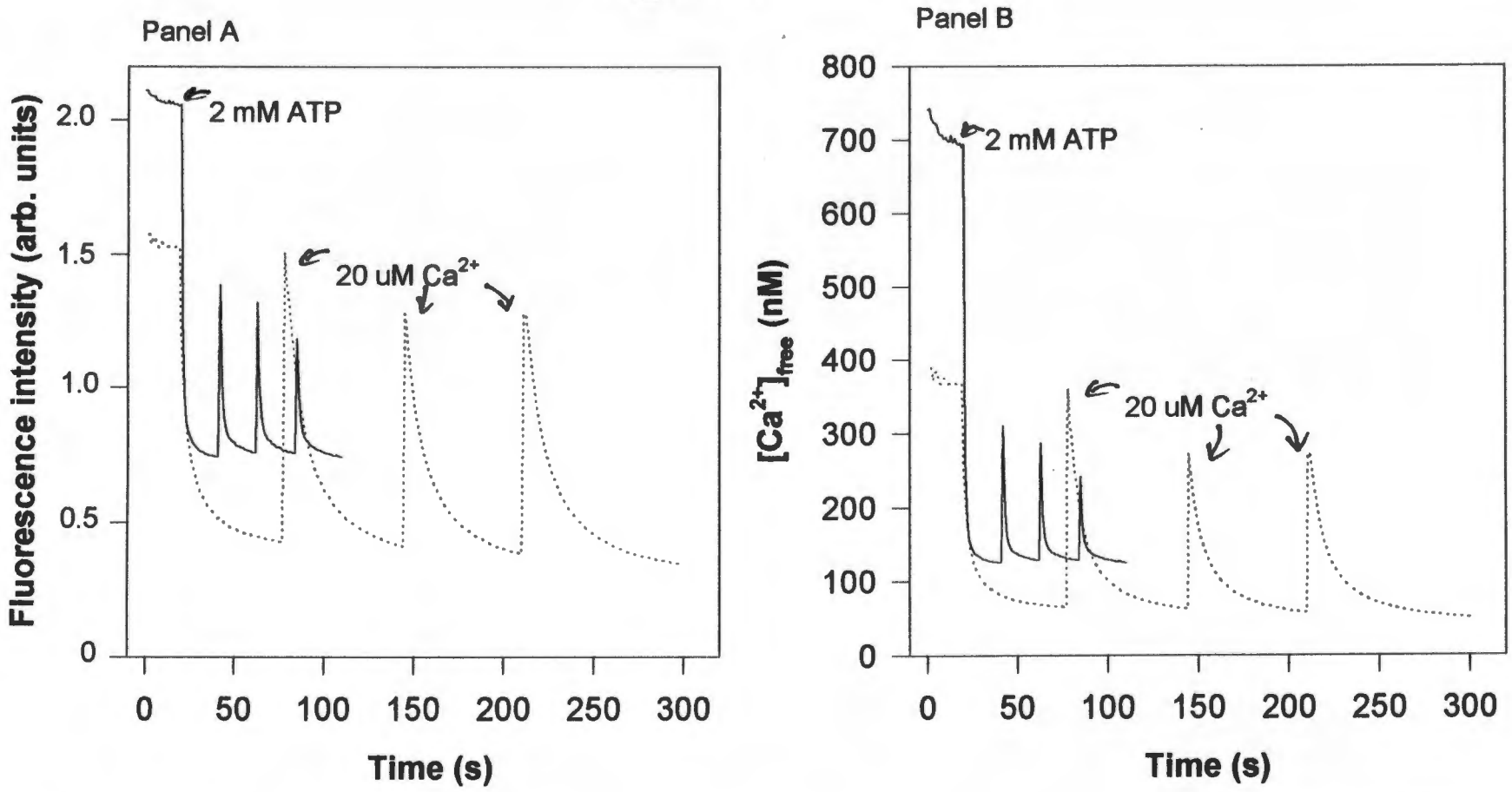

The effect of 7.5 μM EGTA on $[Ca^{2+}]_{lim}$

Panel A, The effect of a chelator on $[Ca^{2+}]_{lim}$ was determined under similar reaction conditions, as described in the legend of Fig 29. Here, SRV were pre-incubated in a medium containing 7.5 μM EGTA. The enzyme was activated as before and 20 μM $CaCl_2$ aliquots were added to the mixture as indicated in the plot.
Panel B, The fluorescence signal was transformed into $[Ca^{2+}]_{free}$ with the transformation equation $[Ca^{2+}]_{free} = K_d[(F-F_{min})/F_{max} - F)]$. The solid and dotted lines refer to the control experiment and when 7.5 μM EGTA was present, respectively.

Figure 32

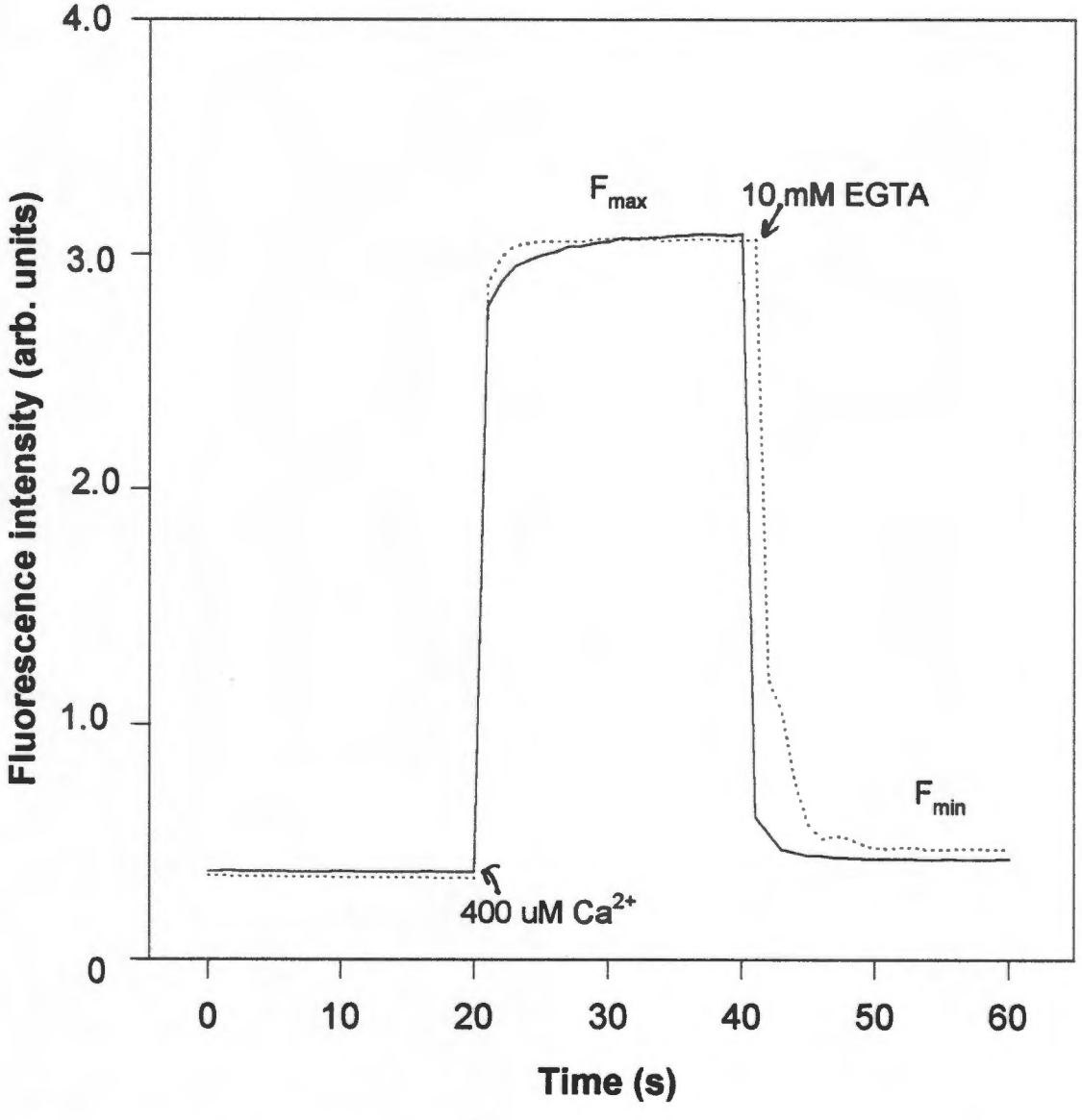

Influence of 7.5 μM EGTA on Fmax and Fmin
F_{max} and F_{min} were obtained by the addition of 400 uM $CaCl_2$ and 10 mM EGTA, respectively for both the control experiments and in the presence of 7.5 μM EGTA. See legends of Fig 29 and Fig 30 for details. The solid and dotted lines refer to the control experiment and in the presence of EGTA, respectively.

20 μM Ca^{2+} aliquots, the fluorescence increased immediately due to the formation of the highly fluorescent CaFluo-3 complex and decreased again to the baseline value over a time frame of 20 s, due to Ca^{2+} transport into SRV lumen. A saturated fluorescence level was achieved upon addition of 400 mM Ca^{2+}, the F_{max} value. The minimum fluorescence (F_{min}) level was obtained with the addition of excess EGTA (10 mM). When the baseline fluorescence value was converted to $[Ca^{2+}]$free, it was found to be in the range of 100-200 nM. The $[Ca^{2+}]$free always decreased to a value in this range, the so-called $[Ca^{2+}]_{lim}$ value.

3.2.2. The effect of micromolar EGTA on $[Ca^{2+}]_{lim}$:

The presence of 7.5 μM EGTA in the medium resulted in a lower fluorescence baseline value on addition of ATP, in other words, a lower $[Ca^{2+}]_{lim}$ value (Fig 31). Adding an aliquot of 20 μM Ca^{2+}, resulted in an immediate fluorescence increase. The time for the fluorescence signal to reach the baseline value, was slowed from 20 s to 70 s. Thus Ca^{2+} uptake was retarded in the presence of EGTA. No change in F_{max} or F_{min} was observed (Fig 32).

3.2.3. Effect of various chelators on $[Ca^{2+}]_{lim}$:

It was of interest to investigate whether Ca^{2+} chelators other than EGTA would produce a similar effect (i.e. lowering $[Ca^{2+}]_{lim}$). The above mentioned experiments were performed with EDTA, BAPTA, NTA, DTPA, HEDTA and EGTA at various concentrations (1-50 μM) (Fig 33). The average baseline fluorescence value after the addition of ATP and 20 μM Ca^{2+} aliquots was calculated for each chelator and from that, the $[Ca^{2+}]_{lim}$. The $K_{0.5}$ values for each chelator were obtained from a plot of $[Ca^{2+}]_{lim}$ versus [chelator] at

Figure 33

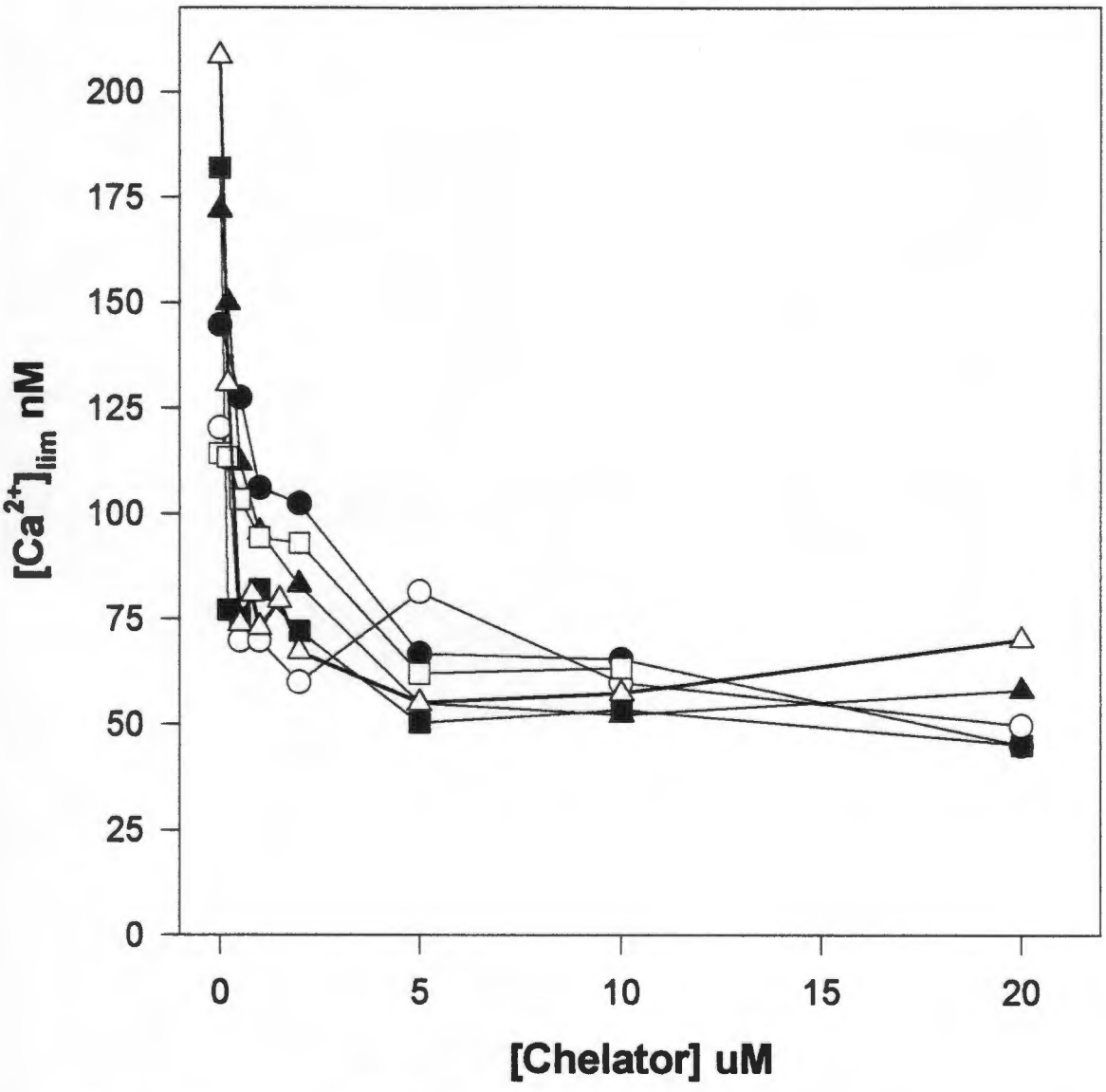

The effect of various chelators on $[Ca^{2+}]_{lim}$
The previous experiments were repeated for each chelator at a specific concentration. The average baseline fluorescence value was calculated and from that, the $[Ca^{2+}]_{lim}$ with the transformation equation. The obtained $[Ca^{2+}]_{lim}$ values were plotted against the chelator concentrations. The solid circles, squares and triangles refer to EGTA, EDTA and BAPTA, respectively, whilst the open circles, squares and triangles refer to DTPA, NTA and HEDTA, respectively.

Figure 34

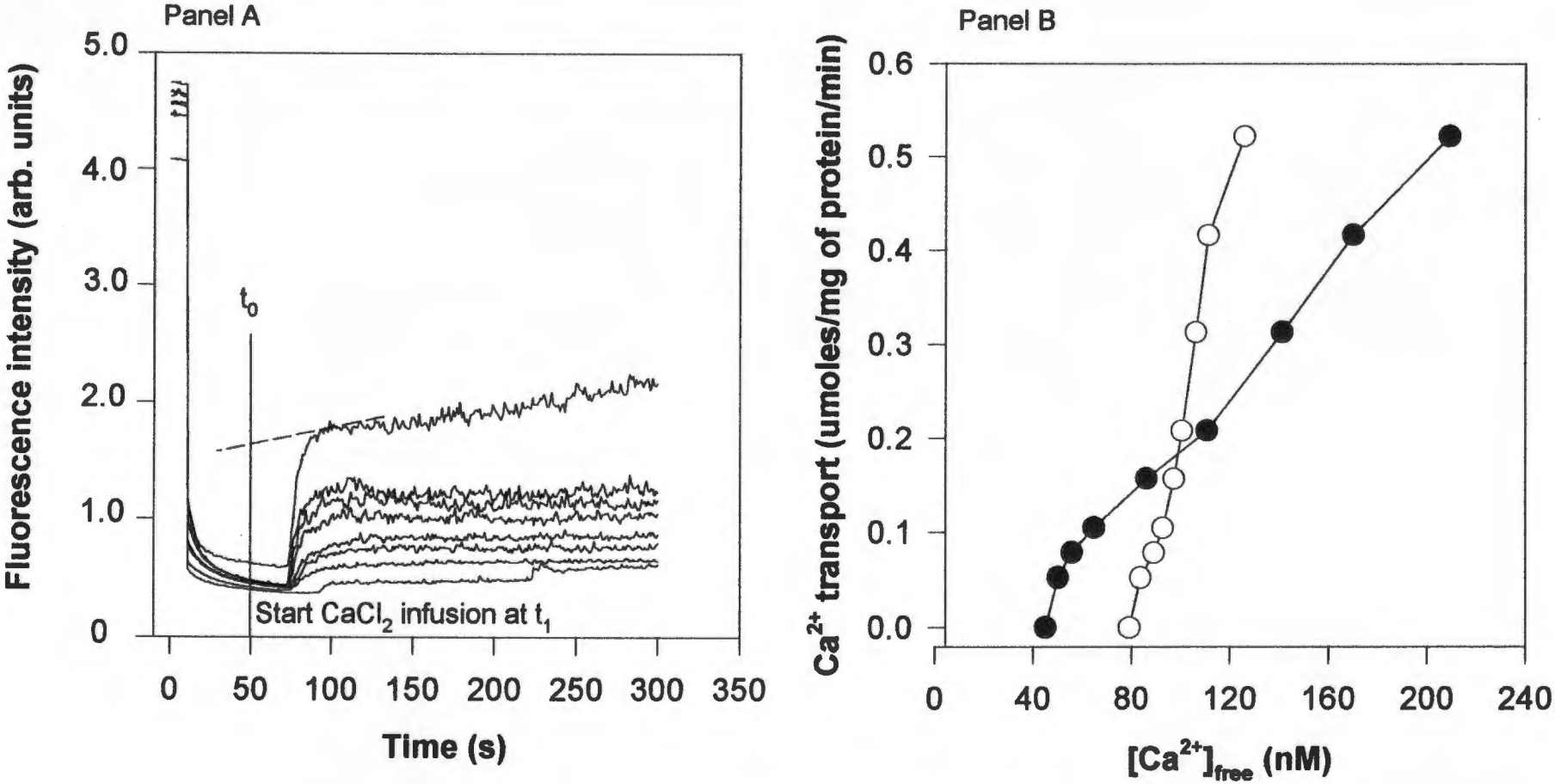

Effect of chelator on Ca^{2+} activation of Ca^{2+} ATPase measured by a Ca^{2+}-infusion method

Panel A, The experiments were carried out in the standard buffer solution, mentioned in Fig 29. The Ca^{2+}ATPase was activated by the addition of 2 mM ATP and at time t_1 the infusion of 1 mM $CaCl_2$ at a specific rate was started. The slopes of the plots were extrapolated to time to, the fluorescence intensity was recorded and converted to $[Ca^{2+}]_{free}$ with the transformation equation.

Panel B, Data was collected as described in Panel A. 2.5 μM EGTA was added to the standard buffer solution, prior to the start of the reaction. The control contained no EGTA.The open and solid circles refer to the control experiment and when EGTA was present, respectively.

Figure 35

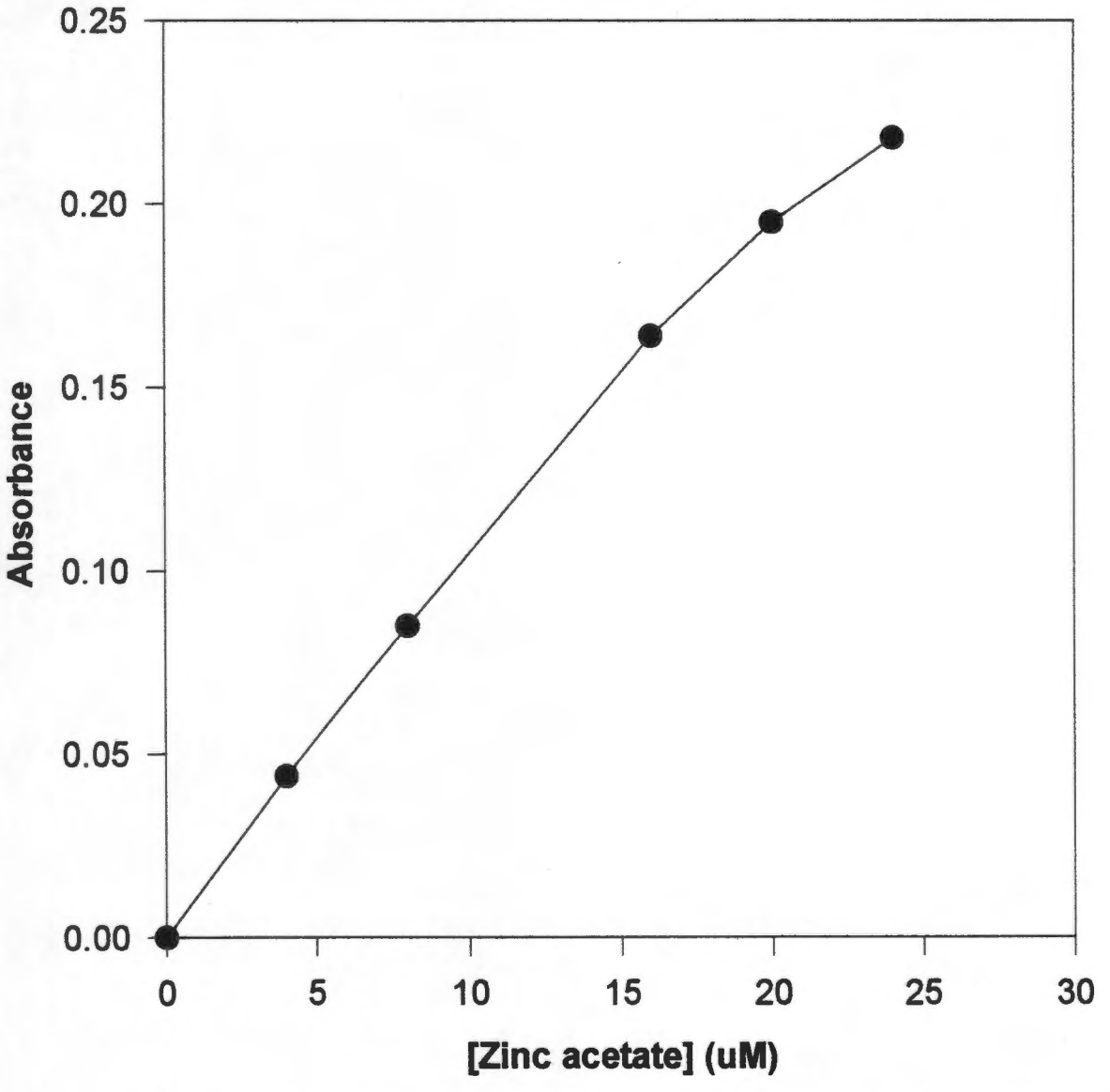

Calibration curve for determining Zn^{2+} levels in SRV preparations

50% change. These values, or potency of the chelator to lower $[Ca^{2+}]_{lim}$, and were found to be similar for each chelator, namely 0.5 μM. One explanation for the chelator effect might be the presence of heavy metal ions, such as Zn^{2+}, Al^{3+}, Cu^{2+} or Cd^{2+}.

3.2.4. Activation of the pump by micromolar EGTA at low Ca^{2+} concentrations:

Previously Berman (1982) found that CaEGTA appears to activate the pump at low free Ca^{2+} concentrations, by measuring Ca^{2+} transport with a Ca^{2+}-electrode and Ca^{2+}-stat method. This effect was also produced with the Fluo-3 system, using a Ca^{2+}-infusion method (Fig 34). At low free Ca^{2+} concentrations (lower than 100 nM), the binding affinity of Ca^{2+} to Ca^{2+}ATPase was increased in the presence of 2.5 μM EGTA.

3.2.5. Determination of Zn^{2+} levels in SRV preparations

Zn^{2+} content of SRV preparation was determined by atomic absorption spectrometry. A calibration curve was obtained using standard zinc solutions (Fig 35).

Table 5 lists four SRV preparations and the Zn^{2+} levels. On average a SRV preparation contained 18 μM Zn^{2+} or 0.52 nmole/mg of protein. The concentration of SR protein used in the fluorescence experiments was 0.25 mg of protein/ml, thus on average a minimum of about 0.13 μM Zn^{2+} was present in the assay medium.

Figure 36

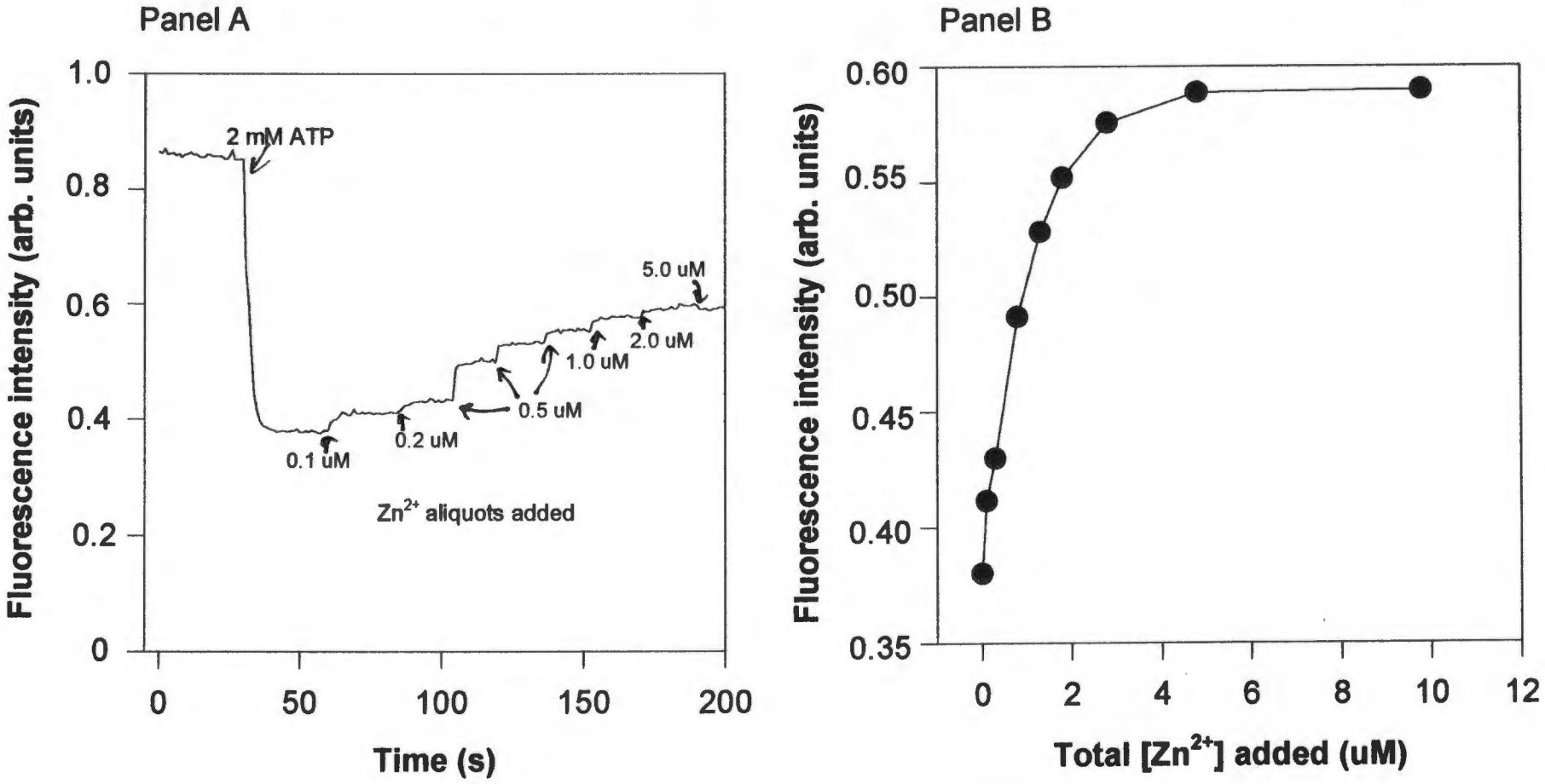

Influence of Zn^{2+} on Fluo-3 fluorescence signal
Panel A, SRV (0.25 mg of protein/ml) were incubated in 20 mM TRIS/MOPS, pH 6.8, 5 mM $MgCl_2$, 5 mM potassium oxalate. The Ca^{2+}ATPase was activated with 2 mM ATP. Increasing concentration of a 250 µM stock zinc acetate solution was added and the fluorescence increase recorded.
Panel B, The observed fluorescence increase was plotted against total Zn^{2+} added.

Table 5

Calculating $[Zn^{2+}]$ in SRV preparations with atomic absorption spectrometry

SRV preparation	[SRV] (mg/ml)	$[Zn^{2+}]$ (μM)	$[Zn^{2+}]$ (nmole/mg)
1	37.3	25	0.67
2	37.7	17	0.45
3	33.2	16	0.48
4	29.4	14	0.48

3.2.6. Influence of Zn^{2+} on the Fluo-3 fluorescence signal

To investigate the contribution of ZnFluo-3 fluorescence to the overall fluorescence signal, aliquots of Zn^{2+} were added to the standard assay mixture. Addition of Zn^{2+} caused an increase in the fluorescence signal, in much the same way as Ca^{2+} does (Fig 36). A plot of fluorescence versus total $[Zn^{2+}]$ indicates that 0.13 μM Zn^{2+} would bring about a 0.018 arb. unit fluorescence increase. Thus complexing Zn^{2+} by the chelators could significantly lower the apparent $[Ca^{2+}]_{lim}$.

3.2.7. Effect of 1 μM HEDTA on ZnFluo-3 fluorescence signal:

To test this possibility further, SRV (0.25 mg of protein/ml) were incubated in the standard assay medium. After activation with 2 mM ATP, 1 μM HEDTA was added. This led to the predicted drop in fluorescence, i.e. a lower fluorescence baseline value and $[Ca^{2+}]_{lim}$ (Fig 37A). Addition of 0.1 and 0.2 μM Zn^{2+} aliquots led to a transient increase in fluorescence, with a fast rise and slow decrease. Higher

Figure 37

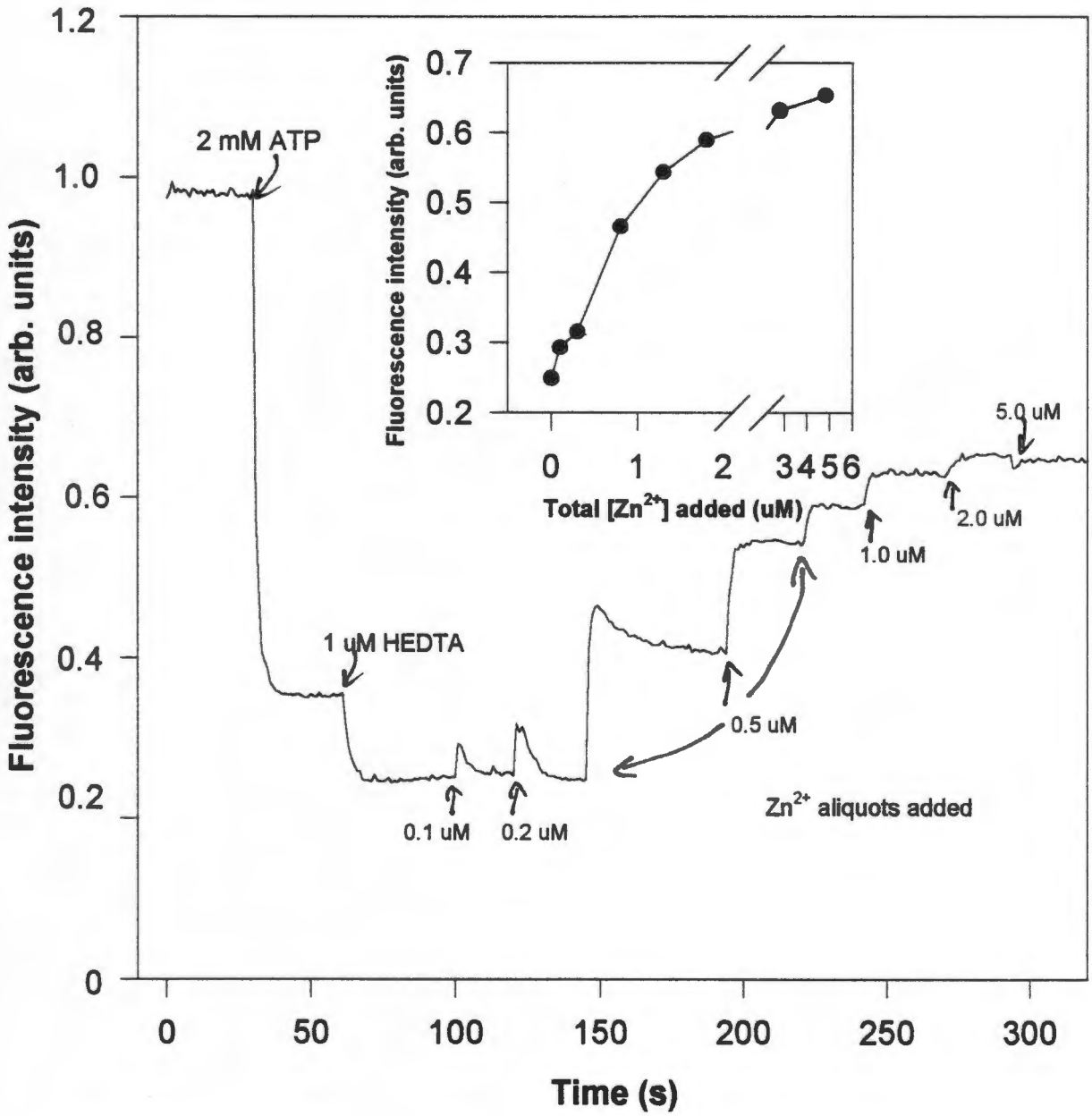

Effect of 1 uM HEDTA on Zn^{2+}Fluo-3 fluorescence

SRV were incubated in the same buffer solution and Ca^{2+}ATPase activated with 2 mM ATP, as mentioned in the legend of Fig 26. HEDTA (1 μM) and increasing concentration of 250 μM zinc acetate was added as before.

concentrations raised the baseline fluorescence and resulted in a higher final, steady state fluorescence. Further additions caused only increases in fluorescence. This possibly indicates that HEDTA was saturated with Zn^{2+}. The fluorescence level reached saturation with 0.8 µM total Zn^{2+}. The rise and subsequent decrease in fluorescence on addition of small amounts of Zn^{2+} might possibly be explained by Zn^{2+} binding rapidly to Fluo-3 followed by the slow chelation of Zn^{2+} by HEDTA. The drop in fluorescence after the addition of 1 µM HEDTA, is equivalent to the presence of 0.4 µM Zn^{2+} (see insert panel, Fig 37).

3.2.8. Effect of HEDTA and Zn^{2+} on Ca^{2+} transport characteristics:

Apart from the observation that the baseline fluorescence was lowered in the presence of a chelator, the time frame (t_{frame}) it took for the fluorescence to decrease to the baseline value upon the addition of a 20 µM aliquot of Ca^{2+} was retarded (Fig 38B). This suggest that the chelator removed an activator, eg. heavy metal ion. This was investigated further (Fig 38A). The pump was activated as before with ATP and a 20 µM Ca^{2+} aliquot was added to obtain the t_{frame}. 1 µM HEDTA was added, which resulted in a fluorescence drop, as was seen previously. Adding the same amounts of Zn^{2+} as in Fig 36, the t_{frame} was increased 3-4 fold as before. After the addition of total 0.8 µM Zn^{2+}, a steady state fluorescence level was reached. Addition of 20 µM Ca^{2+}, led again to an increase in fluorescence, and time frame for Ca^{2+} transport was not retarded as was the case when only HEDTA was present and no Zn^{2+} (Fig 38B).

Figure 38

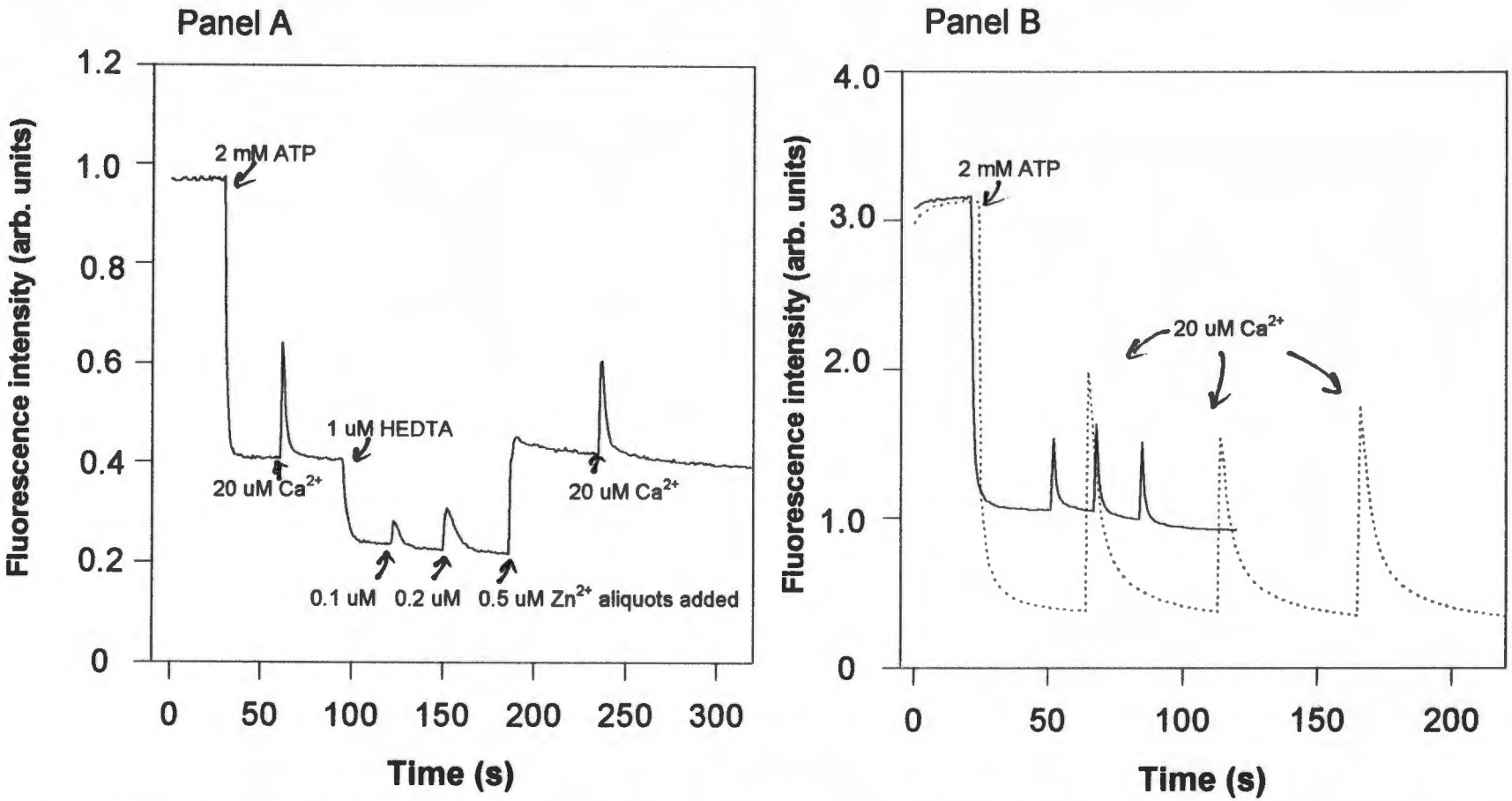

The effect of Zn^{2+} and HEDTA on Ca^{2+} transport characteristics measured by Fluo-3

Panel A, The effect of HEDTA on $[Ca^{2+}]_{1im}$ and Ca^{2+} transport characteristics was determined under similar reaction conditions, as described in the legend of Fig 20. Here, SRV were pre-incubated in a medium containing 0.7 μM HEDTA. The enzyme was activated as before and 20 μM $CaCl_2$ aliquots were added to the mixture as indicated on the trace.

Panel B, Similar reaction conditions were used as described in Panel A. Only one aliquot of 20 μM $CaCl_2$ was added, initially. Aliquots of HEDTA (1 μM), zinc acetate (0.1, 0.2, and 0.5 μM), and $CaCl_2$ (20 μM) were added as indicated on the traces.

Figure 39

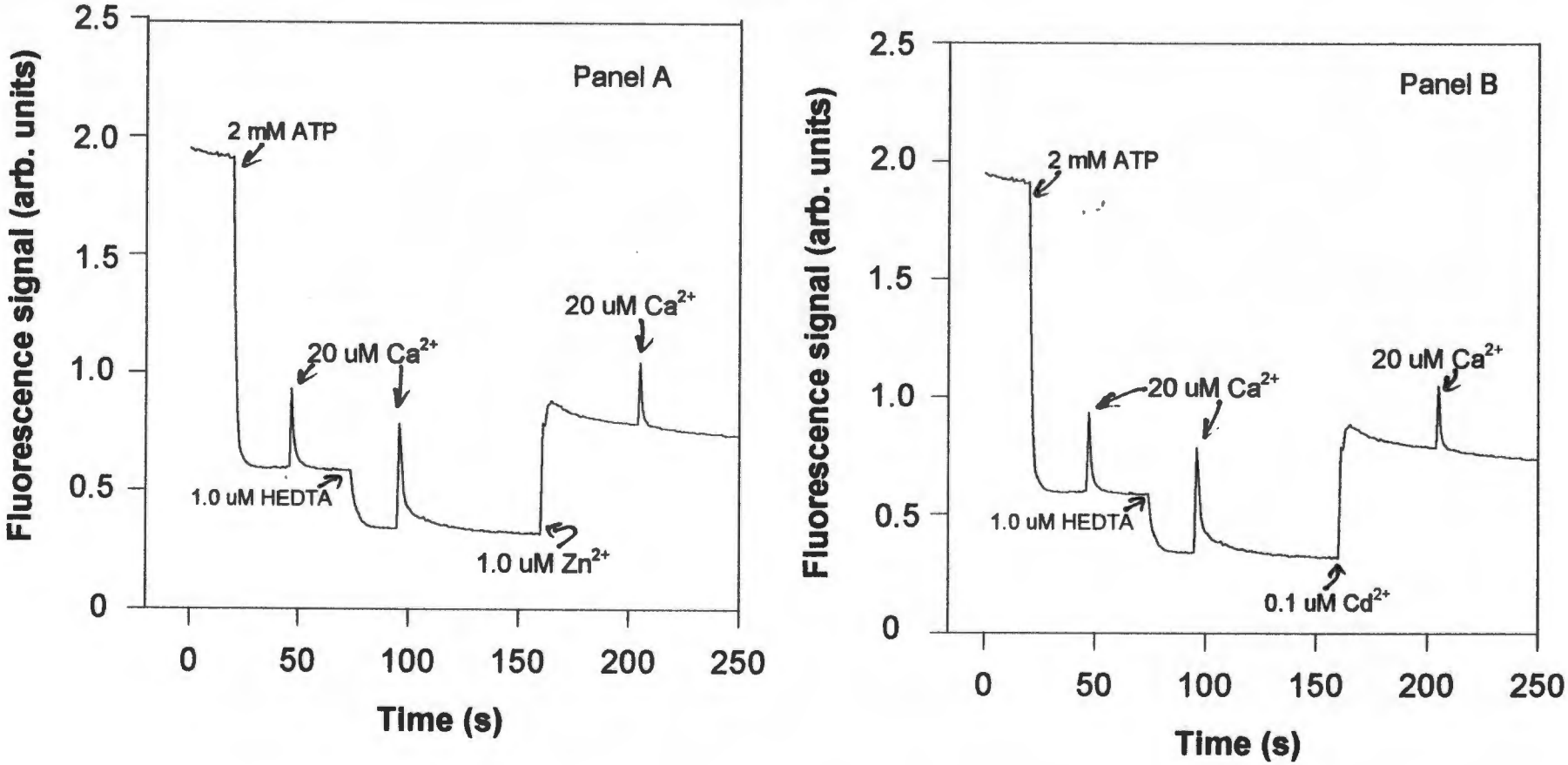

The effect of Zn^{2+} and Cd^{2+} on the Ca^{2+} transport rate

Panel A, The effect of Zn^{2+} on the Ca^{2+} transport rate was determined under similar reaction conditions, as described in the legend of Fig 38. SRV pre-incubated in the standard assay medium and the enzyme activated with 2 mM ATP. 20 µM $CaCl_2$, 1.0 µM HEDTA and 1.0 µM Zn^{2+} aliquots were added to the mixture as indicated on the trace.

Panel B, See panel A. An aliquot of 0.1 µM Cd^{2+} was added instead of 1.0 µM Zn^{2+}.

3.2. 9. Effect of Cd^{2+}, Fe^{2+} and Cu^{2+} on Ca^{2+} transport characteristics:

The Zn^{2+} effects were also examined with respect to other heavy metals, such as Cd^{2+}, Fe^{2+} and Cu^{2+}. The experimental protocol is first demonstrated with Zn^{2+} in Fig 39A, where aliquots of Ca^{2+} are added before and after 1 μM HEDTA addition and then after 1 μM of the heavy metal. It can be seen that 50 nmoles of Ca^{2+} is taken up more slowly after HEDTA addition and then accelerated back to the original speed on the addition of Zn^{2+}, although the difference is not as pronounced as when the chelator is added prior to the addition of ATP (compare Fig 39A with 38B). Rather surprisingly very small amounts of Ca^{2+} appeared to elicit a similar effect. Higher concentrations resulted in a huge increase in Fluo-3 fluorescence, and obviously Cd^{2+} interacts more strongly with the fluorophore than with the chelator. Cu^{2+} and Fe^{2+} caused the baseline fluorescence to drop and did not appear to accelerate transport (Fig 40). Thus use of heavy metal ions with Fluo-3 and chelators is complicated by differing stability constants and firm conclusions regarding stimulation of Ca^{2+} transport cannot be drawn, but there is some indication that the effect may be attributable to Zn^{2+}.

Figure 40

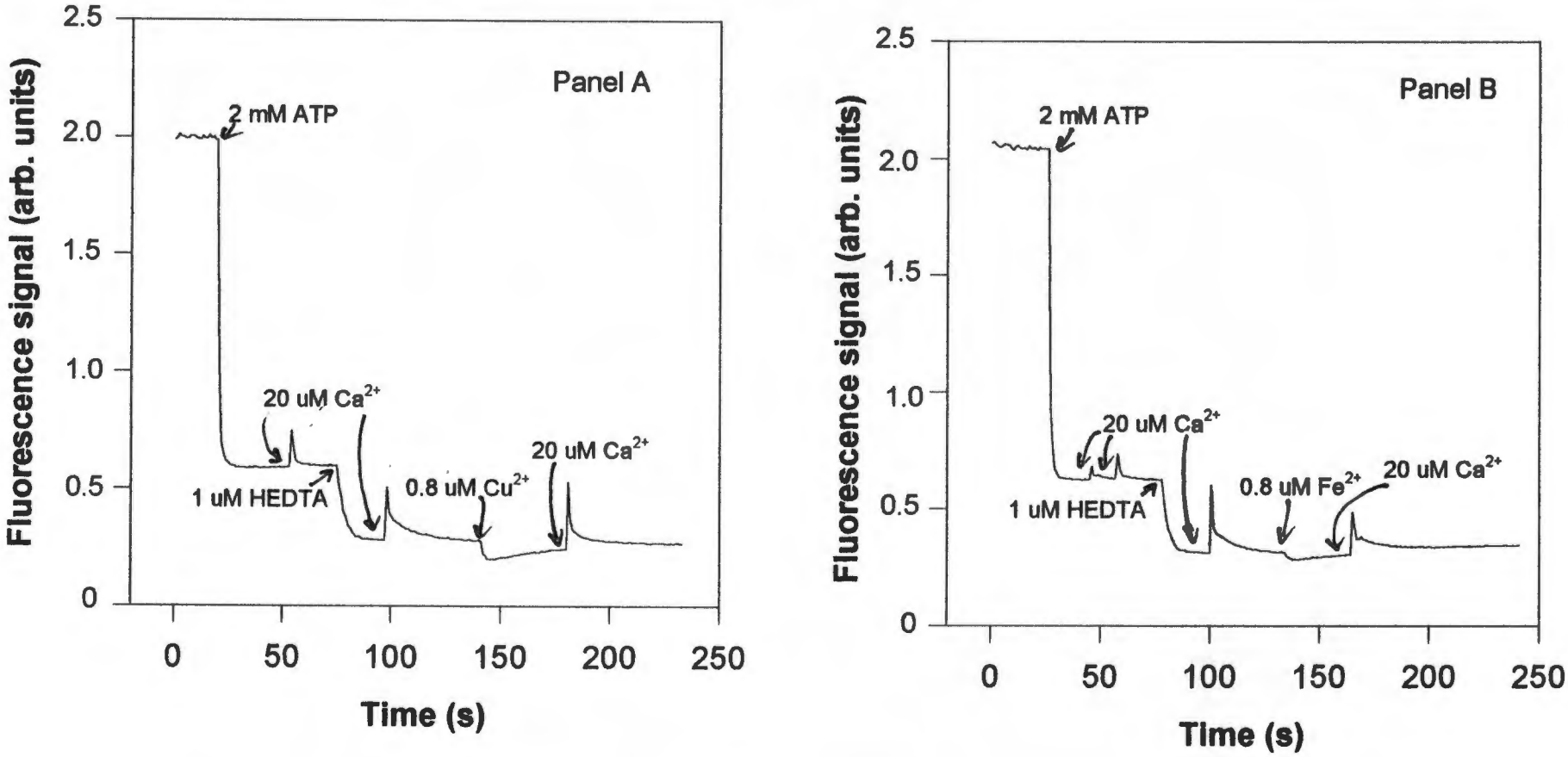

The effect of Fe^{2+} and Cu^{2+} on the Ca^{2+} transport rate

Panel A, See panel A of Fig 39. An aliquot of 0.8 μM Cu^{2+} was added as indicated in the trace.

Panel B, See panel A. An aliquot of 0.8 μM Fe^{2+} was added as indicated in the trace.

4. DISCUSSION

In this study two phenomena have been investigated.
One had to do with the relationship of the catalytic and regulatory nucleotide binding site(s) and the role of Lys492. It arose from the observation that the quenching of TNP-8N_3-AMP superfluorescence by Ca^{2+} is retarded if the nucleotide is covalently attached to Lys492 through light activation of the azido group. It was hoped that a comparison of the quench kinetics of mono-, di-, and triphospho TNP-nucleotides, tethered and untethered to Lys492 could provide some insights into ATP acceleration of the steps in the cycle.

The other phenomenon was an apparent inhibition of the pump by low concentrations of EGTA, seemingly enabling the pump to generate a greater Ca^{2+} concentration gradient across the SR membrane. It appeared as if the chelator could provide the Ca^{2+}ATPase with greater coupling efficiency.

Investigation of the Ca^{2+}-induced quench of the fluorescence of TNP-nucleotides tethered to Lys492 revealed that increasing the number of phospho groups had no effect on the slow kinetics. Neither did altering the pH in the range pH 5.5 to 6.5. Quenching the fluorescence with EDTA was very fast, too fast in fact for manual injection, showing that the step monitored following addition of Ca^{2+} was probably the E_2 to E_1 transition. The kinetics with untethered (free) TNP-8N_3-AMP and TNP-AMP were similar and showed an increase in the quench rate constant with a rise in pH from 5.5 to 6.5. The kinetics with the di- and triphospho TNP-nucleotides were complicated and suggested utilization of these nucleotides as substrates. Use of the nonhydrolysable

analogue, TNP-AMP-PCP, failed to elicit acceleration of the Ca^{2+} quench. The E_2 to E_1 transition is dependent on pH (Pick and Karlish, 1982; Froud and Lee, 1986; Wakabayashi *et al.*, 1990; Forge *et al.*, 1993). Three H^+ are involved in the equilibrium in the absence of Ca^{2+} (Forge *et al.*, 1993). The kinetics of Ca^{2+} binding is limited by the deprotonation steps (Forge *et al.*, 1993). Mg^{2+} also modifies the Ca^{2+} binding kinetics (Champeil *et al.*, 1983; Moutin and Dupont, 1991) and high Mg^{2+} can induce biphasic kinetics by altering the equilibrium in favour of deprotonated species producing a mixture of protonated and deprotonated forms (Forge *et al.*, 1993). ATP accelerates Ca^{2+} binding (Guillain *et al.*, 1981; Stahl and Jencks, 1984; Fernandez-Belda *et al.*, 1984; Wakabayashi and Shigekawa, 1990). The effect is pH dependent (Mintz *et al.*, 1995). ADP and AMP-PCP increase the rate of Ca^{2+} binding up to 20-fold at pH 6.0 and change biphasic kinetics to a single fast phase at pH 7.0.

There is an order of magnitude time scale difference between the $E_2 \leftrightarrow E_1$ transition in our fluorescence experiments and that normally observed for Ca^{2+} binding at pH 6.0, which is complete within 2 s (Forge *et al.*, 1993), whereas the Ca^{2+} quench of superfluorescence of untethered and tethered TNP-$8N_3$-AMP occurs over approximately 50 and 500 s, respectively. This slowness can probably be attributed to the presence of glycerol in the medium. Glycerol is added to enhance phosphorylation and hence superfluorescence (Watanabe and Inesi, 1982). Phosphoenzyme decay induced by Ca^{2+} addition at pH 6.0 or 6.2 occurs at 0.35 s^{-1}; 0.002 s^{-1}; 0.0115 s^{-1} and 0.035 s^{-1} in aqueous medium, 40% dimethyl sulphoxide, 40% glycerol, and 30% dimethyl sulphoxide, respectively (de Meis *et al.*, 1980). The cosolvents probably slow the conformational changes associated with the deprotonation

events. It can be seen from the pH dependence of the quench experiments with tethered nucleotide that the ionizations still occur. The very much slower $E_2 \leftrightarrow E_1$ transition for the tethered nucleotide and its pH independence suggest that another conformational change is rate limiting here. Tethering TNP-8N_3-ATP to Lys492 accelerates phosphorylation slightly in the forward direction of catalysis and partially uncouples the pump (McIntosh and Woolley, 1994). A small nonstoichiometric amount of Ca^{2+} transport is only observed at low pH. These findings, together with our fluorescence results, suggest that tethering principally effects steps $E_1P \leftrightarrow E_2P$ and $E_2 \leftrightarrow E_1$. Perhaps not coincidentally these are the main steps accelerated by ATP binding in a regulatory mode.

Site-directed mutagenesis of Lys492 has recently implicated it in ATP binding and ATP dependent conformational changes associated with regulation of the cycle (McIntosh *et al.*, 1991). There may be a pronounced change in the configuration of the nucleotide binding site during the $E_1P \leftrightarrow E_2P$ and $E_1 \leftrightarrow E_2$ steps. These changes in the microenvironment of the nucleotide binding site maybe necessary for ATP regulation to take place. Tethering TNP-8N_3-ATP to Lys492 might inhibit these changes and therefore no acceleration of the $E_1 \leftrightarrow E_2$ step can occur. Yamamoto *et al.* (1989) have provided evidence through a Ca^{2+}-induced change in conformation around the nucleotide binding site as adenosinetriphosphopyridoxal (AP_3PL) labels Lys492 in EGTA and both Lys684 and Lys492 in the presence of Ca^{2+}. Thus, the target specificity of AP_3PL changes significantly, but not entirely on Ca^{2+} binding, so that the spatial arrangement around the γ-phosphate group of the bound ATP is affected by Ca^{2+} bound at the transport sites.

The E_2 intermediates of SR Ca^{2+}ATPase and Na^+K^+ATPase have different affinities for ATP. Both the E_1 and E_2 intermediates of SR Ca^{2+}ATPase display micromolar affinity for ATP (Meissner, 1973; Lacapere *et al.*, 1990; Wakabayashi *et al.*, 1990). The E_2 intermediates of Na^+K^+ATPase have a lower affinity for ATP compared to the E_1 intermediates (Post *et al.*, 1972, Esmann and Skou, 1983; Skou and Esmann; 1983; Esman, 1994). However, TNP-ATP display a higher affinity for the E_2 intermediates, as it is increased 4-fold by K^+ binding, from 0.09 to 0.38 μM (Moczydlowski and Fortes, 1981).

The deocclusion rate constant of Rb^+ from the Na^+K^+ATPase E_2.Rb intermediate is accelerated by ATP and ADP, and both appear to act at low affinity sites, without phosphorylating the enzyme. The difference in ATP affinities for the E_2 intermediates of SR Ca^{2+}ATPase and Na^+K^+ATPase, can possibly be explained that the SR Ca^{2+}ATPase does not reach an intermediate that is similar to the occluded Rb^+ intermediate of Na^+K^+ATPase at low pH. However, thapsigargin, a specific inhibitor of Ca^{2+}ATPase, binds to the E_2 intermediate to form the E_2.thapsigargin complex. It is possible that this E_2.thapsigargin intermediate complex is similar to the occluded form of Na^+K^+ATPase (E_2.Rb). The E_2.thapsigargin intermediate complex has a 100-fold lower affinity for ATP, although the affinity for TNP-ATP is not affected (DeJesus *et al.*, 1993; McIntosh *et al.*, 1994). It is clear that the TNP-moiety plays a major role in the binding of TNP-ATP to the low affinity ATP binding site. TNP-ATP accelerates ATP hydrolysis (Dupont *et al*, 1985) and phosphoenzyme hydrolysis (Champeil *et al.*, 1988). However, no acceleration of the $E_2 \leftrightarrow E_1$ step was observed. Mintz *et al* (1995) have shown that ADP, AMP-PCP and AMP-PNP

accelerate the conformational change $E_2 \leftrightarrow E_1$. The deprotonation steps involved in the conformational change $E_2 \leftrightarrow E_1$ can be represented in a scheme (Mintz *et al.*, 1995):

Scheme 7

Mintz *et al.* (1995)

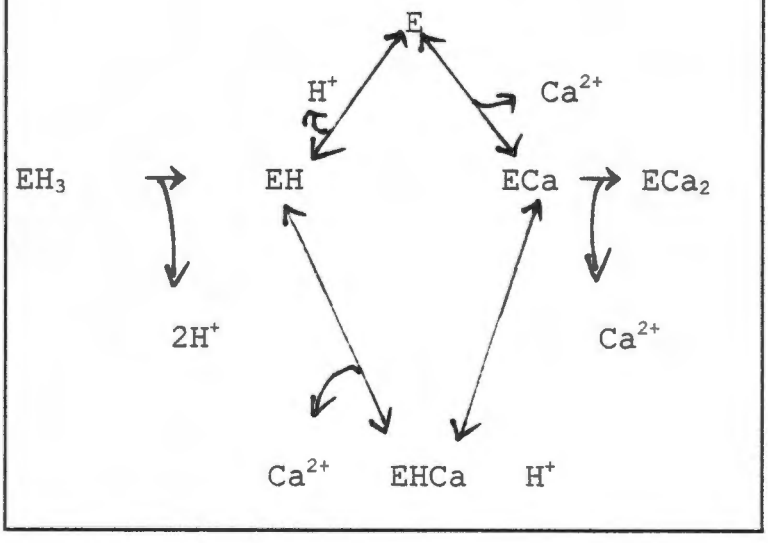

It is not known which deprotonation step is the slowest and accelerated by ATP. It is possible that in the presence of glycerol a different slow step prevails, one that is not accelerated by ATP. It would be interesting to check by direct $^{45}Ca^{2+}$ binding measurements using rapid filtration whether glycerol eliminates ATP activation of the binding kinetics. Alternatively the TNP-nucleotides may not accelerate the slow step as ATP does. There does not appear to be any report in the literature of TNP-nucleotides accelerating Ca^{2+} binding.

Our results show that the complicated kinetics following Ca^{2+} addition to Ca^{2+}ATPase in the presence of the di- and

triphospho TNP-nucleotides can be explained by utilization of the nucleotides as substrates in the forward direction of catalysis. Hydrolysis of the nucleotides was directly demonstrated by monitoring each mono-, di- and triphospho species by HPLC. This result contradicts previous reports that TNP-ATP is not a substrate of Ca^{2+}ATPase (Watanabe and Inesi, 1982; Dupont *et al.*, 1985). This discrepancy is probably due to the very low rate of hydrolysis and suboptimum conditions previously used, particularly the pH. It is in agreement with our previous study that TNP-8N_3-ATP is a well coupled substrate of the Ca^{2+}ATPase (McIntosh and Woolley, 1994). Hydrolysis of TNP-ATP by Ca^{2+}ATPase could not be unequivocally demonstrated by HPLC analysis as there was a significant amount of Ca^{2+}-independent activity that was not inhibitable by thapsigargin. However, there was no lag in TNP-ATP stimulation of Ca^{2+} transport or of superfluorescence in the forward direction of catalysis, suggesting direct activation by the triphosphonucleotide. The rate of Ca^{2+} transport with TNP-ATP and TNP-ADP are similar and the lag in the quench of superfluorescence on addition of Ca^{2+} was approximately double with TNP-ATP compared to TNP-ADP, again suggesting that the triphospho species is utilized directly, followed by the diphospho form. Hydrolysis of TNP-ATP in the presence of EGTA or thapsigargin is probably catalysed by the small amount of myosin contaminating the preparation. Myosin hydrolyses TNP-ATP almost as well as ATP (Hiratsuka and Uchida, 1973). The azido species seem to be only hydrolysed by the Ca^{2+}ATPase.

This is the first time that an ADP analogue has been found to be a substrate of Ca^{2+}ATPase in the forward direction of catalysis. Normally ADP is a substrate in the reverse direction, interacting with E_1P to form ATP. There seem to be no priori or physiological reason why

ADP should not also be a substrate in the forward direction, unless activation of Ca^{2+}ATPase by reversal of the pump is a physiologically important pathway for Ca^{2+} release, which seems not to be the case. Rather it is likely that the failure of ADP to act as a substrate is due to configuration constraints, exact fitting of the substrate into its binding pocket and stabilization through binding energy. The structure of a substitution-inert $Co(NH_3)_4ATP_2$ at the active site of the homologous Na^+K^+ATPase has been determined by NMR (Stewart and Grisham, 1988; Stewart *et al.*, 1989). The molecule adopts a U-shape with the phosphates lying parallel to the adenine ring. In this way, if the adenine and ribose are interacting fairly strongly with their binding site it is impossible for the β-phosphate of ADP to be placed in the same position as the γ-phosphate of ATP. However, if the TNP-moiety of TNP-ATP interacts more strongly with another pocket such that the adenine and ribose are pulled out of position, the β-phosphate of TNP-ADP may align itself with the position normally occupied by the γ-phosphate of ATP (Fig 41). A site-directed mutagenesis study of the amino acids around Lys492 indicates that TNP-$8N_3$-ATP and ATP interact in a different way with this putative loop (McIntosh *et al.*, 1997). Some amino acid mutations that change the affinity for ATP by 1000-fold, have no effect on TNP-$8N_3$-ATP affinity. Clearly the TNP-moiety changes the interaction of the remaining portion of the nucleotide with the active site.

The hydrolysis rate of TNP-$8N_3$-ATP was similar to -ADP, 15 and 10-12 nmoles/min/mg of protein, respectively. In the case of the nonazido derivatives, TNP-ADP was hydrolysed twice as fast as -ATP, 10-12 and 5 nmoles/min/mg of protein, respectively. All four TNP-nucleotides support Ca^{2+} transport. TNP-ADP and -ATP

Figure 41

Mechanism of TNP-ADP utilization as a substrate

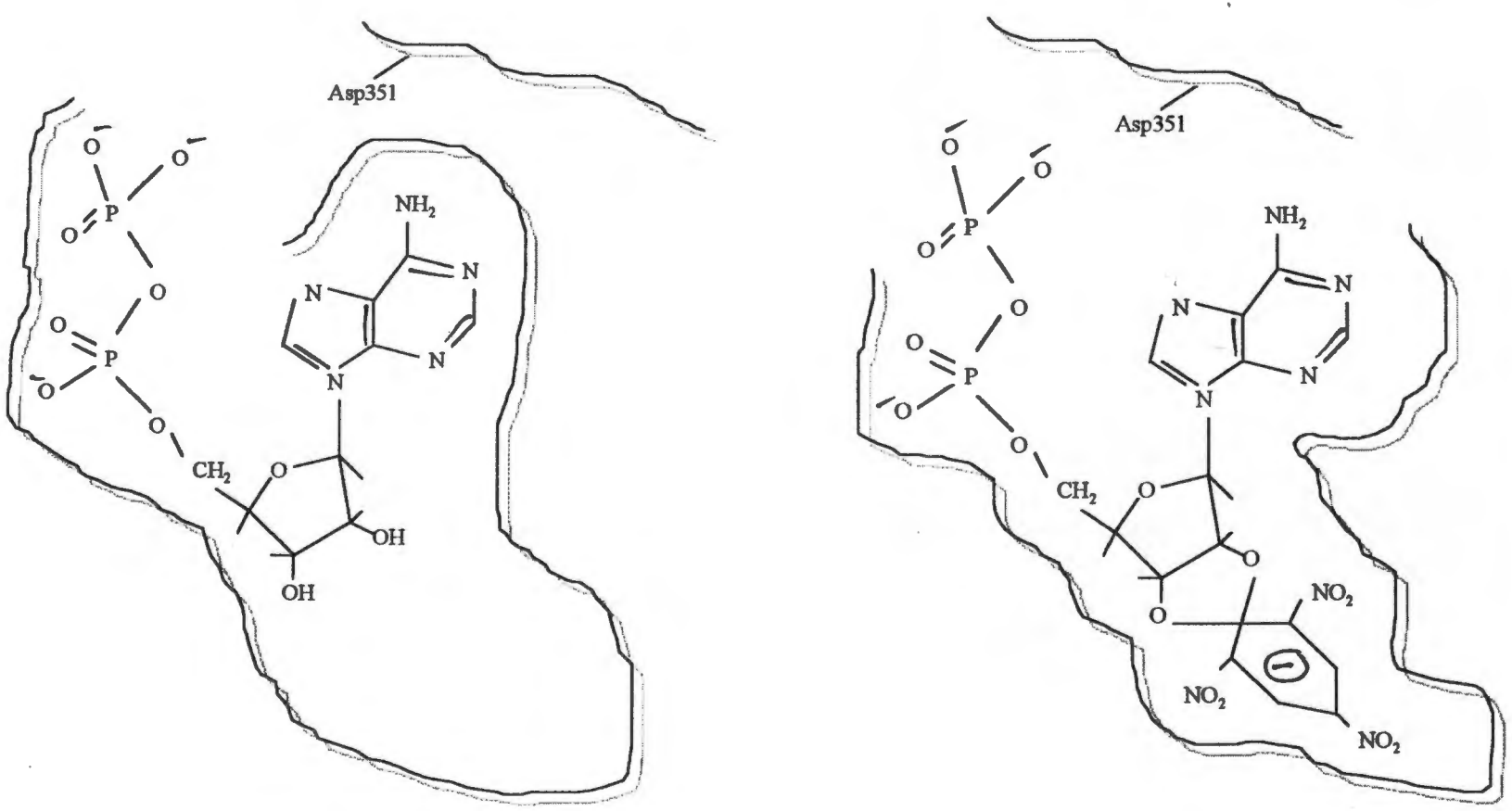

displayed lower transport rates (8-10 nmol/min/mg of protein) than their azido derivatives (25 and 32 nmol/min/mg of protein). The low rate for the nonazido nucleotides coupled with apparent tight binding did not permit distinction between rates at different nucleotide concentrations. The azido nucleotides have an approximate K_m of 0.5 μM.

It is interesting to consider whether the true substrate of Ca^{2+}ATPase is the protonated or deprotonated TNP-nucleotide (Scheme 5). The transport assays were performed at pH 5.5 and the TNP-nucleotides have a pK_a of 5.1 (Hiratsuka, 1975), which means that 40% of the nucleotide will be protonated. Upon protonation, the Meissenheimer complex is destroyed and this renders the nucleotide nonfluorescent and much more flexible. Our results show that, at least in the presence of glycerol, a rise in pH from 5.5 to 6.5 increase the rate of TNP-ATP, -ADP, TNP-$8N_3$-ATP and -ADP hydrolysis (Fig 13 and 14). This suggests that the unprotonated forms are the substrates. However, this pH dependence is opposite to that obtained in the absence of glycerol for TNP-$8N_3$-ATP (McIntosh and Woolley, 1994), and the pH dependence of hydrolysis may be a poor means of answering this question. The tight binding of the TNP species is almost certainly due to the Meissenheimer complex as this high affinity is observed at alkaline pH. It seems likely that the possible forms exhibit a low affinity for the Ca^{2+}ATPase and possibly can be discounted as significant substrates.

As mentioned above, TNP-$8N_3$-ATP and TNP-$8N_3$-ADP are hydrolysed by Ca^{2+}ATPase with equal facility. Tethering TNP-$8N_3$-ATP to Lys492 has been shown to accelerate the Ca^{2+}-dependent hydrolysis of the γ-phospho group about

3-fold and Ca^{2+} transport can be observed at low pH (McIntosh and Woolley, 1994). Can tethered TNP-$8N_3$-ADP also be utilized as a substrate? The tri-, di-, and monophospho TNP nucleotide label Lys492 with equal ease, suggesting that the adenine and TNP-ribose moieties bind independently of the phospho groups, and one could predict that if the untethered nucleotide are substrates, so should the tethered form as well. We obtained no evidence in the form of complicated kinetics with the tethered nucleotides that they were being utilized as substrates. The low levels of E_2P that could be generated probably renders their detection impossible. It would be interesting to test out the hydrolysis of [β-^{32}P]TNP-$8N_3$-ADP directly.

The superfluorescence generated in the forward direction of catalysis was enhanced in the presence of P_i. This superfluorescence enhancement was turnover dependent, as it was not observed with the monophospho TNP-nucleotides. Therefore, a reasonable explanation is that E_2 that is generated as a result of enzyme turnover and the slowness of the $E_2 \leftrightarrow E_1$ step, reacts with P_i to form the superfluorescent E_2P species. Quite distinct superfluorescence kinetics was observed for the azido and nonazido nucleotides under these conditions. These differences might be explained by the *anti* and *syn* configuration of the nonazido and azido nucleotides and their different binding affinities for Ca^{2+}ATPase.

The other phenomenon investigated was an effect of small amounts of EGTA to apparently lower the limiting concentration of Ca^{2+} to which the Ca^{2+}ATPase can pump ($[Ca^{2+}]_{lim}$). This effect was observed using Fluo-3 as the Ca^{2+} monitoring chromophore and otherwise under standard conditions of transport in the presence of oxalate.

Addition of aliquots of Ca^{2+} showed that the pump was partially inhibited by the presence of chelator. This effect was not unique to EGTA, and chelators EDTA, BAPTA, NTA, DTPA and HEDTA all exhibited very similar behaviour in lowering $[Ca^{2+}]_{lim}$ with the same $K_{0.5}$ (0.5 μM) and retarding Ca^{2+} uptake.

This particular chelator effect appears to be different, and yet perhaps related, from a phenomenon previously described where at low Ca^{2+} concentrations, low enough to limit pump turnover, CaEGTA appears to activate the pump (Berman, 1982). This activation occur when Ca^{2+} transport is measured by a Ca^{2+}-stat method using a Ca^{2+}-electrode and Ca^{2+} infusion. The activation occurs with a $K_{0.5}$(CaEGTA) of 19 μM and is specific for EGTA. This effect could be produced with the Fluo-3 system, if Ca^{2+} uptake was measured by statting and infusion (Fig 34).

Returning to the nonspecific chelator effect of lowering $[Ca^{2+}]_{lim}$ coupled with pump inhibition, it is difficult to conceive of a mechanism in which such an effect is executed through direct interaction of such diverse chelators with the Ca^{2+}ATPase, rather indirect mechanisms need to be considered.

One possibility that we considered was that the ability of the pump to apparently increase the Ca^{2+} gradient is due to the increased thermodynamic efficiency (Gafni and Boyer, 1985). This requires that less Ca^{2+} is pumped per ATP hydrolysed, i.e. more energy from the latter being used to raise the gradient. Gafni and Boyer (1985) associated this possibility with a change in stoiciometry from 2 to 1 Ca^{2+}/ATP in going from high to low Ca^{2+} concentrations. Evidence for low Ca^{2+}/ATP stoichiometry has been obtained previously with a Ca^{2+}-electrode stat

method (Meltzer and Berman, 1984). There is general consensus now that 2 Ca^{2+} are required for phosphorylation by ATP to occur (Jencks, 1982) and any decrease in stoichiometry would have to implicate other steps in the cycle. While this mechanism remains a possibility it is difficult to prove.

Another possibility that we considered was an effect of heavy metal ions. One property which the chelators have in common is a very high affinity for heavy metal ions. The stability constants of metal ion/chelator complexes Zn^{2+}, Al^{3+}, Cd^{2+}, Cu^{2+}, Fe^{2+}/EGTA, BAPTA, EDTA, NTA, DTPA and HEDTA were calculated for our conditions using the Fabiato programme (Fabiato and Fabiato, 1973)(Fig 42). These complexes are all more stable than Ca^{2+} or Mg^{2+}/chelator complexes. The values obtained for the Zn^{2+} and Ca^{2+}/chelator complexes are listed in Table 5.

Table 5
Apparent stability constants of Zn^{2+} and Ca^{2+} chelator complexes

Chelator	K(Zn^{2+}chelator) (μM)	K(Ca^{2+}chelator) (μM)
EGTA	8.68e+00	1.03e6
BAPTA	Unknown	9.33e6
NTA	1.74e+14	5.75e8
EDTA	9.753e12	1.01e7
DTPA	Unknown	1.38e5
HEDTA	3.75e+11	1.47e5

It therefore seems possible that at low Ca^{2+} concentrations and sufficient contaminating heavy metal

Figure 42
Apparent stability constants of metal chelator complexes

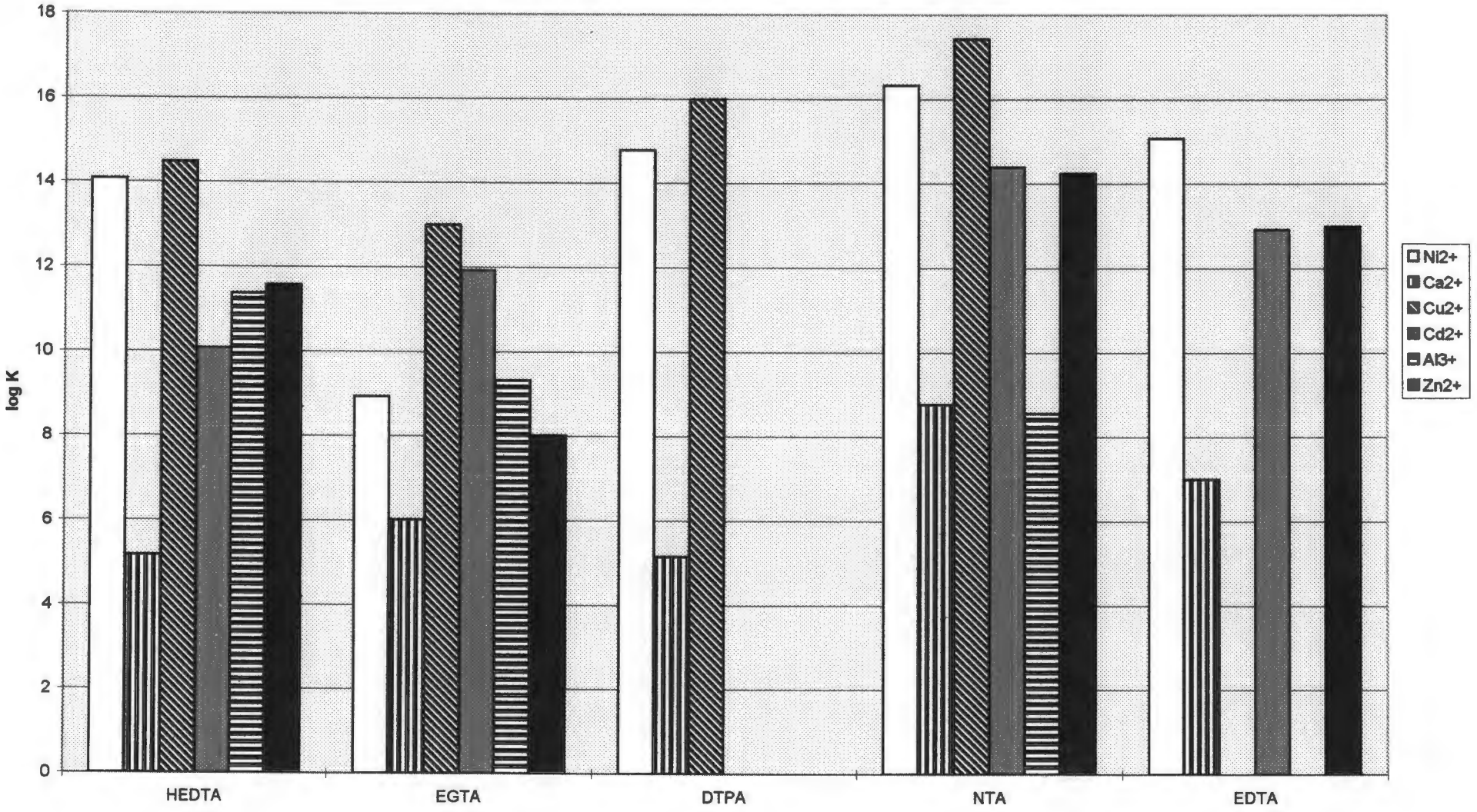

ions, there may be significant Fluo-3 interaction and the addition of low concentrations of chelators could preferentially complex the heavy metal ions, lowering the chromophore fluorescence and hence the apparent $[Ca^{2+}]_{lim}$.

The ability of heavy metal ion/Fluo-3 interaction to yield fluorescence was tested directly and, indeed low concentrations of Zn^{2+} produced significant Fluo-3 fluorescence. Cd^{2+} seemed particularly effective in this regard, although it was not explored in detail.

Atomic absorption analysis of several SRV preparations indicated the presence of Zn^{2+} at 0.52 nmol/mg of protein, or approximately 0.1 mol Zn^{2+}/mol ATPase. At the concentration of protein used in the assay medium, this translated to a concentration of Zn^{2+} of 0.13 μM. As demonstrated, this amount of Zn^{2+} would account for approximately 50% of the fluorescence change produced by the addition of chelator under the conditions of the Ca^{2+} uptake assay. It is very likely that SRV are not the only source of Zn^{2+} and/or other heavy metal ions could also be present from buffers, cation solutions and potassium oxalate. Thus we consider it likely that most of the drop in fluorescence on the addition of chelators is due to the complexation of heavy metals and the rest due to Ca^{2+} chelation.

The involvement of heavy metal ions in the observed effects is strengthened somewhat by our finding that following chelator addition and drop in apparent $[Ca^{2+}]_{lim}$, addition of exogenous Zn^{2+} to bring the baseline fluorescence back to the original $[Ca^{2+}]_{lim}$ level, results in activation of the pump with an aliquot of Ca^{2+} to the original rate.

Activation of Ca^{2+} uptake by Zn^{2+} would be a puzzle, as heavy metal ions are expected to inhibit the pump by either binding to the Ca^{2+} sites or generating sufficient ZnATP to compete with MgATP for the active site. It is not clear what steps is rate-limiting under our conditions in the presence of oxalate. It is possible it is the precipitation of Ca^{2+}oxalate in the vesicle lumen or the diffusion of oxalate into the lumen. However it is difficult to imagine how small amounts of Zn^{2+} could facilitate either of these processes in the face of millimolar concentrations of oxalate. Oxalate does not appear to chelate Zn^{2+} significantly in the presence of 5 mM $MgCl_2$ as judged from expected Zn^{2+}/Fluo-3 fluorescence and the amount obtained. Therefore a direct effect of heavy metals in facilitating Ca^{2+} release from the Ca^{2+}ATPase to the lumen should be considered.

The structure of heavy metal binding sites of many proteins have been elucidated. Amino acid residues cysteine, histidine, aspartic acid and glutamic acid are almost always involved. For example, Zn^{2+} enzymes, Aspartyltranscarbamylase, RNA polymerases, carboxy-peptidase A, Thermolysin, Alkaline phosphotase, Phospholipase C, and Zn^{2+} containing transcription factors all contain clusters of histidine and/or cysteine residues alone or in association with acidic residues (Coleman, 1993). Cu^{2+}ATPases from mammals and bacteria contain Cu^{2+} binding motifs on the amino acid terminal tail (Solioz *et al.*, 1994). They are mostly made up of clusters of MTCXSC and MDHSH segments.

The Ca^{2+}ATPase contains 5 short lumenal loops. The sequences of loops 1,2, and 4 are shown in Fig 43. Loop 1 contains a cluster of 4 glutamates, Loop 2, 2 histidines, and Loop 4, 4 histidines, 2 cysteines, and 7 acidic residues. The cluster of histidines and cysteines in the

latter loop is especially significant and occurs nowhere else in the sequence. Three of the histidines are not conserved in the slow twitch SERCA2 isoform, and are

Figure 43

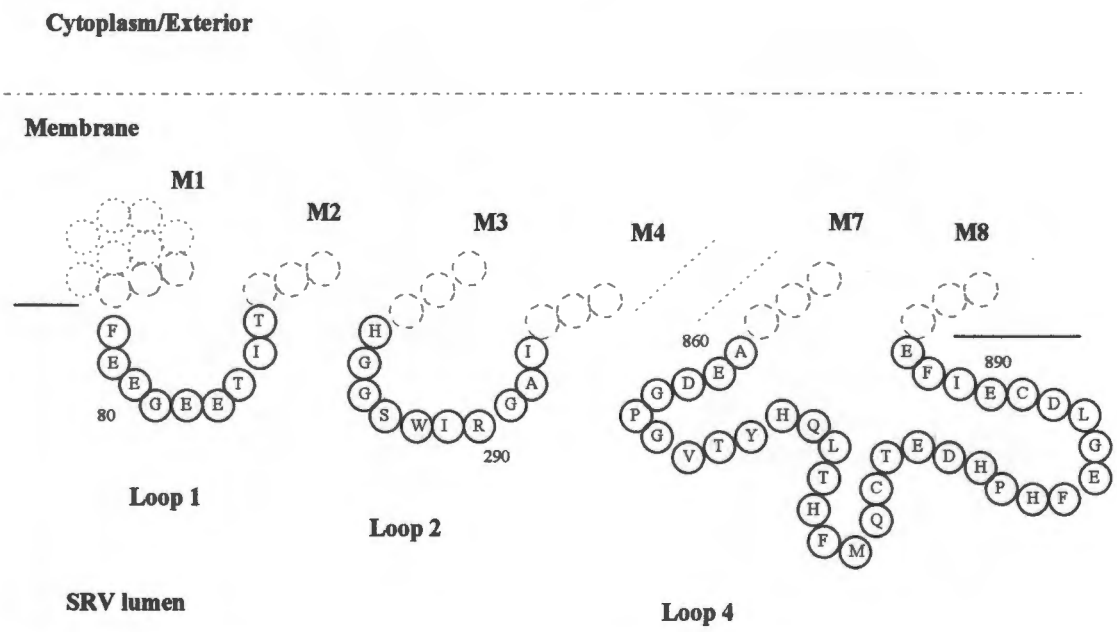

evidently not essential for Ca^{2+} transport. It seems possible that Loop 4 contains 1-2 heavy metal ion binding sites that when occupied accelerate the off rate of Ca^{2+} to the lumen. Membrane helix M8 has been implicated in a peripheral role in the Ca^{2+} binding site and M7 is considered to be obliquely angled with respect to the axis normal to the mebrane (Stokes and Green, 1994). Binding of a heavy metal ion in Loop 4 could pull the ends together significantly repositioning helix M8 (and M7) and facilitating Ca^{2+} dissociation to the lumen.

Examination of the effects of other heavy metal ions (i.e. Cd^{2+}, Cu^{2+} and Fe^{2+}) on the chelator phenomonen revealed that the assay system is complicated and future investigation would be necessary before firm conclusions of the Zn^{2+} effect on Ca^{2+} release can be drawn. In this

regard it would be interesting to examine the effects of Zn^{2+} and other heavy metal ions on $^{45}Ca^{2+}$ release to the lumen. However, it would be difficult to distinguish an effect on the substrate site from one on the luminal sites (Wakabayashi and Shigekawa, 1987).

5. REFERENCES

Ah-Kow, G., Turner, F., Pouet, M.-J., and Simonnin, M.-P., (1980) *J. Org. Chem.* **45**, 4399-4404

Al-Jobore, A., and Roufogalis, B. D., (1981) *Biochim. Biophys. Acta* **645**, 1-9

Allen, G., and Green, N. M., (1976) *FEBS Lett.* **63**, 188-192

Andersen, J. P., Moller, J. V., and Jorgensen, P. L., (1982) *J. Biol. Chem.* **257**, 8300-8307

Anderson, K. W., and Murphy, A. J., (1983) *J. Biol. Chem.* **258**, 14276-14278

Andersen, J. P., (1989) *Biochim. Biophys. Acta.* **988**, 47-72

Andersen, J. P., Vilsen, B., Leberer, E., and MacLennan, D. H., (1989) *J. Biol. Chem.* **264**, 21018-21023

Andersen, J. P., (1995) *J. Biol. Chem.* **270**, 908-914

Andersen, J. P., and Vilsen, B., (1996) *Biochim. Biophys. Acta.* **1275**, 118-122

Banks, R. D., Blake, C. C. F., Evans, P. R., Haser, R., *Biochemistry* **29**, 7040-7045

Bayley, H., and Knowles, J. R., (1077) *Methods Enzymol.* **46**, 69-114

Beil, F. U., Chak, D., and Hasselbach, W., (1977) *Eur. J. Biochem.* **81**, 151-164

Berman, M. C., (1982) *J. Biol. Chem.* **257**, 1953-1957

Berman, M. C., King, S. B., (1990) *Biochim. Biophys. Acta* **1029**, 235-240

Bigelow, D. J., and Inesi, G., (1992) *Biochim. Biophys. Acta* **1113**, 323-338

Bishop, J. E., Johnson, J. D., and Berman, M. C., (1984) *J. Biol. Chem.* **259**, 15163-15171

Bishop, J. E., Nakamoto, R. K., and Inesi, G. (1986) *Biochemistry* **25**, 696-703

Bishop, J. E., Al-Shawi, M. K., and Inesi, G. (1987)
J. Biol. Chem. **262**, 4658-4663

Bishop, J. E., and Al-Shawi, M. K., (1988)
J. Biol. Chem.. **263**, 1886-1892.

Bodley, A. L., and Jencks, W. P. (1987)
J. Biol. Chem. **262**, 13997-14004

Branden, C. I., Jornvall, H., Eklund, H., and Furugren, B., (1975) in The Enzymes (Boyer, P. D., ed) Vol. 11, pp. 103-190, Academic Press, New York

Brandl, C. J., Green, N. M., Korczak, B., and MacLennan, D. H., (1986) *Cell.* **44**, 597-607

Brandl, C. J., and Struhl, K., (1989) *Proc. Natl. Acad. Sci. USA* **86**, 2652-2656

Cable, M. B., Feher, J. J., and Briggs, F. N., (1985)
Biochemistry **24**, 5612-5619

Canet, D., Forge, V., Guillain, F., and Mintz, E., (1996)
J. Biol. Chem. **271**, 20566-20572

Carvalho, M. G. C., Souza, D. O., and de Meis, L., (1976)
J. Biol. Chem. **251**, 3629-3639

Carvalho-Alves, P.C., Oliviera, C. R. G., and Verjovski-Almeida, S., (1985) *J. Biol. Chem.* **260**, 4282-4287

Chaloub, R. M., Guamaraes-Motto, H., Verjovski-Almeida, S., de Meis, L., and Inesi, G., (1979)
J. Biol. Chem. **254**, 9464-9468

Champeil, P., Gingold, M. P., Guillain, F., and Inesi, G., (1983) *J. Biol. Chem.* **258**, 4453-4458

Champeil, P., Guillain, F., Venien, C., and Gingold, M. (1985) *Biochemistry* **24**, 69-81

Champeil, P., and Guillain, F., (1986)
Biochemistry **25**, 7623-7633

Champeil, P., le Maire, M., Andersen, J. P., Guillain, F., Gingold, M., Lund, S., and Moller., J. V., (1986)
J. Biol. Chem. **261**, 16372-16384

Champeil, P., Riollet, S., Orlowski, S., Guillain, F., Seebregts, C. J., and McIntosh, D.B., (1988) *J. Biol. Chem.* **263**, 12288-12294

Chang, A., and Slayman, C. W., (1990) *J. Biol. Chem.* **265**, 15531-15536

Chen, Z., Coan, C., Fielding, L., and Cassafer, G., (1991) *J. Biol. Chem.* **266**, 12386-12394

Chen, Z. D., Sumbilla, C., Lewis, D., Zhong, L., Strock., C., Kirtley, M. E., and Inesi, G. (1996) *J. Biol. Chem.* **271**, 10745-10752

Chowdry, V., and Westheimer, F. H., (1979) *Annu. Rev. Biochem.* **48**, 293-325

Clarke, D. M., Loo, T. W., Inesi, G., and MacLennan, D. H., (1989) *Nature*. **339**, 476-478

Clarke, D. M., Loo, T. W., MacLennan, D. H., (1990) *J. Biol. Chem.* **265**, 14088-14092

Clarke, D. M., Loo, T. W., MacLennan, D. H., (1990) *J. Biol. Chem.* **265**, 22223-22227

Clore, G. M., Gronenborn, A. M., Mitchinson, C., and Green, N. M., (1982) *Eur. J. Biochem.* **128**, 113-117

Coan, C., and Keating, S., (1982) *Biochemistry* **21**, 3214-3220

Coan, C., Jakobs, P., Ji, J.Y., and Murphy, A.J., (1993) *FEBS Lett.* **335**, 33-36

Coleman, J. E., (1992) *Ann. Rev. Biochem.* **61**, 897-946

Coll, R. J., and Murphy, A. J., (1984) *J. Biol. Chem.* **259**, 14249-14254

Coll, R. J., and Murphy, A. J., (1985) *FEBS Lett.* **187**, 131-134

Coll, R. J., and Murphy, A. J., (1991) *Biochemistry* **30**, 1456-1461

Cotton, F. A., and Wilkenson, G., 1972 *Advanced Inorganic Chemistry*, Interscience Publishers, Third Edition

Davidson, G. A., and Berman, M. C., (1985)

J. Biol. Chem. **260**, 7325-7329

Davidson, G. A., and Berman, M. C., (1987)
J. Biol. Chem. **262**, 7041-7048

de Meis, L., (1969) *Biochim. Biophys. Acta.* **172**, 343-344

de Meis, L., and Hasselbach, (1971)
J. Biol. Chem. **246**, 4759-4763

de Meis, L. and Sorenson, (1975)
Biochemistry **14**, 2739-2744

de Meis, L., (1976) *J. Biol. Chem.* **251**, 2055-2062

de Meis, L., and Tume, R., (1977)
Biochemistry **16**, 4455-4463

de Meis, L., and Vianna, A. L., (1979)
Annu. Rev. Biochem. **48**, 275-292

de Meis, L., Martins, O. B., and Alves, E. W., (1980)
Biochemistry **19**, 4252-4261

de Meis, L., (1981) The Sarcoplasmic Reticulum, Wiley, New York

de Meis, L., (1985) *Biochem Soc Symp.* **50**, 97-125

de Meis, L. (1991) *J. Biol. Chem.* **266**, 5736-5742

Degani, C., and Boyer, P. D., (1973)
J. Biol. Chem. **248**, 8222-8226

DeJesus, F., Girardet, J.- L., and Dupont, Y., (1993)
FEBS Lett. **332**, 229-232

Dupont, Y., (1976) Biochim. Biophys. Res. Commun. **71**, 544-550

Dupont, Y., (1977) *Eur. J. Biochem.* **72**, 185-190

Dupont, Y., Leigh, J. B., (1978) *Nature* (Lond.) **273**, 369-398

Dupont, Y., (1980) *Eur. J. Biochem.* **109**, 231-238

Dupont, Y., (1982) *Biochim. Biophys. Acta* **688**, 75-87

Dupont, Y., Chapron, Y., and Pougeois, R., (1982) Biochim. Biophys. Res. Commun. **106**, 1272-1279

Dupont, Y., and Pougeois, R., (1983) *FEBS Lett.* **156**, 93-98

Dupont, Y., (1985) *J. Biol. Chem.* **260**, 7241-7248

Dupont, Y., Pougeois, R., Ronjat, M., and Verjovski-Almeida, S., (1985) *J. Biol. Chem.* **260**, 7241-7249

Ebashi, S., (1961) *J. Biochem. (Tokyo)* **50**, 236-244

Ebashi, S., and Lipmann, F., (1962) *J. Cell. Biol.* **14**, 389-400

Esmann, M., and Skou, J. C., (1983) *Biochim. Biophys. Acta* **748**, 413-417

Esmann, M., (1994) *Biochemistry* **33**, 8558-8565

Fabiato, A., and Fabioto, F., (1979) *J. Physiol. (Paris)* **75**, 463-505

Faller, L. D., (1989) *Biochemistry* **28**, 6771-6778

Faller, L. D., (1990) *Biochemistry* **29**, 3179-3186

Feirrera, S. T., and Verjovski-Almeida, S., (1988) *J. Biol. Chem.* **263**, 9973-9980

Fernandez-Belda, F., Kurzmack, M., and Inesi, G., (1984) *J. Biol. Chem.* **259**, 9687-9698

Forge, V., Mintz, E., Guillain, F., (1993) *J. Biol. Chem.* **268**, 10961-10968

Forge, V., Mintz, E., Canet, D., and Guillain, F., (1995) *J. Biol. Chem.* **270**, 18271-18276

Foster, R., Fyfe, C. A., and Morris, J. W., (1965) *Recl. Trav. Chim. Pays-Bas* **84**, 516-520

Frey, W. H., Senogles, S. E., Tuason, V. B., and Nicol, S. E., (1981) *Biochim. Biophys. Acta* **658**, 369-376

Friedman, Z., and Makinose, M., (1970) *FEBS Lett.* **11**, 69-72

Froud, R. J., and Lee, A. G., (1986) *Biochem. J.* **237**, 197-206

Froud, R. J., and Lee, A. G., (1986)
Biochem. J. **237**, 207-215

Gafni, A., and Boyer, P.D., (1985)
Proc. Natl. Acad. Sci. USA **82**, 98-101

Gantzer, M. L., Klevickis, C., and Grisham, C. M., (1982)
Biochemistry **21**, 4083-4088

Geahlen, R. L., and Haley, B. E., (1977)
Proc. Natl. Acad. Sci. USA **74**, 4375-4377

Gould, G. W., East, J. M., Froud, R. J., McWhirter, J. M., Stefanova, H. I., and Lee, A. G., (1986)
Biochem. J. **237**, 217-227

Green, N. M., (1989) Biochem. Soc. Trans. **17**, 972-974

Green, N. M., and Stokes, D. L., (1992)
Acta Physiol. Scand. **146**, 59-68

Guillain, F., Gingold, M. P., Buschlen, S., and Champeil, P., (1980) *J. Biol. Chem.* **255**, 2072-2076

Guillain, F., Champeil, P., Lacapere, J.-J., and Gingold, M. P., (1981) *J. Biol. Chem.* **256**, 6140-6147

Guillain, F., Gingold, M. P., Champeil, P., (1982)
J. Biol. Chem. **257**, 7366-7371

Guillory, R. J., (1979) *Curr. Top. Bioenerg* **9**, 267-414

Haley, B. E., and Hoffman, J. F., (1974)
Proc. Natl. Acad. Sci. USA **71**, 3367-3371

Haley, B. E., (1975) *Biochemistry* **14**, 3852-3857

Hellam, D. C., and Podolsky, R. J., (1969)
J. Physiol. (Lond.) **200**, 807-819

Hanel, A. M., and Jencks, W. P., (1990)
Biochemistry **29**, 5210-5220

Hanel, A. M., and Jencks, W. P., (1991)
Biochemistry **30**, 11320-11330

Hasselbach, W., and Makinose, M. (1961)
Biochem. Z. **333**, 518-528

Hasselbach (1981) *Arzneimittelforschung.* **31**, 191-193

Hau, S., and Inesi, G., (1997) *Biophys. J.* **73**, 2149-2155

Hendersen, I. M. J., Khan, Y. M., East, J. M., and Lee, A. G., (1994) *Biochem. J.* **297**, 615-624

Hendersen, I. M. J., Starling, A. P., Wictome, M., East, J. M., and Lee, A. G., (1994) *Biochem. J.* **297**, 625-636

Highsmith, S., Murphy, A. J., (1984) *J. Biol. Chem.* **259**, 14651-14656

Highsmith, S., (1986) *Biochemistry* **25**, 1049-1054

Hill, T. L., (1977) *"Free Energy Transduction in Biology"* New York, Academic Press

Hill, T. L., Eisenberg, E., (1981) *Q. Rev. Biophys.* **14**, 463

Hiratsuka, T., and Uchida, K., (1973) *Biochim. Biophys. Acta* **320**, 635-647

Hiratsuka, T., (1975) *J. Biochem. (Tokyo)* **78**, 1135-1147

Hiratsuka, T., (1982) *Biochim. Biophys. Acta* **719**, 509-517

Holbrook, J. J., Liljas, A., Steindel, S. J., and Rossmann, M. G., (1975) in The Enzymes (Boyer, P. D., ed) Vol. 11, pp. 191-292, Academic Press, New York

Ikehora, M., Ohtsuka, E., Kitagawa, S., Yagi, K., and Tonomura, Y., (1961) *J. Am. Chem. Soc.* **83**, 2679-2686

Ikehora, M., Uesugi, S., and Yoshida, K. (1972) *Biochemistry* **11**, 830-842

Ikemoto, N., Morgan, J. F., and Yamada, S., (1978) *J. Biol. Chem.* **253**, 8027-8033

Ikemoto, N., Garcia, A. M., Kurobe, Y., and Scott, T. L., (1981) *J. Biol. Chem.* **256**, 8593-8601

Inesi, G., Goodman, J. J., and Watanabe, S., (1967) *J. Biol. Chem.* **242**, 4637-4643

Inesi, G. (1971) *Science* **171**, 901-903

Inesi, G., Kurzmack, M., and Verjovski-Almeida, S., (1978) *Ann N Y Acad Sci.* **307**, 224-227

Inesi, G., Kurzmack, M., Coan, C., and Lewis, D. E., (1980) *J. Biol. Chem.*. **255**, 3025-3031

Inesi, G., Nakamoto, R., Hymel, L., and Fleischer, S., (1983) *J. Biol. Chem.* **258**, 14804-14809

Inesi, G., (1987) *J. Biol. Chem.* **262**, 16338-16342

Inesi, G., and de Meis, L., (1989) *J. Biol. Chem.* **264**, 5929-5936

Inesi, G., and Kirtley, M. E., (1990) *J. Membrane Biol.* **116**, 1-8

Inesi, G., Chen, L., Sumbilla, C., Lewis, D., and Kirtley, M. E., (1995) *Biosci Rep* **15**, 327-339

Jencks, W. P. (1975) *Adv Enzymol Relat Areas Mol Biol.* **43**, 219-410

Jencks, W. P., (1980) *Adv. Enzymol. Relat. Areas. Mol. Biol.* **51**, 75-106

Jencks, W. P., (1983) *Curr. Top. Membr. Transp.* **19**, 1-19

Jencks, W. P., (1992) *Membr. Transp.* **20**, 555-559

Jencks, W. P., Yang, T., Peisach, D., and Myung, J., (1993) *Biochemistry* **32**, 7030-7034

Jeng, S. J., and Guillory, R. J., (1975) *J. Supramol. Struct.* **3**, 448-468

Kawakita, M., Yasuoka, K., and Kaziro, Y., (1980) *J. Biochem.* **87**, 609-617

Kawakita, M., and Yamashita, T., (1987) *J. Biochem.* **102**, 103-109

Khan, Y. M., East, J. M., and Lee, A. G., (1997) *Biochem. J.* **321**, 671-676

Khnanshvili, D., and Jencks, W. P., (1988) *Biochemistry* **27**, 2943-2952

Klevickis, C., and Grisham, C. M., (1982)
Biochemistry **21**, 6979-6984

Knowles, A. F., and Racker, E., 1975
J. Biol. Chem. **250**, 1949-1951

Kotagel, N., Colca, J. R., and McDaniel, M. L., (1983)
J. Biol. Chem. **258**, 4808-4813

Kronman, M. J., and Bratcher, S. C., (1983)
J. Biol. Chem. **258**, 5707-5709

Lacapere, J. J., and Guillain, F., (1990)
J. Biol. Chem. **265**, 8583-8589

Lacapere, J. J., and Guillain, F., (1993)
Eur. J. Biochem. **211**, 117-126

Lecoeq, D. I., (1968) *J. Med. Chem.* **11**, 1096-1097

Levy, D., Seigneuret, M., Bluzat, A., and
Rigaud, J. L., (1990) *J. Biol. Chem.* **265**, 19524-19534

Lowry, O. H., Rosenbrough, N. Y., Farr, A. L., and Randall,
R. J., (1951) *J. Biol. Chem.* **193**, 696-700

Lunardi, J., Lauquin, G., and Vignais, P. V., (1977)
FEBS Lett. **80**, 317-323

MacLennan, D. H., and Holland, P.C., (1975)
Annu. Rev. Biophys. Bioeng. **4**, 377-404

MacLennan, D. H., Brandl, C. J., Korczak, B., and
Green, N. M., (1985) *Nature*. **316**, 696-700

MacLennan, D. H., (1990) *Biophys J.* **58**, 1355-1365

MacLennan, D. H., Clarke, D. M., Loo, T. W., and
Skerjanc, I. S., (1992)
Acta Physiol Scand Suppl **607**, 141-150

Mahaney, J. E., Froehlich, J. P., and Thomas, D. D., (1995)
Biochemistry **34**, 4864-4879

Makinose, M. and Hasselbach, W., (1965)
Biochem. Z. **343**, 360-382

Makinose, M., and The, R., (1965) *Biochem. Z.* 343, 383-393

Martell, A. E., and Smith, R. M., (1974) *Critical Stability Constants*, Vol. 1, Plenum Press, New York

Martin, (1984) *Metal ions in Biological Sytems* (Sigel, H., ed.) Vol 17, 1-43

Martin, R., Maune, J. F., Beckingham, K., and Bayley, P. M., (1992) *Eur. J. Biochem.* **205**, 1107-1114

Martonosi, A., (1995) *Biosci Rep.* **15**, 263-281

Maruyama, K., and MacLennan, D. H., (1988) *Proc. Natl. Acad. Sci. USA* U.S.A. **85**, 3314-3318

Maruyama, K., Clarke, D. M., Fujii, J., Inesi, G., Loo, T. W. and MacLennan, D. H., *J. Biol. Chem.* **264**, 13038-13042

Masuda, H., and de Meis, L., (1973) *Biochemistry* **12**, 4581-4585

McIntosh, D.B., and Boyer, P. D., (1983) *Biochemistry* **22**, 2867-2875

McIntosh, D.B., and Ross, D., (1988) *J. Biol. Chem.* **263**, 12220-12223

McIntosh, D. B., Ross, D. C., Champeil, P., and Guillain, F., (1991) *Proc. Natl. Acad. Sci. USA* **88**, 6437-6441

McIntosh, D.B. (1992) *J. Biol. Chem.* **267**, 22328-22335

McIntosh, D.B., Woolley, D. G., and Berman, M. C., (1992) *J. Biol. Chem.* **267**, 5301-5309

McIntosh, D.B., and Woolley, D. G., (1994) *J. Biol. Chem.* **269**, 21587-21595

McIntosh, D. B., Woolley, D.G., Vilsen, B., and Andersen, J. P., (1996) *J. Biol. Chem.* **271**, 25778-25789

Meissner, G., (1973) *Biochim. Biophys. Acta* **298**, 906-926

Meissner, G., Conner, G. E., and Fleicher, S., (1973) *Biochim. Biophys. Acta* **298**, 246-269

Meltzer, S., and Berman, M. C., (1984) *Anal. Biochem.* **138**, 458-464

Meszaros, L. G., and Bak, J. Z., (1992)

Biochemistry **31**, 1195-1200

Meszaros, L. G., and Bak, J. Z., (1993)
Biochemistry **32**, 10085-10088

Michelangeli, F., Orlowski, S., Champeil, P., Grimes, E. A., East, J. M., and Lee, A. G., (1990)
Biochemistry **29**, 8307-8312

Michelson, A. M., (1964) *Biochim. Biophys. Acta* **91**, 1-13

Miller, D. L., and Westheimer, F. H., (1966)
J. Am. Chem. Soc. **88**, 1511-1513

Mintz, E., Lacapere, J. J., and Guillain, F., (1990)
J. Biol. Chem. **265**, 18762-18768

Mintz, E., Mata, A. M., Forge, V., Passafiume, M., and Guillain, F., (1995) *J. Biol. Chem.* **270**, 27160-27164

Mitchinson, C., Wilderspin, A. F., Trinnaman, B. J., and Green, N. M., (1982) *FEBS Lett.* **146**, 87-92

Moffat, J. G., (1964) *Can. J. Chem.* **42**, 599-604

Moller, J. V., Lind, K. E., and Andersen, J. P., (1980)
J. Biol. Chem. **255**, 1912-1920

Moller, J. V., Juul, B., and le Maire, M., (1996)
Biochim. Biophys. Acta **1286**, 1-51

Moras, D., Olsen, K. W., Sabesan, M. N., Buchner, M., Ford, G. C., and Rossmann, M. G., (1975)
J. Biol. Chem. **250**, 9137-9162

Moutin, M. J., and Dupont, Y., (1991)
J. Biol. Chem. **266**, 5580-5586

Mozydlowski, E. G., and Fortes, P. A. G., (1981)
J. Biol. Chem. **256**, 2346-2356

Mozydlowski, E. G., and Fortes, P. A. G., (1981)
J. Biol. Chem. **256**, 2357-2366

Murphy, A. J., and Morales, M. F., (1970)
Biochemistry **9**, 1528-1532

Murphy, A. J., (1977) *Arch. Biochem. Biophys.* **180**, 114-120

Murphy, A. J., (1990) *Biochemistry* **29**, 11236-11242

Murto, J., (1965) *Suom. Kem.* (B) **38**, 255-257

Myung, J., and Jencks, W. P., (1994)
Biochemistry **33**, 8775-
8785

Nakamoto, R. K., and Inesi, G. (1984)
J. Biol. Chem. **259**, 2961-2970

Nakamura, J., (1986) *Biochim. Biophys. Acta* **870**, 495-501

Nakamura, J., (1987) *J. Biol. Chem.* **262**, 14492-14497

Nakamura, J., and Tanjima, G., (1997)
J. Biol. Chem. **272**, 19290-19294

Nakamura, Y., and Tonomura, Y. (1982)
J. Bioenerg. Biomembr. **14**, 307-318

Neet, K. E., and Green, N. M., (1977)
Arch. Biochem. Biophys. **178**, 588-597

Onodera, M., and Yagi, K., (1971)
Biochim. Biophys. Acta **253**, 254-265

Orlov, S. N., Pokudin, N. I., Reznikova, M. B., Rjazhsky, G. G., and Postnov, Y. V., (1983)
Eur. J. Biochem. **132**, 315-319

Orlowski, S., and Champeil, P., (1991)
Biochemistry **30**, 352-361

Pauls, H., Bredenbrocker, B., and Schoner, W., (1980)
Eur. J. Biochem. **109**, 523-533

Petithory, J. R., and Jencks, W. P. (1986)
Biochemistry **25**, 4493-4497

Petithory, J. R., and Jencks, W. P. (1988)
Biochemistry **27**, 5553-5564

Pick. U., (1981) *Eur. J. Biochem.* **121**, 187-195

Pick. U., (1982) *J. Biol. Chem.* **257**, 6111-6119

Pick. U., and Bassilian, S., (1981) *FEBS Lett.* **123**, 127-130

Pick. U., and Karlish, S. J. D., (1980)
Biochim. Biophys. Acta **626**, 255-261

Pick, U., and Karlish, S. J., (1982)
J. Biol. Chem. **257**, 6120-6126

Pickart, C. M., and Jencks, W. P. (1982)
J. Biol. Chem. **257**, 5319-5322

Pickart, C. M., Jencks, W. P., (1984)
J. Biol. Chem. **259**, 1629-1643

Post, R. L., Hegyvary, C., and Kume, S., (1972)
J. Biol. Chem. **247**, 6530-6540

Prager, R., Punzengruber, C., Kolassa, N., Winkler, F., and Suko, J., (1979) *Eur. J. Biochem.* **97**, 239-250

Prescott, D. M., (1988) *Cells: Principles of molecular structure and function*, Jones and Bartlett Publishers

Pucell, A., and Martonosi, A., (1971)
J. Biol. Chem. **246**, 3389-3397

Punzengruber, C., Prager, R., Kolassa, N., Winkler, F., and Suko, J., (1978) *Eur. J. Biochem.* **92**, 349-359

Rauch, B., von Chak, D., and Hasselbach, W., (1978) *FEBS Lett.* **93**, 65-68

Reinstein, J., and Jencks, W. P., (1993)
Biochemistry **32**, 32, 6632-6642.

Reynolds, J. A., Johnson, E. A., and Tanford, C., (1985)
Proc. Natl. Acad. Sci. USA **85**, 3658-3661

Rice, D. W., Hardy, G. W., Merrett, M., and Phillips, A. W., (1979) *Nature (Lond.)* **279**, 773-777

Rice, W. J., and MacLennan, D. H., (1996)
J. Biol. Chem. 271, 31412-31419.

Ross, D., and McIntosh, D.B., (1987)
J. Biol. Chem. **262**, 2042-2049

Ross, D., and McIntosh, D.B., (1987)
J. Biol. Chem. **262**, 4613-4621

Ross, D., Davidson, G. A., and McIntosh, D.B., (1991)

J. Biol. Chem. **266**, 4613-4621

Rossi, B., Leone, F. A., Gache, C., and Lazdunski, M., (1979) *J. Biol. Chem.* **254**, 2302-2307

Rossi, J. P. F. C., and Rega, A. F., (1989) *Biochim. Biophys. Acta* **996**, 153-159

Roufogalis, B. D., Al-Jobore, A., (1983) *Cell Calcium* **1**, 27-32

Sarma, R.H., Lee, C. H., Evans, F. E., Yathrinda, N., and Sundralingam, M., (1974) *J. Biol. Chem.* **96**, 7337-7348

Schatzmann, H. J., (1973) *J. Physiol. (Lond.)* **235**, 551-569

Scheiner-Bobis, G., Antonipillai, J., and Farley, R. A., (1993) *Biochemistry* **32**, 9592-9599

Schwarzenbach, G., Senn, H., and Anderegg, G., (1957) *Helv. Chim. Acta* **40**, 1886-1900

Scofano, H.M., Vieyra, A. R., and de Meis, L. (1979) *J. Biol. Chem.* **254**, 10227-10231

Scofano, H.M., Barrabin, H., Inesi, G., and Cohen, J. A., (1985) *Biochim. Biophys. Acta* **819**, 93-104

Scott, T. L., (1985) *J. Biol. Chem.* **260**, 14421-14423

Seebregts and McIntosh, D.B., (1989) *J. Biol. Chem.* **264**, 2043-2052

Segel, G. B., Simon, W., Lichtman, A. H., and Lichtman, M. A., (1981) *J. Biol. Chem.* **256**, 6629-6632

Serpersu, E. H., Kirch, U., and Schoner, W., (1982) *Eur. J. Biochem.* **122**, 347-354

Silva, J. L., and Verjovski-Almeida, S., (1983) *Biochemistry* **22**, 707-716

Silva, J. L., and Verjovski-Almeida, S., (1985) *J. Biol. Chem.* **260**, 4764-4769

Smith, G. L., and Berger, R. L., and Podolsky, R. J., (1977) *Biophys. J.* **17**, 159

Solioz, M., Odermatt, A., and Krapf, R., (1994)
FEBS Lett. **346**, 44-47

Squier, T. C., Bigelow, D. J., Fernandez-Belda, F., de Meis, L., and Inesi, G., (1990) *J. Biol. Chem.* **265**, 13713-13720

Stahl, N., and Jencks, W. P. (1984)
Biochemistry **23**, 5389-5392

Stahl, N., and Jencks, W. P. (1987)
Biochemistry **26**, 7654-7667

Stefanova, H. I., East, J. M., Gore, M. G., and Lee, A. G., (1992) *Biochemistry* **31**, 6023-6031

Stefanova, H. I., Mata, A. M., East, J. M., Gore, M. G., and Lee, A. G., (1993) *Biochemistry* **32**, 356-362

Stefanova, H. I., Mata, A. M., Gore, M.G., East, J.M., and Lee, A.G., (1993) *Biochemistry* **32**, 6095-6103

Stein, W. D., and Honig, B., (1977) *Mol. Cell. Biochem.* **15**, 27-44

Stewart, J. M. MacD., and Grisham, C. M., (1988)
Biochemistry **27**, 4840-4848

Stewart, J. M. MacD., Jorgensen, P. L., and Grisham, C. M., (1989) *Biochemistry* **28**, 4695-4701

Stokes, D. L., and Green, N. M., (1994)
FEBS Lett. **346**, 32-38

Stokes, D. L., and Lacapere, J. J. (1994)
J. Biol. Chem. **269**, 11606-11613

Stokes, D. L., Taylor, W. R., and Green, N. M., (1994)
FEBS Lett. **346**, 32-38

Sumida, M., Schwartz, A., and Froehlich, J. P., (1978)
Ann.
NY Acad. Sci. **307**, 228

Suzuki, H., Kubota, T., Kubo, K., and Kanazawa, T. (1990)
Biochemistry **29**, 7040-7045

Suzuki, H., and Kanazawa, T., (1996)
J. Biol. Chem. **271**, 5481-5486

Takisawa, H., and Tonomura, Y., (1978)
J. Biochem. (Tokyo) **83**, 1275-1284

Tanford, C., (1981) *J. Physiol.* **77**, 223-229

Tanford, C., Reynolds, J.A., and Johnson, E.A., (1987)
Proc. Natl. Acad. Sci. USA **84**, 7094-7098

Tavale, S. S., and Sobell, M., (1970)
J. Mol. Biol. **48**, 109-123
Taylor, W.R., and Green, N. M., (1989)
Eur. J. Biochem. **179**, 241-248

Tonomura, Y., (1961) *J. Am. Chem. Soc.* **83**, 2679-2686

Toyofuku, T., Curotto Kurzydlowski, K., Narayanan, N., and MacLennan, D.H., (1994) *J. Biol. Chem.* **269**, 26492-26496

Toyoshima, C., Sasabe, H., and Stokes, D. L., (1993)
Nature **362**, 469-471

Trosper, T. L., and Philipson, K. D., (1984)
Cell Calcium **5**, 211-222

Tsien, R. Y., (1980) *Biochemistry* **19**, 2396-2404

Verjovski-Almeida, S., and Inesi, G. (1979)
J. Biol. Chem. **254**, 18-21

Verjovski-Almeida, S., and Silva, J. L., (1981)
J. Biol. Chem. **256**, 2940-2944

Viannna, A. L., (1975) *Biochim. Biophys. Acta* **410**, 389-406

Vilsen, B., Andersen, J. P., and MacLennan, D. H., (1991)
J. Biol. Chem. **266**, 16157-16164

Vilsen, B., and Andersen, J. P., (1992)
J. Biol. Chem. **267**, 3539-3550

Wakabayashi, S., Ogurusu, T., and Shigekawa, M., (1986)
J. Biol. Chem. **261**, 9762-9769

Wakabayashi, S., and Shigekawa, M., (1987)
J. Biol. Chem. **262**, 11524-11531

Wakabayashi, S., Ogurusu, T., and Shigekawa M., (1990)
Biochemistry **29**, 10613-10620

Wakabayashi, S., and Shigekawa, M., (1990)
Biochemistry **29**, 7309-7318

Watanabe, S. and Inesi, G. (1982)
J. Biol. Chem. **257**, 11510-11516

Wawrzynow, A., Collins, J. H., and Coan, C., (1993)
Biochemistry **32**, 10803-10811

Webb and Trentham, D. R., (1981)
J. Biol. Chem. **256**, 4884-4887.

Weiner, M. L., and Lee, K. S., (1972)
J. Gen. Physiol. **59**, 462-475

Wyman, J., Jr., (1964) *Adv. Protein Chem.* **19**, 223

Yakamoto, H., Tagaya, M., Fukui, T., and Kawakita, M.,
(1988) *J. Biochem.* **103**, 905-914

Yamagata, K., Daiho, T., and Kanazawa, T., (1993)
J. Biol. Chem. **268**, 20930-20936

Yamagata, K., Daiho, T., and Kanazawa, T., (1994)
J. Biol. Chem. **269**, 4129-4134

Yamaguchi, M., and Kanazawa, T., (1984)
J. Biol. Chem. **259**, 9526-9531

Yamaguchi, M., and Kanazawa, T., (1985)
J. Biol. Chem. **260**, 4896-4900

Yamamoto, H., Imamura, Y., Tagaya, M., Fukui, T., and
Kawakita, M., (1989) *J. Biochem. (Tokyo)* **106**, 1121-1125

Yamamoto, T., and Tonomura, Y., (1967)
J. Biochem. (Tokyo) **62**, 558-575

Yamasaki, K, Daiho, T., and Kanazawa, T., (1994)
J. Biol. Chem. **269**, 4129-4134

Yates, D. W., and Duance, V. C., (1976)
Biochem. J. **159**, 719-728